USER MANUAL FOR RTE2002
Version 1

A COMPUTER CODE FOR THREE-DIMENSIONAL ROCKET THERMAL EVALUATION

M.H.N. Naraghi
Tara Technologies, LLC
3126 Highridge Rd.
Yorktown Heights, NY 10598
www.tara-technologies.com

January 2002

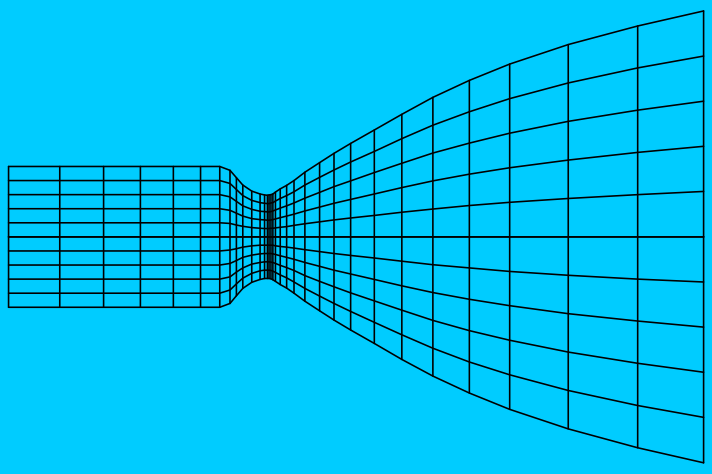

ACKNOWLEGMENT

The original version of RTE was developed through funding by NASA Lewis research center (grant NAG 3-892) and a number of NASA/ASEE summer faculty fellowships to the author this code. Since the public domain version of the code was release (1991), RTE has been substantially improved through private funds. The public domain version of this code can be obtained from NASA Glenn Research Center (see NASA's code publication web site:
http://www.lerc.nasa.gov/WWW/TU/Computer_Tech_Briefs_1991_to_1994.htm).

TABLE OF CONTENTS

SUMMARY

This manual describes the theoretical model and input/output of a computer code for three-dimensional thermal analysis of regeneratively cooled rocket thrust chambers and nozzles (RTE). A unique feature of this code is conjugating all thermal/fluids processes in the propulsion system in order to obtain matched results for the thermal field. These thermal/fluids processes include: convection and radiation heat transfer from hot combustion gases to the liner of the engine; conduction heat transfer with walls; and convection to the coolant. RTE uses an iterative marching scheme to match the heat flux and temperature fields of these thermal processes. The program uses GASP (GAS Properties), WASP (Water and Steam Properties) and a module for properties of RP1 to evaluate coolant flow properties. Hence, it is capable of handling all commonly used coolants in propulsion systems (e.g., H_2, O_2, H_2O, CH_4 and RP1). CET (Chemical Equilibrium with Transport Properties) code is used for evaluation of hot gas properties. The inputs to RTE consist of the composition of fuel/oxidant mixtures and flow rates, chamber pressure, coolant entrance temperature and pressure, dimensions of the engine, materials and number of nodes in different parts of the engine. It allows temperature variations in axial, radial and circumferential directions and by implementing an iterative scheme, it provides a listing of nodal temperatures, rates of heat transfer, and hot-gas and coolant thermal and transport properties. The O/F (oxidant/fuel) ratio can be varied along the thrust chamber. This feature allows the user to incorporate a non-equilibrium model or an energy release model for the hot-gas-side. The mixture ratio at each station can be calculated using ROCCID. Thermal radiation from hot gases within the chamber is also included in the analysis. The exchange factors for radiation calculations are evaluated using an external module (RTE_RAD, Rocket Thermal Evaluation Discrete Exchange Factor), which can be input to the main rocket thermal evaluation code.

This code can be used for both regeneratively and radiatively cooled engines. For regeneratively cooled engines, the code can be used for one pass as well as pass-and-half cooling cycles. Additionally, the blocked channel option allows a user to assess the thermal performance of a regeneratively cooled engine when a cooling channel is blocked. The user has the option of bypassing the hot-gas-side calculations and directly inputting gas side fluxes. This feature can be used to link RTE to a boundary layer program for the hot-gas-side heat flux calculation. The procedure for linking RTE to a hot-gas side program, TDK (Two Dimensional Kinetics Nozzle Performance Computer Program) is described in this manual.

RTE is written in Fortran and has been successfully compiled on a number of UNIX systems and Microsoft Windows. Shell programs have been developed for UNIX and WINDOWS operation systems to link RTE and TDK. To ease inputting the large data sets needed to run the program a Graphic User Interface (preprocessor) based on Excel is provided. A user can fill in engine specifications in designated Excel cells and choose the right engine information from combo boxes. Then by clicking on a command button, data from the Excel interface would be transferred into RTE's input file. Also, RTE and its radiation module can be run from Excel. RTE provides a number of output files, each

provide useful information regarding the engine's thermal performance. The Graphic postprocessor of RTE is based on Techplot software. It produces a number of output files that can be processed by Tecplot for temperature isotherms and graphic results.

NOMENCLATURE

A	area
C	correlation factor for heat transfer coefficient
C_p	specific heat
D	diameter
$\overline{DG_k S_n}$	total exchange factor between gas and surface differential elements
$\overline{DS_k S_n}$	total exchange factor between two surface differential elements
e	cooling channel surface roughness
E	surface and gas emissive power
f	friction factor
g_c	gravitational constant, 32.2 $ft.lb_m/lb_f.s^2$
h	heat transfer coefficient
i	enthalpy
J	work/heat proportionality factor
k	conductivity
K_a	absorption coefficient
K_s	scattering coefficient
K_t	total extinction coefficient
m	total number of axial stations
N	total number of cooling channels
P	pressure
Pr	Prandtl number
q	heat flux
Q_r	radiative heat transfer at inner surface
r	radius
R_{cur}	radius of curvature
R_n	thermal resistance
Re	Reynolds number
s	entropy
T	temperature
V	velocity
W	weight flow
W	weight factor for discrete exchange factor method
x	station position in longitudinal direction

Greek Symbols

β	angle between a vector normal to the nozzle surface and axial direction
ΔS	length of cooling channel between two stations
Δp	pressure drop
Δr	radial mesh size
Δφ	circumferential mesh size

ε	convergence criteria or error limit
μ	dynamic viscosity
ρ	density
σ	Stefan-Boltzmann coefficient
φ	entrance and curvature effect correction factors
ω	successive overrelaxation coefficient
ω_0	$=K_s/K_t$, scattering albedo

Subscripts

A	adiabatic
Avg	average
C	coolant
Cur	curvature
f	viscous or friction
G	gas
i	node i
j	node j
k	secant method iteration number
M	momentum
n	related to station n
r	radiation
S	static
s	surface
t	throat
W	wall
X	reference
0	stagnation

Superscripts

j	iteration number
l	iteration number for conduction model
n	related to station n

INTRODUCTION

Thermal analysis is an essential and integral part in the design of rocket engines. The need for thermal analysis is especially important in the reusable engines where an effective and efficient cooling system is crucial in expanding the engine life. The rapid and accurate estimation of propulsion system aerothermodyanamic heat loads and thermal protection system effectiveness is required if new vehicle propulsion concepts are to be evaluated in a timely and cost effective manner. In the high-pressure engines hot-gas temperatures are very high (they can reach 7000R at the throat area). It is therefore essential to be able to estimate the wall temperature and ensure that the material can withstand such high temperature. Furthermore, an accurate thermal model enables an engine designer to modify the cooling channel configuration for the optimum cooling at high temperature areas. It should be noted that the under-cooling of an engine would result in catastrophic failure of the engine and over-cooling would cause loss of engine performance. This loss of performance can be due to the need for a bigger coolant compressor or decreased effective flow area at the throat when the liner temperature is very low (larger boundary layer displacement when the liner is over-cooled).

The thermal phenomena in rocket engines involve interactions among a number of processes, including, combustion in the thrust chamber, expansion of hot-gases through the nozzle, heat transfer from hot-gases to the nozzle wall via convection and radiation, conduction in the wall, and convection to the cooling channel. The complexity of the thermal analysis in rocket engines is due to three-dimensional geometry, coolant and hot gas heat transfer coefficient dependence on the pressure and wall temperature, unknown coolant pressure drop and properties, axial conduction of heat within the wall, and radiative heat transfer between gases and surfaces of the engine. A comprehensive thermal model must account for all of these items.

RTE (Rocket Thermal Evaluation) is a comprehensive rocket thermal analysis code that uses a number of existing codes and allows interaction among them via iterative procedures. The code is based on the geometry of a typical regeneratively-cooled engine similar to that shown in Figures 1 and 2. It uses CET (Chemical Equilibrium with Transport Properties) [1-2] and GASP [3-4] for the evaluation of hot gas and coolant properties. The inputs to this code consist of the composition of fuel/oxidant mixtures and flow rates, chamber pressure, coolant entrance temperature and pressure, dimensions of the engine and materials in different parts of the engine, as well as the grid generation data. This program allows temperature variations in axial, radial and circumferential directions, and by implementing an iterative scheme it provides a listing of nodal temperatures, rates of heat transfer, and hot gas and coolant thermal and transport properties. The fuel/oxidant mixture ratio can be varied along the thrust chamber. This feature allows the user to incorporate a non-equilibrium model or an energy release model for the hot-gas-side. The mixture ratio along the thrust chamber is calculated using ROCCID [5] (ROCket Combustor Interactive Design and Analysis Computer Program). ROCCID has been modified to take RTE input and make the mixture ratio variable along the thrust chamber. Thermal radiation from hot gases within the chamber is also included in the analysis. The user has the option of bypassing the hot-gas-side calculations and

directly inputting gas side fluxes. This feature is used to link RTE to a boundary layer program for the hot-gas-side heat flux calculation. A shell program was developed to link RTE to a hot-gas side program, TDK [6] (Two Dimensional Kinetics Nozzle Performance Computer Program). This shell program runs RTE and TDK in an iterative loop to match wall temperatures and fluxes computed based on the two codes. Additionally, another feature is devised such that a user can input hot-gas-side fluxes via a matrix whose rows are axial positions along the chamber and nozzle, and columns are different temperatures.

This manual describes the numerical model and the computer code (RTE) developed to analyze rocket engine thrust chamber heat transfer characteristics. This code can be used to determine the temperature distribution in both regeneratively and radiatively cooled thrust chambers by allowing for temperature variations in the radial, circumferential and axial directions.

NUMERICAL MODEL

Overview of the Numerical Model

The numerical procedure for the thermal analysis is summarized below. A flowchart of this model is given in Appendix A. The model is based on the geometry of a typical regeneratively cooled thrust chamber (shown in Figure 1 and 2). The user specifies the combustion chamber and nozzle wall materials and thicknesses. The wall can consist of three layers: a coating, the channel, and the closeout, which can be made of different materials. The user also specifies the number of cooling channels in the wall. For the numerical procedure, the rocket thrust chamber and nozzle are subdivided into a number of stations along the longitudinal direction, as shown in Figure 3.

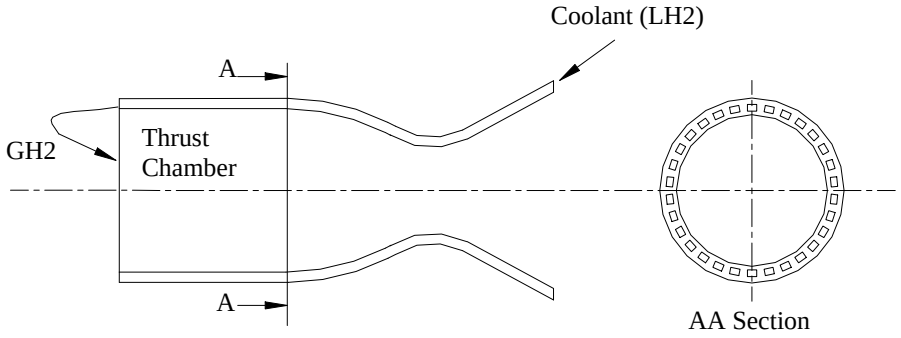

Figure 1: Configuration of a typical regeneratively cooled rocket engine

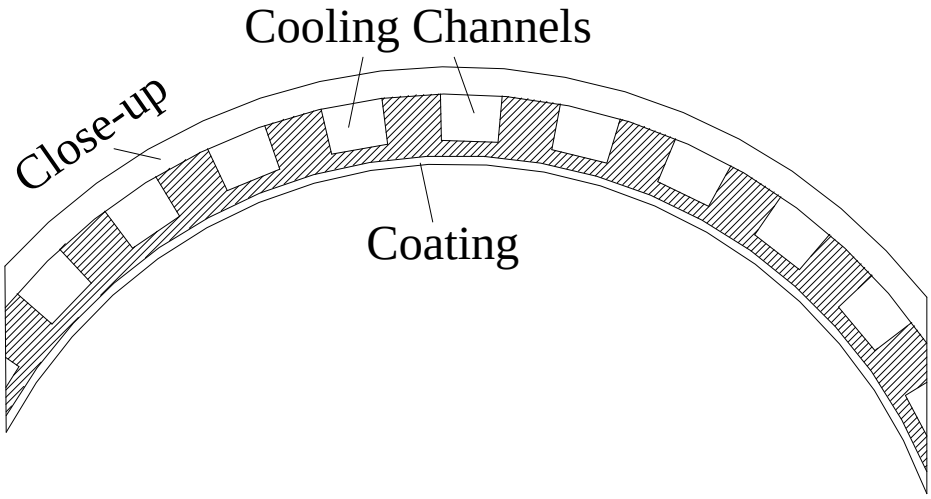

Figure 2: Detailed layout of cooling channels in a typical regeneratively cooled rocket engine

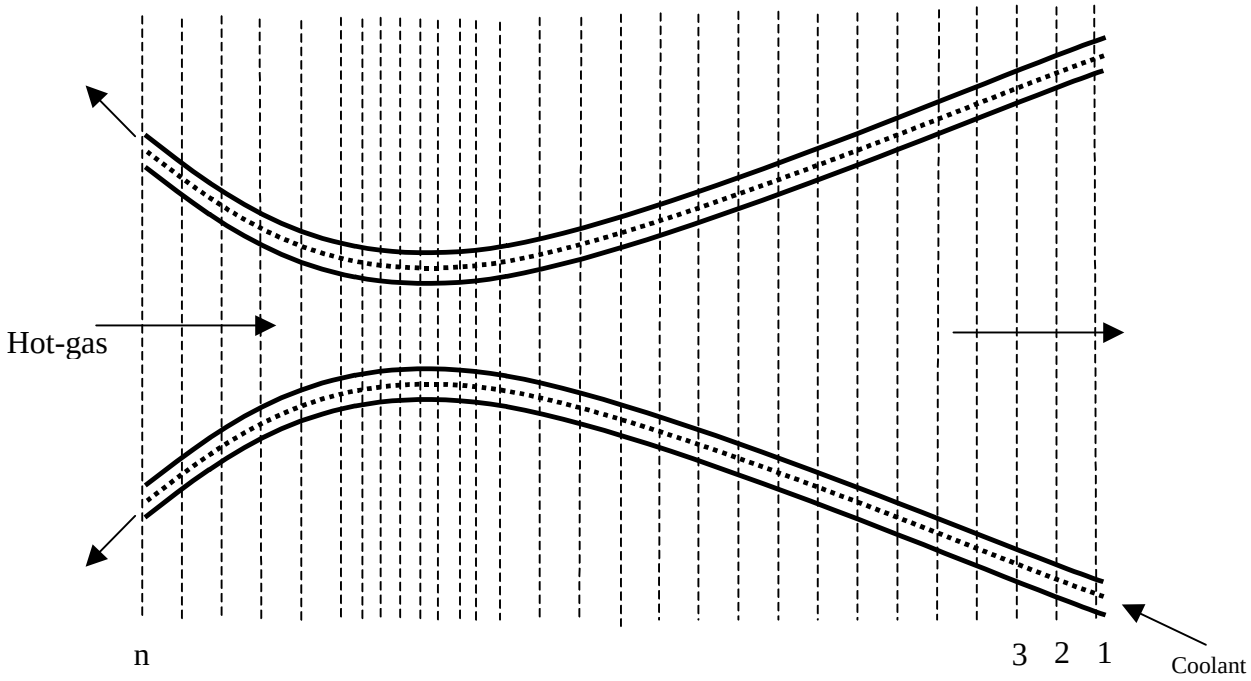

Figure 3: A rocket thrust chamber subdivided into a number of stations

These stations do not have to be equally spaced; in fact, it is desirable to put more stations near the throat where the heat flux and temperature gradients are largest. The numbering of stations starts with the inlet to the cooling channels and ends at their exit. Figure 3 shows a counter flow nozzle liner cooling arrangement. There are other cooling arrangements where the coolant enters at a point in the middle or the other end of the nozzle liner, travels parallel to the hot-gas, makes a U-turn at the exit of nozzle, and returns as a counter flow coolant into different cooling channels. This arrangement is known as "pass-and-half" or "wrapped" flow cooling. The numbering for the pass-and-half or wrapped coolant flow stations starts at the negative value of the station that coolant flow enters the nozzle liner. For example, if the coolant flow enters at station 10, the down stream flow (the same direction as the hot-gas flow) the starting point station index is –10; then the next index is –9, -8, …-1 (see Figure 4 for details). Up to this point the coolant flow is parallel to the hot-gas flow. The coolant flow makes a U-turn from station 1 and moves upstream (opposite to the hot-gas flow) all the way to the last station (station n). RTE's numerical model starts with the station that coolant enters (cooling station –10 for the case shown in Figure 4). The model marches along the cooling channel, and at each station the heat picked up by coolant is calculated using the heat balance among several heat transfer modes (convection and radiation from hot-gases, conduction within the chamber and nozzle liner, and convection to the coolant). In this model, the heat transfer between downstream and upstream channels is neglected, i.e., no heat transfer between sections –8 and 8. This assumption will produce reasonable results since the temperature difference between the coolant and hot gas is on the order of 100 times the temperature difference between two adjacent cooling channels. This assumption has no effects on the overall heat picked up by the coolant since the heat

transfer from hot-gases to the wall at a given station is either picked up by downstream or upstream flows.

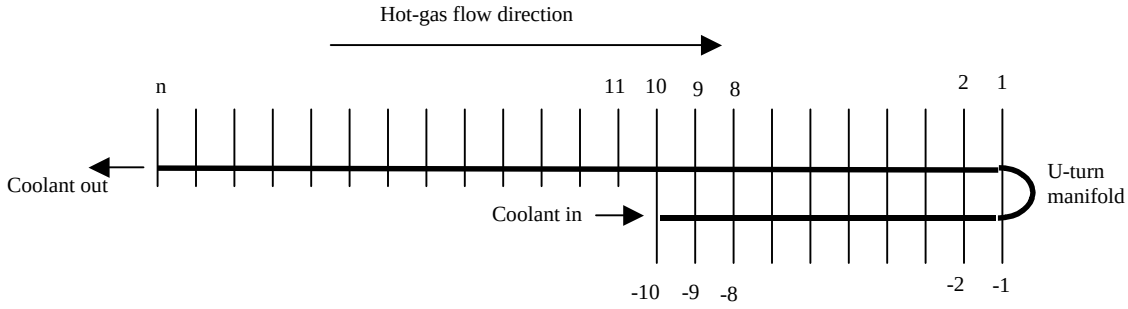

Figure 4: Schematic of a typical pass-and-half (wrapped) cooling channel with station numbering

The thermodynamic and transport properties of the combustion gases are evaluated using the chemical equilibrium composition computer program developed by Gordon and McBride [1-2] (CET, Chemical Equilibrium with Transport properties). The GASP (GAS Properties) [3] or WASP (Water And Steam Properties) [4] programs are implemented to obtain coolant thermodynamic and transport properties. For RP1 a separate subroutine is based on properties given in [7]. Since the heat transfer coefficients of the hot gas and coolant sides are related to surface temperatures, an iterative procedure is used to evaluate heat transfer coefficients and adiabatic wall temperatures.

The temperature distribution within the wall is determined via a three-dimensional finite difference scheme. In this method, finite difference grids are superimposed throughout the wall at different stations. The temperature of each node is then written in terms of temperatures of neighboring nodes (the four closest nodes at the same station and two nodes at the neighboring stations). The program marches axially from one station to another. At each station the Gauss-Siedel iterative method is used to obtain convergence for the temperature distribution along the radial and circumferential directions. When the axial march is completed, comparison is made between the results of the present march and that of the previous one to see if the convergence criteria in the axial direction have been met. If it is not met, the code starts again at the first station and makes another march along the cooling channels. The process continues until convergence is achieved. A detailed description of this numerical model is outlined below.

Geometric Data and Hot-Gas-Side Equilibrium Properties

First, the area ratio for each station and the distance between neighboring stations are calculated via the following equations:

$$\frac{A_n}{A_t} = \left(\frac{d_{G_n}}{d_{G_t}}\right)^2 \qquad (1)$$

and

$$S_{n-1.n} = \sqrt{(\frac{d_{G_n} - d_{G_{n-1}}}{2})^2 + (x_n - x_{n-1})^2} \tag{2}$$

Then, the static pressures, temperatures, enthalpies and Mach numbers for the combustion gases are evaluated using the ROCKET subroutine from [1]. It should be noted that these properties are independent of wall temperature and are only dependent on the cross-sectional area of the nozzle; the propellant used and chamber pressure. Indeed, the heat transfer from hot gases to the chamber and nozzle wall will cause very little change in the gas temperature (the thermodynamic process dominates the transport process).

Geometry of the nozzle is inputted into RTE via two variables, axial position (x_n) and the corresponding nozzle diameter (d_{G_n}). The axial position, x_n, is zero at throat, positive downstream of the throat and negative upstream of the throat. These two variables in the NAMELIST of RTE are defined as X and DG.

Coolant Properties at the Cooling Channel Entrance

On the coolant side, the stagnation enthalpy and density at the entrance to the cooling channel are evaluated as functions of the coolant stagnation pressure and temperature $i_{C0} = i_{C0}(P_{C0}, T_{C0})$ and $r_{C0} = r_{C0}(P_{C0}, T_{C0})$ using the coolant properties modules (e.g., GASP and WASP).

Axial Marches

The model now begins its axial marches (passes) starting from the first station. At the first axial march an initial guess for the wall temperature distribution is made. For the next march, however, the results of temperature distribution for the previous march can be used as an initial guess. The hot gas and coolant adiabatic wall temperatures and wall properties can be evaluated at a given station based on the assumed wall temperature distribution using the properties computer codes [1-4] for the combustion gases and the coolant. The reference enthalpy of the gas side, i_{GX_n} is given by [8-9]

$$i_{GX_n} = 0.5(i_{GW_n} + i_{GS_n}) + 0.180(i_{G0_n} - i_{GS_n}) \tag{3}$$

where i_{GW_n} is a function of gas static pressure P_{GS_n} and gas-side wall temperature T_{GW_n} and is evaluated using the program given in [1]. The gas-side adiabatic wall enthalpy, i_{GAW_n} is calculated using the following equation [8-9]

$$i_{GAW_n} = i_{GS_n} + (\mathrm{Pr}_{GX_n})^{1/3}(i_{G0_n} - i_{GS_n}) \tag{4}$$

where the gas reference Prandtl number Pr_{GX_n} is

$$\mathrm{Pr}_{GX_n} = \frac{C_{p_{CX_n}} m_{GX_n}}{k_{GX_n}} \tag{5}$$

$C_{p_{CX_n}}$, m_{GX_n} and k_{GX_n} are functions of P_{GS_n} and i_{GX_n} .

Once the gas-side adiabatic wall temperature is determined, the wall adiabatic temperature is calculated via

$$T_{GAW_n} = f(P_{GS_n}, i_{GAW_n}) \tag{6}$$

and using the combustion codes [1-2]. The hot-gas side heat transfer coefficient, h_{G_n} is given by [6-7]

$$h_{G_n} = \frac{C_{G_n} k_{GX_n}}{d_{G_n}} \mathrm{Re}_{GX_n}{}^{0.8} \mathrm{Pr}_{GX_n}{}^{0.3} \tag{7}$$

where C_{G_n} is the gas-side correlation coefficient given as input and the Reynolds number is defined by

$$\mathrm{Re}_{GX_n} = \frac{4\dot{W}_G}{p d_{G_n} m_{GX_n}} \frac{T_{GS_n}}{T_{GX_n}} \tag{8}$$

$$T_{GX_n} = f(P_{GS_n}, i_{GX_n}) \tag{9}$$

$$T_{GS_n} = f(P_{GS_n}, i_{GS_n}) \tag{10}$$

Once the hot-gas-side heat transfer coefficient is determined the wall heat flux can be evaluated via

$$q_n = h_{G_n}(T_{GAW_n} - T_{GW_n}) \tag{11}$$

or

$$q_n = \frac{h_{G_n}}{C_{p_{GX_n}}}(i_{GAW_n} - i_{GW_n}) \tag{12}$$

Later, the adiabatic wall temperature and gas-side heat transfer coefficient, calculated from equations (6) and (7), or wall heat flux calculated using equations (11) and (12) will be used in the conduction subroutine to evaluate a revised wall temperature distribution. It should be noted that the formulation given by equations (7-12) yields an approximate value for the wall heat flux.

In addition to the formulation given by equation (7-12), the heat fluxes can be input directly at specified station. The program then bypasses wall heat flux computations and uses the specified heat fluxes. Additionally this feature allows interfacing RTE with a boundary layer module.

The variable in the NAMELIST of RTE that controls the method of hot-gas-side calculations is IWFLUX. By setting IWFLUX=0, equations (3-12) are used to calculate hot-gas-side fluxes. For this case REACTANT compositions data file described in [1-2] are needed. If hot-gas-side wall heat fluxes are known the IWFLUX is set to 1 (IWFLUX=1) and an array of wall heat flux (QW) for every station must be included in the NAMELIST of the RTE.

If another software is being used for hot-gas-side computations then the resulting wall heat fluxes can be linked to RTE via a matrix. Rows of this matrix represent location along axial direction of the engine and its columns represent various temperature. Running the user-preferred hot-gas-side software for a constant wall temperature can generate each column of this matrix. It should be noted that positions of points for which heat fluxes are evaluated do not have to coincide with positions of stations defined in the RTE's input. RTE has an interpolation routine that calculates wall heat flux based on the wall temperature and location of the station. This feature of RTE can be used by setting IWFLUX=2, and providing another input file (FLUX.DAT), which contains fluxes matrix. A sample of FLUX.DAT is given in Appendix B.

Interfacing RTE and TDK's Boundary Layer Module

To interface RTE and TDK a shell program is written which allow iterations between RTE and TDK. First RTE's internal heat flux calculation (equations (6-12)) is used to predict wall temperature. Then the calculated wall temperature via and RTE and TDK interface program (TDK_RTE) is inserted into input of TDK. Then by running TDK (with one of its boundary layer modules, BLM or MABL) the wall heat flux based on TDK's boundary layer module is calculated. The heat fluxes for each station are inserted into the input file of RTE via an interface program (RTE_TDK). This cycle is repeated several times until convergence is achieved. At each iterative cycle heat fluxes at all stations are compared to those of pervious iteration. This iterative calculation stops when the difference between wall heat fluxes of two consecutive iteration become negligibly small. The flow chart of this iterative scheme is given in Figure 5. More detailed descriptions of this feature of RTE are presented in "HOT-GAS_SIDE BOUNDARY LAYER ANALYSIS" and Appendix D.

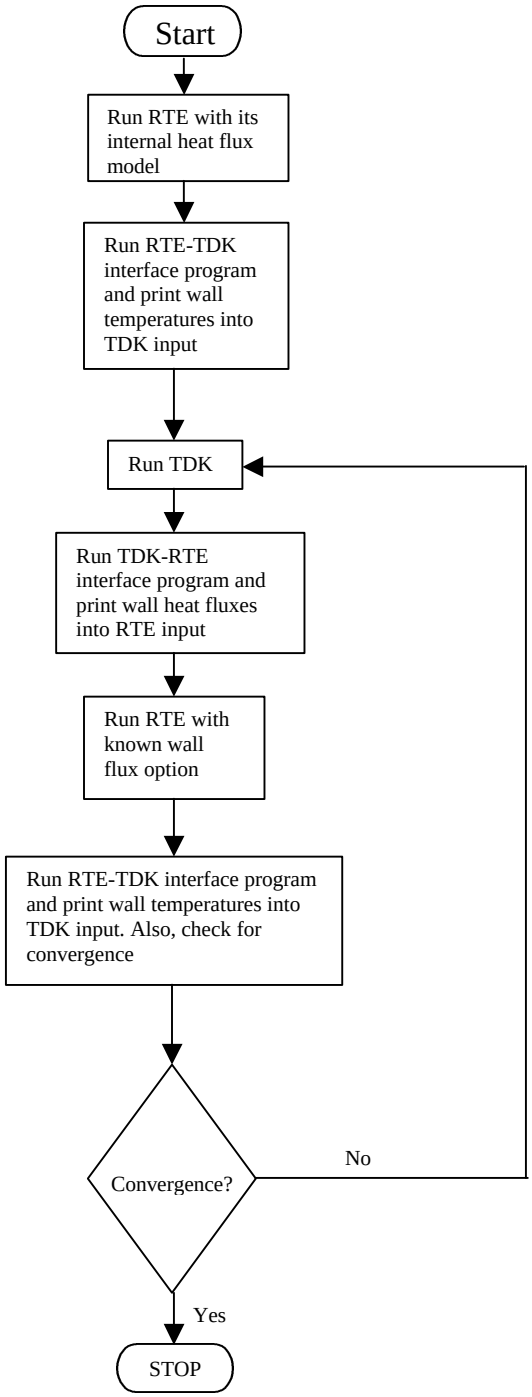

Figure 5: Flow chart of shell program for interfacing RTE and TDK

Next, attention will be focused on calculating the coolant-side properties and heat transfer calculations.

Coolant Properties

For the first station the coolant stagnation enthalpy, static pressure and static density are set equal to the stagnation enthalpy, pressure, and density at the entrance to the cooling channel (i.e., $i_{C0_1} = i_{C0}$, $P_{CS_1} = P_{C0}$ and $r_{CS_1} = r_{C0}$. For the other stations, the coolant stagnation enthalpy is calculated via

$$i_{C0_n} = i_{C0_{n-1}} + \frac{(q_n{}^{j-1} + q_{n-1})\Delta S_{n-1,n}}{2W_C} \tag{13}$$

where $\Delta S_{n-1,n}$ is the distance between two neighboring stations $n-1$ and n which is calculated from equation (2) and $q_n{}^{j-1}$ is the heat transferred per unit length of the cooling channel from the hot gases to the coolant at station n (calculated from the conduction subroutine at iteration $j-1$). For the first iteration at station n, $q_n{}^{j-1}$ in equation (13) is not known; therefore the following equation is used to evaluate the stagnation enthalpy

$$i_{C0_n} = i_{C0_{n-1}} + \frac{q_{n-1}\Delta S_{n-1,n}}{W_C} \tag{14}$$

Note that q_{n-1} in equations (13) and (14) are the heat transfer per unit length of cooling channel at the previous station.

The coolant velocity is calculated from the following equation:

$$V_{CS_n} = \frac{W_C}{r_{CS_n} A_{C_n} N_n} \tag{15}$$

Note that r_{CS_n}, is set equal to r_{C0_n} for the first station, and for the other stations is evaluated, using the GASP, WASP programs [3-4] or RP1 subroutine, based on the static pressure and enthalpy at the previous iteration, i.e.,

$$r_{CS_n} = r(P_{CS_n}^{j-1}, i_{CS_n}^{j-1}) \tag{16}$$

At the first iteration, however, it is set equal to the static density of the previous station ($r_{CS_n}^1 = r_{CS_{n-1}}$).

Once the coolant velocity is determined, the static enthalpy can be calculated using the following equation:

$$i_{CS_n} = i_{C0_n} - \frac{V_{CS_n}{}^2}{2 g_c J} \tag{17}$$

Coolant Friction Factor Calculations

In order to determine the coolant friction factor first the Reynolds numbers must be evaluated. The coolant static and reference Reynolds numbers, respectively, are given by:

$$Re_{CS_n} = \frac{W_C d_{C_n}}{A_{C_n} N_n m_{CS_n}} \tag{18}$$

and

$$Re_{CX_n} = Re_{CS_n} \left(\frac{r_{CW_n}}{r_{CS_n}} \right) \left(\frac{m_{CS_n}}{m_{CW_n}} \right) \tag{19}$$

where m_{CS_n} is a function of P_{CS_n} and i_{CS_n} are calculated using the GASP program [3], the WASP program [4] if the coolant is water or Rp1 subroutine. Note also that d_{C_n} is the coolant hydraulic diameter at station n. To employ a better value for the Reynolds number, an average Reynolds number between the entrance and exit to each station is evaluated, i.e.,

$$Re_{CS_{Avg.}} = 0.5(Re_{CS_{n.}} + Re_{CS_{n-1}}) \tag{20}$$

$$Re_{CX_{Avg.}} = 0.5(Re_{CX_{n.}} + Re_{CX_{n-1}}) \tag{21}$$

The Reynolds number in the cooling channel is within the turbulent flow range; hence, the Colebrook equation [10] is used to calculate the friction factor. This equation is given by:

$$\frac{1}{\sqrt{f}} = -2.0 \log \left(\frac{e}{3.7065 D} + \frac{2.5226}{\mathrm{Re}_{CX_{Avg.}} \sqrt{f}} \right) \tag{22}$$

This implicit equation very closely approximated by the explicit formula [11]

$$\frac{1}{\sqrt{f}} = -2.0\log\left[\frac{e}{3.7065D} - \frac{5.0452}{\mathrm{Re}_{CX_{Avg.}}}\log\left(\frac{1}{2..8257}\left(\frac{e}{D}\right)^{1.1098} + \frac{5.8506}{\mathrm{Re}_{CX_{Avg.}}^{0.8981}}\right)\right] \tag{23}$$

Curvature Effect

The correlation given by equation (23) is only valid for straight channels. To include the curvature effect, the friction factor obtained from equation (23) must be multiplied by the curvature factor given by Ito's correlation [12]:

$$f_{Cur.} = \left[Re_{CX_{Avg.}}\left(\frac{r_{C_n}}{R_{Cur._n}}\right)^2\right]^{1/20} \tag{24}$$

where r_{C_n} is the hydraulic radius of cooling channel, $R_{Cur._n}$ is the radius of curvature. The curvature factor given by equation (24) is valid when $Re_{CX_{Avg.}}\left(\frac{r_{C_n}}{R_{Cur._n}}\right)^2 > 6$, otherwise, $f_{Cur.} = 1$.

Pressure Drop

Once the friction factors are determined, the viscous pressure drop between stations $n-1$ and n is calculated using Darcy's law [13] which is given by:

$$\left(\Delta P_{CS_{n-1,n}}\right)_f = \frac{f_n}{8g_c}\left(\frac{r_{CS_n} + r_{CS_{n-1}}}{d_{C_n} + d_{C_{n-1}}}\right)\left(V_{CS_n} + V_{CS_{n-1}}\right)^2 \Delta S_{n-1,n} \tag{25}$$

and the momentum pressure drop is calculated via

$$\left(\Delta P_{CS_{n-1,n}}\right)_M = \left(\frac{2}{(A_C N)_{n-1} + (A_C N)_n}\right)\frac{W_C^{\,2}}{g_c}\left(\frac{1}{(r_{CS} A_C N)_n} - \frac{1}{(r_{CS} A_C N)_{n-1}}\right) \tag{26}$$

An average value of variables between stations n and $n-1$ in equations (25) and (26) are used to improve the accuracy. Pressure drop due to change in size of cooling channels (contraction or expansion) is incorporated through the following equation:

$$\left(\Delta P_{CS_{n-1,n}}\right)_K = K\frac{r_{CS_n} V_{CS_n}^2}{2g_c} \tag{27}$$

where $K = \left[\left(\frac{d_{C_{n-1}}}{d_{C_n}}\right)^2 - 1\right]^2$ for expansion,

and $K = 0.5 - 0.167\left(\frac{d_{C_n}}{d_{C_{n-1}}}\right) - 0.125\left(\frac{d_{C_n}}{d_{C_{n-1}}}\right)^2 - 0.208\left(\frac{d_{C_n}}{d_{C_{n-1}}}\right)^3$ for contraction

The static pressure at each station is calculated based on the viscous and momentum pressure drops and is given by:

$$P_{CS_n} = P_{CS_{n-1}} - \left[\left(\Delta P_{CS_{n-1,n}}\right)_f + \left(\Delta P_{CS_{n-1,n}}\right)_M + \left(\Delta P_{CS_{n-1,n}}\right)_K\right] \tag{28}$$

Coolant Wall and Reference Properties

Once the coolant static pressure is determined, the coolant wall properties which are functions of the static coolant pressure P_{CS_n} and wall temperature, i.e.,

$$C_{PCW_n}, m_{CW_n}, k_{CW_n}, i_{CW_n} = f(P_{CS_n}, T_{CW_n}) \tag{29}$$

are evaluated using the coolant properties modules (GASP, WASP or RP1). It should be noted that the wall temperature is not constant at a given station; hence, three coolant wall properties, which are based on the lower, upper and side-wall temperatures are determined. The reference and adiabatic wall enthalpies at the station are, respectively, calculated from the following equations [9]

$$i_{CX_n} = 0.5(i_{CS_n} + i_{CW_n}) + 0.194(i_{C0_n} - i_{CS_n}) \tag{30}$$

and

$$i_{CAW_n} = i_{CS_n} + (\mathrm{Pr}_{CX})^{1/3}\left(i_{C0_n} - i_{CS_n}\right) \tag{31}$$

The adiabatic wall temperature is a function of the coolant static pressure and the adiabatic wall enthalpy and is evaluated using the GASP program [3]. Note that the Prandtl number in equation (28) is expressed by:

$$\mathrm{Pr}_{CX} = \frac{C_{p_{CX}} m_{CX}}{k_{CX}} \tag{32}$$

where

$$C_{p_{CX}}, m_{CX}, k_{CX} = f(P_{CS}, i_{CX}) \tag{33}$$

Coolant Heat Transfer Coefficient Calculations

A number of built-in correlations may be used to evaluate the heat transfer coefficients in the cooling channels. These correlations can be activated via the NAMELIST variable ITYPE. User specified correlation can be used by setting ITYPE=0. The simplest one is given by the following correlation (Dittus-Boelter correlation see [8-9]):

$$Nu = C_{C_n} Re_{CX}^{0.8} Pr_{CX}^{0.4} \tag{34}$$

This correlation can be used if ITYPE is set to 1. For most supercritical cryogenic fluid flows Hendricks and coworkers suggested a correlation in [14-15]. In this correlation the Nusselt number is given by:

$$\frac{Nu}{Nu_r} = C_{C_n} Re^{0.8} Pr^{0.4} \tag{35}$$

where

$$Nu_r = y^{-0.55}$$

$$y = 1 + g\left(T_W - T_S\right)$$

and

$$g = \left| \frac{1}{r} \frac{\partial r}{\partial T} \right|_P = \frac{1}{r} \frac{\left(\frac{\partial P}{\partial T} \right)_r}{\left(\frac{\partial P}{\partial r} \right)_T}$$

Properties for the above correlation are based on the coolant static temperature T_{CS}, and static pressure P_{CS}. The correlation of equation (35) can be used by setting ITYPE=2. Correlations described by equations (34) and (35) give inaccurate results when the coolant is liquid oxygen. A correlation, specifically for oxygen has been proposed [16]. This correlation is given by:

$$Nu = C_{C_n} Re_{CS} Pr_{CS}^{0.4} \left(\frac{\bar{c}_p}{c_{p_{CS}}} \right) \left(\frac{P_{Cri}}{P_{CS}} \right)^{0.2} \sqrt{\left(\frac{k_{CS}}{k_{CW}} \right) \left(\frac{r_{CW}}{r_{CS}} \right)} \tag{36}$$

where $P_{Cri} = 731.4$ psia is the critical pressure and

$$\bar{c}_p = \frac{i_{CW} - i_{CS}}{T_{CW} - T_{CS}}$$

The oxygen correlation can be used by setting ITYPE=3. When the coolant is RP1, the following two correlations can be used (see [17-19]):

$$Nu = 0.255 Re_{CS}^{0.582} Pr_{CS}^{0.554} \tag{37}$$

for ITYPE=4, and

$$Nu = 0.0056 Re_{CX}^{0.95} Pr_{CX}^{0.4} \tag{38}$$

for ITYPE=5. The user defined correlation can be used by setting ITYPE=0, where correlation has a general form of

$$Nu_{CS} = C_{C_n} Re_{CS}^{b} Pr_{CS}^{c} \left(\frac{r_{CS}}{r_{CW}} \right)^{d} \left(\frac{m_{CS}}{m_{CW}} \right)^{e} \left(\frac{k_{CS}}{k_{CW}} \right)^{f} \left(\frac{\bar{c}_p}{c_{p_{CS}}} \right)^{g} \left(\frac{P_{CS}}{P_{Cri}} \right)^{h} \tag{39}$$

The user can specify exponents of the above correlation in the NAMELIST of RTE by setting REEXP=b, PREXP=c, DENEXP=d, VISCEXP=e, CONDEXP=f, SHEXP=g and PRESEXP=h. Values of these exponents for some hydrocarbon fuels are reported in [19] and given in Table 1.

Fuel	Coefficient/Exponent								No. of Points	Std. Dev.	Correl. Coeff.
	C_{C_n}	b	c	D	e	f	g	h			
RP1	0.0095 0.0068	0.99 0.94	0.4 0.4	0.37 0	0.6 0	-0.2 0	-6.0 0	-0.36 0	274 274	0.16 0.20	0.97 0.96
Chem. Pure Propane	0.011 0.020	0.87 0.81	0.4 0.4	-9.6 0	2.4 0	-0.5 0	0.26 0	-0.23 0	79 79	0.10 0.15	0.99 0.97
Commercial Propane	0.034 0.028	0.80 0.80	0.4 0.4	-0.24 0	0.098 0	-0.43 0	2.1	-0.38 0	285 285	0.27 0.29	0.94 0.93
Natural Gas	0.00069 0.0028 3.7	1.1 1.0 0.42	0.4 0.4 0.4	1.4 1.5 0	-6.5 -6.5 0	6.3 6.4 0	2.6 2.4 0	0.087 0 0	130 130 130	0.16 0.16 0.38	0.92 0.92 0.30
All of the above fuels	0.019	0.81	0.4	-0.059	0.0019	0.053	0.52	0.11	768	0.28	0.97
All of the above fuels except Natural Gas	0.044	0.76	0.4	0	0	0	0	0	638	0.26	0.98

Table 1: Coefficient and exponents of correlations for hydrocarbon fuels

The properties in the above correlations are calculated using the GASP program [3] (for H2, O2, etc.), WASP program [4] (for water) and RP1 properties routine. It should also be noted that there are three coolant heat transfer coefficients and adiabatic wall temperatures. They are for the top, side, and bottom walls of the cooling channel. The variable heat transfer coefficient is due to the variable wall temperature in the cooling channel. The coolant reference and adiabatic wall enthalpies are also functions of wall temperature and are larger for the surface nodes closer to the bottom of the cooling channel. The correlation factors for the heat transfer coefficient, C_{C_n}, in equations (34) and (35) are usually equal to 0.023 for most coolants. When the coolant is liquid oxygen, however, a factor of 0.0025 is used in equation (36).

Entrance Effect

The correlations given by equations (34)-(39) are for fully developed turbulent flow in a smooth and straight tube (channel). To include the effect of the entrance region, they are multiplied by the following coefficient [20]:

$$f_{Ent.} = 2.88\left(\frac{\sum_{i=1}^{n}\Delta S_{i,i+1}}{d_{C_n}}\right)^{-0.325} \tag{40}$$

Other entrance effect factors for different types of cooling channel entrances reported in [20] are given by:

$$f_{Ent.} = \left[1+\left(\frac{\sum_{i=1}^{n}\Delta S_{i,i+1}}{d_{C_n}}\right)^{-0.7}\left(\frac{T_W}{T_b}\right)^{0.1}\right] \tag{41}$$

for a 90^o bend entrance. Taylor [21] suggested the following correction factors:

$$f_{Ent.} = \left(\frac{T_W}{T_b}\right)^{\left[1.59/\left(\sum_{i=1}^{n}\Delta S_{i,i+1}/d_{C_n}\right)\right]} \tag{42}$$

for straight tube and

$$f_{Ent.} = \left(\frac{T_W}{T_b} \right)^{\left[1.59 / \left(\sum_{i=1}^{n} \Delta S_{i,i+1} / d_{C_n} \right) \right]} \left[1 + 5 / \left(\frac{\sum_{i=1}^{n} \Delta S_{i,i+1}}{d_{C_n}} \right) \right] \tag{43}$$

for a 90^o bend entrance. Any of the above four correlations can be selected by setting RTE's NAMELIST variable IENT to 1 for equation 40; 2 for equation 41; 3 for equation 42; and 4 for equation 43. If no number is assigned to IENT then the entrance effect will be neglected.

Curvature Effect

The correction factor for the curvature effect is given by [22]:

$$f_{Cur.} = \left[\mathrm{Re}_{CX_{Avg.}} \left(\frac{r_{C_n}}{R_{Cur._n}} \right)^2 \right]^{\pm 1/20} \tag{44}$$

where r_{C_n} is the hydraulic radius of cooling channel, $R_{Cur._n}$ is the radius of curvature, the sign (+) denotes the concave curvature and the sign (-) denotes the convex one. The radius of curvature (RCURVE) must be input through RTE's NAMELIST for every station. If no RCURVE value is specified in the input then a large value is assigned to this parameter, which corresponds to a straight channel ($f_{Cur.} = 0$).

Surface Roughness Effect on Heat Transfer Enhancement

It is well known that the surface roughness increases the pressure drop in the cooling channel as well as convective heat transfer. The effect of surface roughness on the pressure drop is incorporated in the fanning friction factor given by equations (22) and (23). Norris [23] suggested a simple empirical correlation for incorporating the effect of surface roughness on the heat transfer coefficient. This correlation is given by:

$$\frac{Nu}{Nu_{smooth}} = \left(\frac{f}{f_{smooth}} \right)^n \tag{45}$$

where $n = 0.68 Pr^{0.215}$. For $f / f_{smooth} > 4.0$ Norris finds that the Nusselt number no longer increases with increasing roughness. Cooling channel roughness is defined by RGHNS for each station in the NAMELIST of RTE. The fact that roughness can be varied along the cooling channel allows a user to examine selectively roughening of channel in the area where the most cooling is needed.

Heat Transfer Enhancement due to Twisted Tapes Inserts

In some instances twisted tape inserts (swilers) can be used to enhance heat transfer in the cooling channel [24-25]. A typical twisted tape insert consists of a thin strip that is twisted through 360° per axial distance p_t. Twisted tapes can be described by the twist angle a and twist ratio *y*. The helix angle of the tape is related to the twist ratio via $\tan a = p/(2y)$. Thorsen and Landis [25] recognized that buoyancy effects arising from density variation in the centrifugal field should have an effect on heat transfer. They showed that the swirl-flow-induced buoyancy effect should depend on the dimensionless group Gr/Re^2,

$$\frac{Gr}{Re^2} = \frac{2d_{C_n} b_T \left| T_{C_W} - T_{CS} \right| \tan a}{d_i} \tag{46}$$

where d_i is the insert diameter (note that d_i is always smaller than the cooling channel width). Thorsen and Landis measured the heat transfer coefficient for the cooling of water in tubes having tapes with three different helix angles; a = 11.1, 16.9, and 26.5°. The correction factor for the cooling data is given by

$$f_{\text{swiler}} = F\left(1 + 0.25\sqrt{\frac{Gr}{Re}}\right) \tag{47}$$

where

$$F = 1 + 0.004872\frac{\tan^2 a}{d_i\left(1+\tan^2 a\right)}$$

Swiler inserts in cooling channels result in an increase in pressure drop. The correction factor for the swiler pressure drop is given by

$$f_{\text{swiler } f} = \left(\frac{y}{|y-1|}\right)^{1.15} \tag{49}$$

for $Re > 70000$, and

$$f_{\text{swiler } f} = \left(\frac{y}{|y-1|}\right)^{1.15+.15(7000-\text{Re}_{CX})/650000} \tag{50}$$

for $Re < 70000$

Swilers can be used at stations where heat transfer enhancement is needed by setting ISW=1 in the NAMELIST of RTE. If no swiler is used at some stations the ISW must be set to 0. Swiler angles are defined by SANGLE in degrees (e.g., SANGLE=30).

Edge Effects

The sharp corners of rectangular cooling channels result in an increase in the frictional pressure drop. When all four corners are sharp the following correction factor can be used for frictional pressure drop [26]:

$$f_{\text{edge,f}} = 1.00875 - \frac{0.1125}{Ar} \tag{51}$$

where $Ar=h/w$ is the aspect ration of the cooling channel. In some cases the lower corners of cooling channels are rounded and the upper corners are sharp. The correction factor for two sharp edge corners is given by

$$f_{\text{edge,f}} = \frac{0.0875 - 0.1125/Ar}{2} + 1 \tag{52}$$

The NMELIST variable of RTE for the edge effect is IEDGE. Equation (51) is used when IEDGE=2 and equation (52) when IEDGE=1. When IEDGE is 0 or any other number, no edge effect correction will be implemented.

Wall Temperature Distribution

Once the heat transfer coefficients and adiabatic wall temperatures for the hot gas and coolant are evaluated, a finite difference model is used to re-evaluate the wall temperature distribution. This model has been specifically developed for three-dimensional conduction in a rocket thrust chamber and nozzle, as shown in Figure 1. Because of the symmetry of the configuration, computations are performed for only one cell (see Figure 6). Since no heat is transferred to the two sides of the cell, they are assumed insulated. A finite difference grid is superimposed on the aforementioned cell as shown in Figure 7. In this program the number of nodes in the radial direction for different layers and in the circumferential direction for the land and channel area must be specified. Thus, the grid size can vary from one layer to another. Each node is connected to four neighboring nodes at the same station. It also exchanges heat with its counterpoints at two neighboring stations (i.e., stations $n+1$ and $n-1$). The finite difference equation for a node located in the middle of a material is given by:

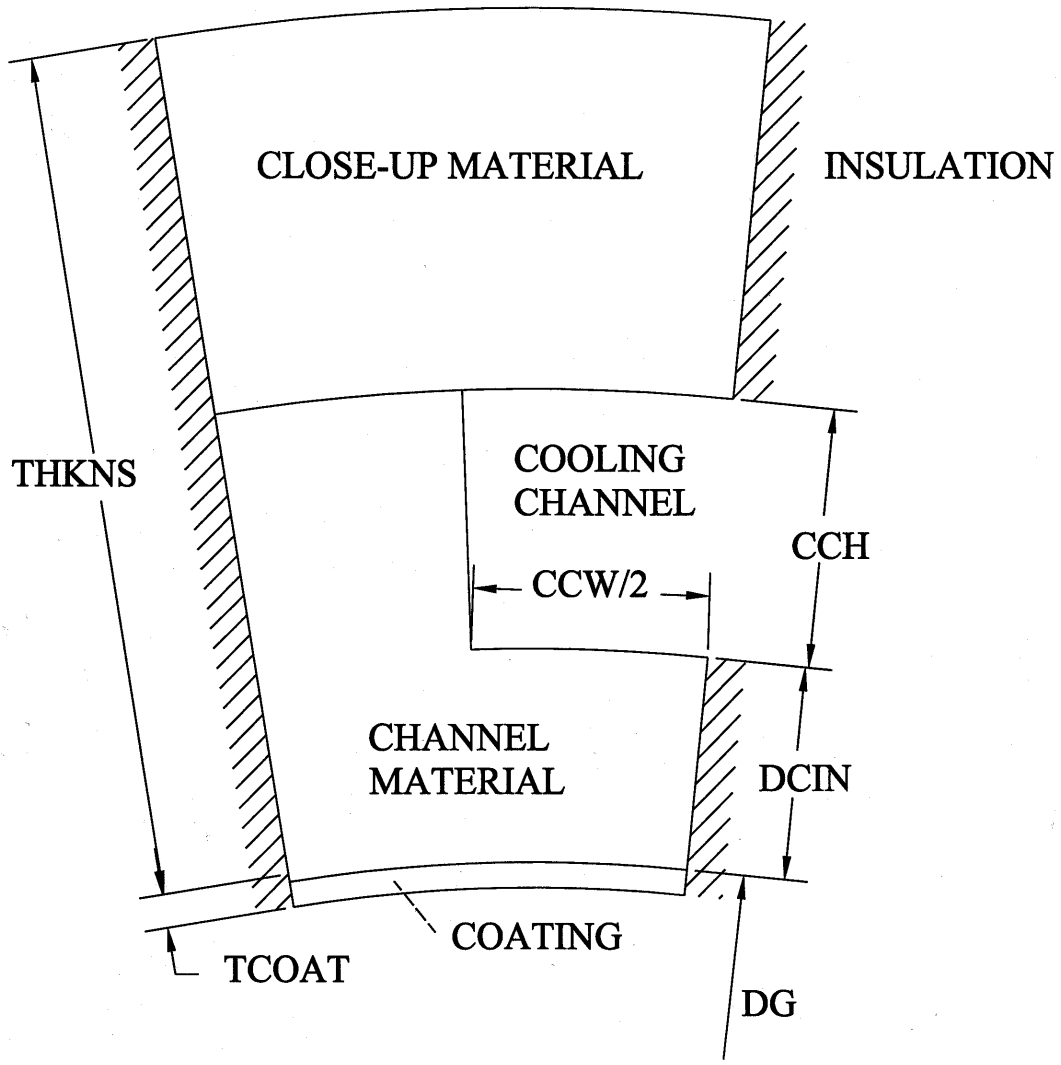

Figure 6: A half cooling channel cell

$$T_{i,j,n}^{l} = \frac{T_{i+1,j,n}^{l-1}/R_1 + T_{i,j-1,n}^{l-1}/R_2 + T_{i-1,j,n}^{l-1}/R_3 + T_{i,j+1,n}^{l-1}/R_4 + T_{i,j,n+1}/R_5 + T_{i,j,n-1}/R_6}{1/R_1 + 1/R_2 + 1/R_3 + 1/R_4 + 1/R_5 + 1/R_6} \quad (53)$$

where R_1, R_2, R_3, R_4, R_5, R_6, are resistances between node i, j, n and its six neighboring nodes. These resistances are given by:

$$R_1 = \frac{r\Delta f}{\Delta r\left(\Delta S_{i,j}^{n-1,n} + \Delta S_{i,j}^{n,n+1}\right)}\left(\frac{1}{k_{i,j,n}^{l-1}} + \frac{1}{k_{i+1,j,n}^{l-1}}\right)$$

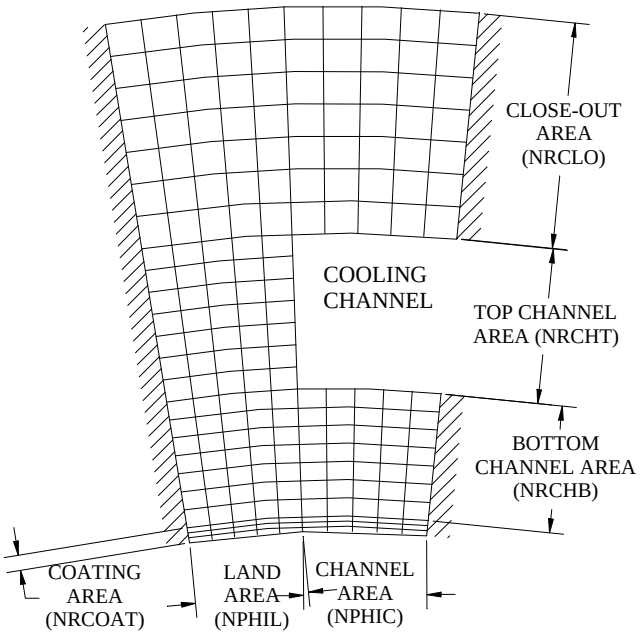

Figure 7: Finite difference grid superimposed on half cooling channel cell

$$R_2 = \frac{\Delta r}{\left(r + \frac{\Delta r}{2}\right)\Delta f\left(\Delta S_{i,j}^{n-1,n} + \Delta S_{i,j}^{n,n+1}\right)}\left(\frac{1}{k_{i,j,n}^{l-1}} + \frac{1}{k_{i,j-1,n}^{l-1}}\right)$$

$$R_3 = \frac{r\Delta f}{\Delta r\left(\Delta S_{i,j}^{n-1,n} + \Delta S_{i,j}^{n,n+1}\right)}\left(\frac{1}{k_{i,j,n}^{l-1}} + \frac{1}{k_{i-1,j,n}^{l-1}}\right)$$

$$R_4 = \frac{\Delta r}{\left(r - \frac{\Delta r}{2}\right)\Delta f\left(\Delta S_{i,j}^{n-1,n} + \Delta S_{i,j}^{n,n+1}\right)}\left(\frac{1}{k_{i,j,n}^{l-1}} + \frac{1}{k_{i,j+1,n}^{l-1}}\right)$$

$$R_5 = \frac{\Delta S_{i,j}^{n,n+1}}{2A_{i,j,n}}\left(\frac{1}{k_{i,j,n}^{l-1}} + \frac{1}{k_{i,j,n+1}}\right)$$

$$R_6 = \frac{\Delta S_{i,j}^{n,n+1}}{2A_{i,j,n-1}}\left(\frac{1}{k_{i,j,n}^{l-1}} + \frac{1}{k_{i,j,n-1}}\right)$$

$$A_{i,j,n} = \frac{(r\Delta f\Delta r)_{n+1} + (r\Delta f\Delta r)_n}{2}$$

and

$$A_{i,j,n} = \frac{(r\Delta f\Delta r)_{n+1} + (r\Delta f\Delta r)_n}{2}$$

and l is the Gauss-Siedel iteration index. Note that the above equation is a three-dimensional finite difference equation. The Gauss-Siedel iteration, however, is only performed for the nodes on the n[th] station and $T_{i,j,n+1}$ and $T_{i,j,n-1}$ are kept constant during this iteration. The value of $T_{i,j,n-1}$ in equation (53) is from the recent march and $T_{i,j,n+1}$ from the previous march. The conductivity in equation (53) is a function of temperature, i.e., $k = k(T)$. Similar equations are derived for other nodes (boundary nodes and nodes at the interface between two different materials) and are being used in the program. It should be noted that at the boundary nodes, depending on the boundary conditions, convective and radiative terms also appear in the nodal balance of energy equation. For example, for a node at the inner surface of the nozzle the finite difference equation is given by

$$T_{i,j,n}^{l} = \frac{T_{i+1,j,n}^{l-1}/R_1 + T_{i,j-1,n}^{l-1}/R_2 + T_{i-1,j,n}^{l-1}/R_3 + T_g/R_4 + T_{i,j,n+1}/R_5 + T_{i,j,n-1}/R_6 + q_r\Delta f(\Delta S_{i,j}^{n-1,n} + \Delta S_{i,j}^{n,n+1})/2}{1/R_1 + 1/R_2 + 1/R_3 + 1/R_4 + 1/R_5 + 1/R_6} \tag{54}$$

where

$$R_1 = \frac{2r\Delta f}{\Delta r\left(\Delta S_{i,j}^{n-1,n} + \Delta S_{i,j}^{n,n+1}\right)}\left(\frac{1}{k_{i,j,n}^{l-1}} + \frac{1}{k_{i+1,j,n}^{l-1}}\right)$$

$$R_2 = \frac{\Delta r}{\left(r + \frac{\Delta r}{2}\right)\Delta f\left(\Delta S_{i,j}^{n-1,n} + \Delta S_{i,j}^{n,n+1}\right)}\left(\frac{1}{k_{i,j,n}^{l-1}} + \frac{1}{k_{i,j-1,n}^{l-1}}\right)$$

$$R_3 = \frac{2r\Delta f}{\Delta r\left(\Delta S_{i,j}^{n-1,n} + \Delta S_{i,j}^{n,n+1}\right)}\left(\frac{1}{k_{i,j,n}^{l-1}} + \frac{1}{k_{i-1,j,n}^{l-1}}\right)$$

$$R_4 = \frac{2}{h_g r\Delta f\left(\Delta S_{i,j}^{n-1,n} + \Delta S_{i,j}^{n,n+1}\right)}$$

$$R_5 = \frac{\Delta S_{i,j}^{n,n+1}}{2A_{i,j,n}}\left(\frac{1}{k_{i,j,n}^{l-1}} + \frac{1}{k_{i,j,n+1}}\right)$$

$$R_6 = \frac{\Delta S_{i,j}^{n,n+1}}{2A_{i,j,n-1}}\left(\frac{1}{k_{i,j,n}^{l-1}} + \frac{1}{k_{i,j,n-1}}\right)$$

$$A_{i,j,n} = \frac{\left[\left(r_0 + \frac{\Delta r}{4}\right)\Delta f\,\frac{\Delta r}{2}\right]_{n+1} + \left[\left(r_0 + \frac{\Delta r}{4}\right)\Delta f\,\frac{\Delta r}{2}\right]_n}{2}$$

$$A_{i,j,n-1} = \frac{\left[\left(r_0 + \frac{\Delta r}{4}\right)\Delta f\,\frac{\Delta r}{2}\right]_n + \left[\left(r_0 + \frac{\Delta r}{4}\right)\Delta f\,\frac{\Delta r}{2}\right]_{n-1}}{2}$$

Note that equation (54) is used when hot-gas-side heat transfer coefficient is known and wall heat flux is evaluated based on the temperature difference, i.e., equation (11). When wall heat flux (q_n) is known, equation (54) becomes

$$\begin{aligned} T_{i,j,n}^{l} = {} & [T_{i+1,j,n}^{l-1}/R_1 + T_{i,j-1,n}^{l-1}/R_2 + T_{i-1,j,n}^{l-1}/R_3 + T_{i,j,n+1}/R_5 + T_{i,j,n-1}/R_6 + \\ & (q_n + q_r)\Delta f(\Delta S_{i,j}^{n-1,n} + \Delta S_{i,j}^{n,n+1})/2]/(1/R_1 + 1/R_2 + 1/R_3 + 1/R_4 + 1/R_5 + 1/R_6) \end{aligned} \tag{55}$$

where q_n is wall heat flux which can be an input of the program or evaluated using equation (12).

Finite difference equations for other nodes, such as cooling channel, interface between two materials, and outer surface nodes, are included in the program. In general, the finite difference equations give the temperature of each node at iteration l in terms of the temperatures of neighboring nodes and/or heat transfer coefficients, conductivities, hot-gas, and coolant temperatures at the previous iteration (iteration $l-1$). To accelerate convergence, the following successive over-relaxation formula is used:

$$T_{i,j}^{l} = T_{i,j}^{l-1} + w(T_{i,j}^{l} - T_{i,j}^{l-1}) \tag{56}$$

The most efficient value of w for the geometry under consideration here is between 1.7 and 1.9 (obtained by a trial and error procedure to minimize the computation time). The successive over-relaxation equation makes the convergence four times faster than when it is eliminated from the calculation for the configuration considered here. It should be noted that the finite difference model presented here is only limited to rectangular cooling channels.

Thermal conductivities in this model are taken as functions of temperatures. Conductivities of twelve commonly used materials in regeneratively cooled rocket are built into RTE. These thermal conductivities can take an input code number of 1 through 12. The material code for coating, channel area and close-up are defined by MTCOAT, MTCH and MTCLO in the namelist of RTE. Figure 8 shows RTE's built-in thermal conductivities as functions of temperature. User-defined materials can be introduced by setting material code –1, -2 or –3 (a user can defined up to three material conductivities). If any of these negative codes are assigned to any layer the corresponding conductivities must be entered as a function of temperature via a separate namelist $CONDDATA. A complete description of the $CONDDATA namelist is presented in the RTE's input file section.

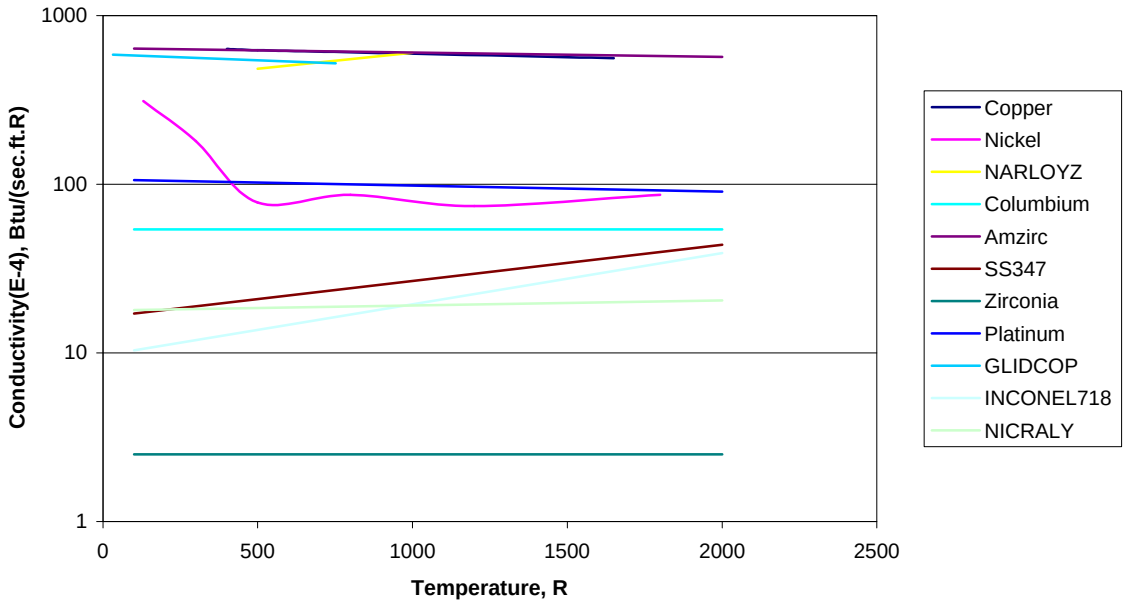

Figure 8: Built-in conductivities in RTE

Radiation Heat Transfer Model

The radiative heat flux, q_r, in the nozzle surface energy balance equations consists of radiative heat transfer from hot-gases and the surface of the nozzle. To evaluate this term the Discrete Exchange Factor (DEF) method [27-31] and is used. The radiation model of RTE is based on the configuration of a typical nozzle shown in Figure 8. In this method radiative exchange between surfaces and/or volumes are expressed by four exchange

factors, between two surface elements ($\overline{dss}(\mathbf{r}_i,\mathbf{r}_j)$), between a surface and gas elements ($\overline{dsg}(\mathbf{r}_i,\mathbf{r}_j)$), between gas and surface elements ($\overline{dgs}(\mathbf{r}_i,\mathbf{r}_j)$) and between two gas elements ($\overline{dgg}(\mathbf{r}_i,\mathbf{r}_j)$). The equations for these four mechanism of radiative transport is given by (see Figure 8 for nomenclature):

$$\overline{dss}(\mathbf{r}_i,\mathbf{r}_j)=\frac{2r_j ds_j}{p}\int_{y_{\min}}^{y_{\max}}\frac{\cos b_i \cos b_j t(\mathbf{r}_i-\mathbf{r}_j)}{\left|\mathbf{r}_i-\mathbf{r}_j\right|^2}dy_j \tag{57}$$

$$\overline{dsg}(\mathbf{r}_i,\mathbf{r}_j)=\frac{2K_{t_j} r_j dr_j dx_j}{p}\int_{y_{\min}}^{y_{\max}}\frac{\cos b_i t(\mathbf{r}_i-\mathbf{r}_j)}{\left|\mathbf{r}_i-\mathbf{r}_j\right|^2}dy_j \tag{58}$$

$$\overline{dgs}(\mathbf{r}_i,\mathbf{r}_j)=\frac{r_j ds_j}{2p}\int_{y_{\min}}^{y_{\max}}\frac{\cos b_j t(\mathbf{r}_i-\mathbf{r}_j)}{\left|\mathbf{r}_i-\mathbf{r}_j\right|^2}dy_j \tag{59}$$

$$\overline{dgg}(\mathbf{r}_i,\mathbf{r}_j)=\frac{K_{t_j} r_j dr_j dx_j}{2p}\int_{y_{\min}}^{y_{\max}}\frac{t(\mathbf{r}_i-\mathbf{r}_j)}{\left|\mathbf{r}_i-\mathbf{r}_j\right|^2}dy_j \tag{60}$$

where symmetry with respect to the azimuth angle y has been incorporated; $\mathbf{r}_i$ denotes the location at which radiation is emitted; $\mathbf{r}_j$ the position at which radiation is received; b is the angle between the surface normal and the vector connecting $\mathbf{r}_i$ and $\mathbf{r}_j$; K_{t_j} is the extinction coefficient at node *j*; t is the transmittance, which can be defined as

$$t(\mathbf{r}_i-\mathbf{r}_j)=e^{-\int_{\mathbf{r}_i}^{\mathbf{r}_j}K_t(\mathbf{r})d\mathbf{r}} \tag{61}$$

The hot-gases in the thrust chamber and nozzle form a non-homogenous medium; hence the extinction coefficient changes with position (composition and pressure of hot-gases change with axial position). If the extinction coefficient, K_t is assumed constant then the transmittance becomes

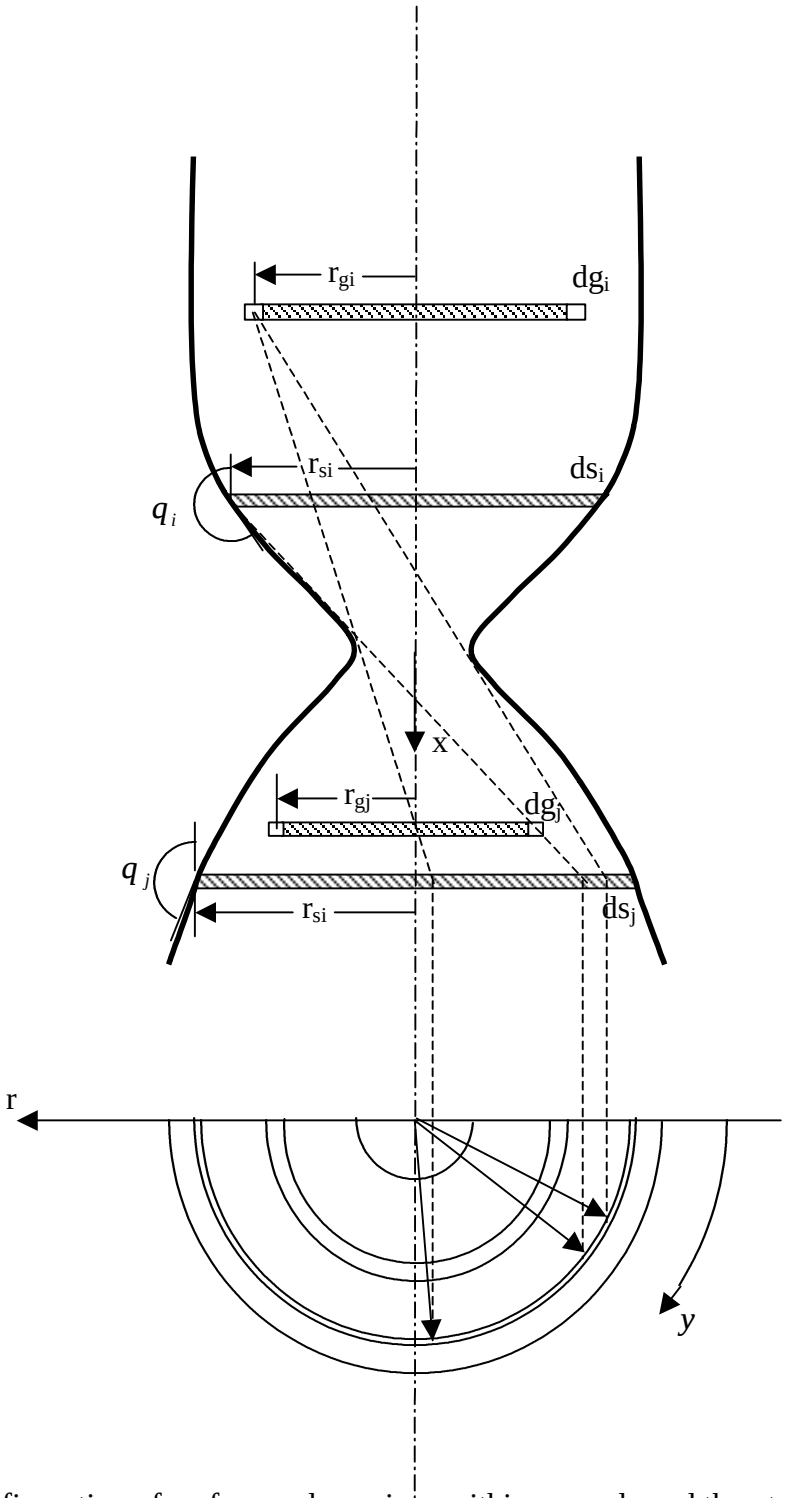

Figure 8: Configuration of surface and gas rings within a nozzle and thrust chamber with throat blockage (shadowing)

$$t(\mathbf{r}_i - \mathbf{r}_j) = e^{-K_t|\mathbf{r}_i - \mathbf{r}_j|} \tag{62}$$

The limits of integration in equations (57-60) are $y_{\min}$ and $y_{\max}$ and these are the minimum and maximum azimuth angles which ring element *j* is seen from a point on ring element *i*.

The allowable range of y is dictated by the orientation and relative position of the ring position of the ring element pair and blockage effects by the throat. Details concerning the determination of the limiting azimuth angles are subsequently presented. Geometric consideration of any ring element pair depicted in Figure 8 reveals

$$\left|\mathbf{r}_i - \mathbf{r}_j\right|^2 = r_i^2 + r_j^2 - 2r_i r_j \cos y + (x_j - x_i)^2 \tag{63}$$

and for surface ring elements,

$$\left|\mathbf{r}_i - \mathbf{r}_j\right| \cos b_i = -(r_i - r_j \cos y)\cos q_i - (x_j - x_i)\sin q_i \tag{64}$$

$$\left|\mathbf{r}_i - \mathbf{r}_j\right| \cos b_j = (r_i \cos y - r_j)\cos q_j + (x_j - x_i)\sin q_j \tag{65}$$

Where q_k is the angle, resting in the *r*-*x* plane, measured from the *z*-axis, in the direction of increasing radius, onto the backside of element *k*. All surface elements satisfy $p/2 \le q \le 3p/2$. Combining equations (57)-(65) gives the resulting exchange factor expressions:

$$\overline{dss}(\mathbf{r}_i, \mathbf{r}_j) = \frac{2r_i r_i^2 \cos q_i \cos q_j ds_j}{p} \int_{y_{\min}}^{y_{\max}} \frac{(f_i - \cos j)(f_j - \cos y)t(\mathbf{r}_i - \mathbf{r}_j)}{\left|\mathbf{r}_i - \mathbf{r}_j\right|^4} dy_j \tag{66}$$

$$\overline{dsg}(\mathbf{r}_i, \mathbf{r}_j) = \frac{-2K_{t_j} r_i^2 \cos q_i \cos q_j dr_j dx_j}{p} \int_{y_{\min}}^{y_{\max}} \frac{(f_i - \cos j)t(\mathbf{r}_i - \mathbf{r}_j)}{\left|\mathbf{r}_i - \mathbf{r}_j\right|^3} dy_j \tag{67}$$

$$\overline{dgs}(\mathbf{r}_i, \mathbf{r}_j) = \frac{-r_i r_j \cos q_j ds_j}{2p} \int_{y_{\min}}^{y_{\max}} \frac{(f_i - \cos j)t(\mathbf{r}_i - \mathbf{r}_j)}{\left|\mathbf{r}_i - \mathbf{r}_j\right|^3} dy_j \tag{68}$$

(69)

$$\overline{dgg}(\mathbf{r}_i,\mathbf{r}_j)=\frac{K_{t_j}r_j dr_j dx_j}{2p}\int_{y_{\min}}^{y_{\max}}\frac{t(\mathbf{r}_i-\mathbf{r}_j)}{\left|\mathbf{r}_i-\mathbf{r}_j\right|^2}dy_j$$

where

$$f_i=\frac{r_i}{r_j}+\frac{z_j-z_i}{r_j}\tan\theta_i \qquad \text{and} \qquad f_j=\frac{r_j}{r_i}+\frac{z_i-z_j}{r_i}\tan\theta_j \tag{70}$$

The limiting angles $\psi_{\min}$ and $\psi_{\max}$ remain to be determined. The limiting azimuth angles for surface-to-surface exchange are governed by the configuration and/or blocking surfaces.

It is possible that, in many instances, the view between ring element pairs is partially obstructed by the throat. The blockage angle, $\cos^{-1}\Gamma$, is evaluated by projecting a line from a point on an emitting ring element (denoted by subscript i) around the periphery of the blocking body at an axial position x_k, such that x_k is between x_i and x_j. The intersection point between the receiving ring element (denoted by subscript j) and the shadowing produced by the blocking body at x_k results in a minimum azimuth angle. This procedure is repeated for several values of x_k and can mathematically stated as:

$$\Gamma=\min\left(\frac{[D_G(x_k)/2]^2(x_j-x_i)^2-r_i^2(x_j-x_k)^2-r_j^2(x_k-x_i)^2}{2r_i r_j(z_k-z_i)(z_j-z_k)}\right)_{x_k\in(x_i,x_j)} \tag{71}$$

The minimum and maximum azimuth angles can then be calculated from the following equations:

$$\psi_{\min}=\cos^{-1}[\min(f_i,f_j,\Gamma,1)] \qquad \text{and} \qquad \psi_{\max}=p \tag{72}$$

The direct exchange factors calculated based on the above formulation account for direct exchange of radiation between surface and gas elements. To account for multiple reflections and scattering of radiation total exchange factors are introduced. The total exchange factor between two elements is defined as the fraction of the radiative energy that is emitted from one element and is absorbed by the other element via direct radiation and multiple reflections and scatterings from surfaces and gas, and are calculated using the following equations:

$$\begin{aligned}\overline{\mathbf{DSS}}=&\left[\mathbf{I}-\left\{\overline{\mathbf{dss}}+\overline{\mathbf{dsg}}w_0\mathbf{W_g}\left[\mathbf{I}-\overline{\mathbf{dgg}}w_0\mathbf{W_g}\right]^{-1}\overline{\mathbf{dgs}}\right\}\tilde{\mathbf{n}}\mathbf{W_s}\right]^{-1}\\&\cdot\left\{\overline{\mathbf{dss}}+\overline{\mathbf{dsg}}w_0\mathbf{W_g}\left[\mathbf{I}-\overline{\mathbf{dss}}w_0\mathbf{W_g}\right]^{-1}\overline{\mathbf{dgs}}\right\}\tilde{\mathbf{a}}\end{aligned} \tag{73}$$

$$\overline{\mathbf{DVS}} = \left[\mathbf{I} - \overline{\mathbf{dgg}} w_0 \mathbf{W_g}\right]^{-1} \overline{\mathbf{dgs}} \cdot \left[\mathbf{I} - \tilde{\mathbf{n}}\mathbf{W_s}\left\{\overline{\mathbf{dss}} + \overline{\mathbf{dsg}} w_0 \mathbf{W_g}\left[\mathbf{I} - \overline{\mathbf{dgg}} w_0 \mathbf{W_g}\right]^{-1} \overline{\mathbf{dgs}}\right\}\right]^{-1} \acute{\mathbf{a}} \quad (74)$$

where $\overline{\mathbf{DSS}} = \left[\overline{DS_i S_j}\right]$, $\overline{\mathbf{DVS}} = \left[\overline{DV_i S_j}\right]$ are matrices of total exchange factors from surface and gas axisymmetric rings to surface elements; $\overline{\mathbf{dss}} = \left[\overline{ds_i s_j}\right]$, $\overline{\mathbf{dsg}} = \left[\overline{ds_i g_j}\right]$, $\overline{\mathbf{dgs}} = \left[\overline{dg_i s_j}\right]$, $\overline{\mathbf{dgg}} = \left[\overline{dg_i g_j}\right]$ are matrices of direct exchange factors between differential surface/volume ring elements; $\mathbf{W_s} = \left[w_{s,i} d_{i,j}\right]$ and $\mathbf{W_g} = \left[w_{g,i} d_{i,j}\right]$ are diagonal matrices of numerical integration weight factors for surface/volume ring elements, respectively; and $= \left[r d_{i,j}\right]$ and $= \left[a d_{i,j}\right]$ are diagonal matrices of reflectivities and absoptivities for surface ring elements.

Once the total exchange factors are evaluated using equation (73) and (74) then the radiative heat flux at the n-th station is computed using the following energy balance equation:

$$q_{r,n} = \sum_{j=1}^{2n_r+m} w_{s,j} \overline{DS_j S_n} E_{s,j} + \sum_{j=1}^{m \cdot n_r} w_{g,j} \overline{DG_j S_n} E_{g,j} - E_{s,n} \quad (75)$$

E_{s_n} and E_{g_n} are surface and gas emissive powers at station n and are related to their temperatures via

$$E_{s_n} = e s T_{s_n}^4$$

$$E_{g_j} = 4K_{t_l}(1-w_0) s T_{g_j}^4$$

Note that the first term in the right-hand-side of equation (75) is the radiative flux at the surface due to emission from other surface elements, the second term is due to the radiative flux from gas elements and the last term is the radiative heat loss due to emission.

The present model is benchmarked against a number of exact solutions and solutions that are available for a number of cylindrical problems. The results reported in [30-31] show excellent agreement between the results of this model and those published.

The radiation module of RTE consists of a separate program (RTE_RAD) that only evaluated total exchange factors based on the Discrete Exchange Factor (DEF) method. In this module the nozzle is subdivided into a number of volume and surface nodes as shown in Figure 9. The number of radial nodes is NCLMN, which is set to 5. The number of axial nodes is the same as the number of stations. The position of axial nodes coincides with that of stations. Since the exchange factors are dependant of gas and surface radiative properties and the geometry of the nozzle they are calculated by running

RTE_RAD and the printed into two files (TSS.DAT and TGS.DAT). Then RTE reads the exchange factors and use them in equation (75) to evaluate radiative flux for surface nodal points. The radiative fluxes, as shown in equation (75) are functions of surface temperatures. These fluxes are evaluated by an iterative procedure.

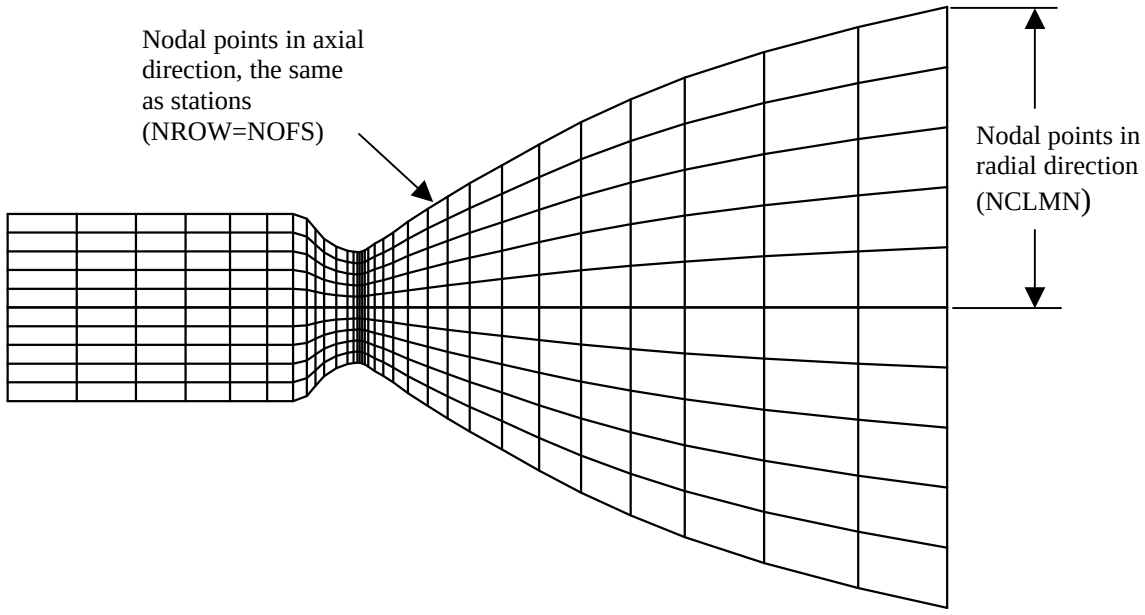

Figure 9: Position of surface nodes and gas nodes for the radiation model

The combustion properties code given by Gordon and McBride [1] does not provide the radiative properties of combustion gases. These properties may be obtained from Ludwig et al. [32] and Siegel and Howell [33]. For example, if the fuel is RP-1, the combustion gas species mole fractions are obtained from the combustion code [1], containing 17% CO_2, 30% CO, 33%H_2O, 6% OH, 2.5% O_2, 3% H, 7% H_2 and 1.5% O. Using an integrated average value of the absorption coefficients of these species, the overall absorption coefficient is found to be $K_a = 2.5\,\text{in}^{-1}$

Iteration and Marching Procedures and Stagnation Coolant Properties

Based on the revised wall temperature, new hot-gas and coolant wall properties, heat transfer coefficients and adiabatic wall temperatures are calculated using equations (3) through (49). Again, a new wall temperature distribution based on the most recent heat transfer coefficients and adiabatic wall temperatures is calculated using the finite difference subroutine for heat conduction within the wall. This procedure is repeated until the relative difference between the temperature distributions of two consecutive iterations becomes negligibly small. After the results for station n converge, the coolant Mach number and entropy as functions of static pressure and enthalpy ($M_{C_n}, s_{C_n} = f(P_{CS_n}, i_{CS_n})$) are evaluated using the GASP or WASP programs.

Next, the coolant stagnation pressure is evaluated based on the coolant entropy and stagnation enthalpy, i.e., $P_{C0_n} = P(i_{C0_n}, s_{C_n})$. The GASP and WASP programs do not have explicit expressions for pressure in terms of entropy and enthalpy. Thus, an implicit relation for stagnation pressure (i.e., $s_{C_n} = s(P_{C0_n}, i_{C_n})$) with the secant method for solving nonlinear equations is used to determine P_{C0_n}. In the secant method, two initial guesses for the stagnation pressures were made ($P_1 = P_{C0_{n-1}} + 20$ and $P_2 = P_{C0_{n-1}} - 20$) and the corresponding entropies s_1 and s_2 were determined. The secant method's iterative equation is given by:

$$P_{k+1} = P_k - s_k \frac{P_{k-1} - P_k}{s_{k-1} - s_k} \tag{76}$$

where k is the iteration index. When equation (76) converges (the difference between two consecutive pressures become negligibly small), the coolant stagnation is set equal to the latest value of P_k. The stagnation pressure obtained based on this procedure would automatically satisfy the relation between coolant stagnation and static pressures, i.e.,

$$P_{C0} = P_{CS} + \frac{rV^2}{2} \tag{77}$$

When the coolant is RP1, GASP is not used to determine the coolant properties the above equation is used to determine the coolant stagnation pressure. Finally, the coolant stagnation temperature is determined based on the coolant stagnation pressure and enthalpy ($T_{C0_n} = T(P_{C0_n}, i_{C0_n})$).

The program then marches axially and performs similar calculations (i.e., equations (3) through (43)) for all stations. Once the results of the last station (station m) converged, the results of this march are compared to those of the previous march. If the relative differences between the results of two consecutive marches are less than the axial convergence criterion the program stops, otherwise it continues its axial marches until convergence is achieved. Setting the axial convergence criterion greater than one or setting the maximum number of passes equal to one can eliminate the effect of axial conduction.

The method described here, i.e., axial marches along axial direction, has several advantages over the direct solution of a three-dimensional finite difference formulation. First, it converges very quickly. Second, it requires less memory. Third, it allows the user to control the importance of axial conduction by allowing for different convergence criterion between the axial and radial and circumferential directions. For example, in analysis of a thin-walled, radiatively-cooled, low-pressure engine, axial conduction is negligible. In this case one might set the convergence accuracy to 5% in the axial direction and 0.1% in the other directions. In the case of a thick-walled, regeneratively-

cooled, high-pressure engine, axial conduction may be significant. Thus, the accuracy in the axial direction may be set to 0.1% and 0.1% in the other directions.

DESCRIPTION OF THE COMPUTER CODE RTE

Rocket Thermal Evaluation (RTE) and its radiation module are written in standard FORTRAN. The numerical model of RTE is based on the numerical method discussed in the previous section. The program provides the temperature distribution in the rocket thrust chamber and nozzle. It also calculates the rate of heat transfer to the cooling channel, coolant temperature and pressure drop. This program can be used for all types of propellants and coolants that are used in regeneratively cooled rockets. The conductivities of several rocket engine materials are included in tabular form as functions of temperatures. These include: Copper, Nickel, Soot (Carbon), NASA-Z (NARloy-Z), Columbium, Zirconia, SS-347, Amzirc, Platinum, Glidcop, Inconel718 and Nicraly. The user can specify conductivities of up to three materials in the input of the RTE . Three options are available for the boundary condition at the outside surface: radiative, natural convective, and forced convective boundary conditions. For the radiative and convective boundary conditions, the outer surface emissivity and convective heat transfer coefficients, respectively, must be specified. The boundary conditions at the inner surface are combined convection and radiation heat transfer from hot gases and other surfaces. The convective heat flux for the hot-gas-side can be specified in the input file. This feature allows the user to interface RTE to the other codes for the hot-gas-side properties and boundary layer analysis. The procedure for linking RTE to a hot-gas-side program will be explained later.

RTE uses three major subprogram modules, hot-gas-side properties (BONNIE, which is a modified CET [1]), coolant properties (GASP, WASP and RP1) and conduction subprogram (COND). Subroutine BONNIE (CET) is for evaluation of thermodynamic and transport properties of combustion gases. A complete description of this subprogram is given in [1] and [2]. Subroutine BONNIE is only capable of predicting hot-gas properties at equilibrium conditions. The combustion in the thrust chamber, however, is a gradual process and might not reach the equilibrium condition within the thrust chamber. As a result of this, the model over-predicts temperatures close to the injector, and a large discrepancy between the computational and experimental temperatures is observed in this part of the engine. To overcome this problem, provisions have been made such that one can input the percentage of fuel burned at each station. Using this option, a low mixture ratio is assigned to the stations close to the injector and is gradually increased to its actual value at stations closer to the throat. The value of mixture ratio at each station depends on the injector and chamber geometries, manifold conditions and many other parameters. To predict the mixture ratio at each station, the user may use ROCCID (ROcket Combustor Interactive Design and Analysis Computer Program) [5]. ROCCID uses state-of-the-art codes and procedures for the analysis of a liquid rocket engine combustor's steady state combustion performance and combustion stability. Modifications have been made on

ROCCID such that it takes the RTE inputs with constant mixture ratios and produces an input file with variable mixture ratios. Details of these modifications will be described later.

The variable IBCASE controls the output of the BONNIE subroutine. When IBCASE=1, the subroutine ROCKET from BONNIE is used to evaluate static temperature and enthalpies of hot gas for all stations. When IBCASE=2 and 3, the thermodynamic and transport properties are calculated based on the specified (P,T) and (P,I), respectively.

The subroutine BONNIE requires three sets of data. The first set of data for the BONNIE subroutine is REACTANT cards that give the chemical composition of the fuel and oxidant. A complete description of REACTANT cards is given in [1]. The next set is THERMO data that gives the thermodynamic properties for different combustion species. These data are valid as long as the gas temperature is between 300 K and 5000 K. The last set of data for BONNIE is TRANS data, which gives the transport properties, namely the viscosities and conductivities of different species. Similar to THERMO data, TRANS data are valid when the gas temperature is between 300 K and 5000 K. When the gas temperature is outside this range, a low or high temperature THERMO and TRANS data should be used. The ASCII files of THERMO and TRANS data are required for the first run of RTE. At the first run BONNIE generates binary files of THERMO and TRANS data files which are used for future runs.

Subroutines GASP and WASP [3-4] are used for evaluation of the thermodynamic and transport properties of the coolant. The GASP subprogram accommodates all commonly used coolants in rockets. Sometimes, water is used as the coolant for colorimeter experiments. In this case, the WASP program is used to calculate the thermodynamic and transport properties of the coolant.

Subroutine COND is used to evaluate the nodal temperature distribution. Based on the specified coolant and hot gas heat transfer coefficient and adiabatic wall temperatures or hot-gas-side wall heat flux. This subroutine calculates the nodal temperatures, heat transfer to the coolant, and heat transfer from the hot gas. Three options are available for the outer surface boundary condition. These options are radiation, free convection and forced convection boundary conditions. This subroutine can take three layers of materials as shown in the rocket wall configuration, Figure 3. The thermal conductivities of each layer can be functions of temperature, and a successive over-relaxation formula is implemented for quick convergence. Note that this subroutine has two versions: CONDWCC (COND With Cooling Channel) and CONDNOCC (COND No Cooling Channel). Subroutine CONDWCC is used when the engine is regeneratively cooled and subroutine CONDNOCC when the engine is radiatively cooled.

Based on the flowchart given in Appendix A, at a given station, the program recalculates nodal temperatures, coolant pressure, thermodynamic and transport properties of the hot gases and coolant for each iteration. The iteration continues until the relative difference of nodal temperatures between two consecutive iterations become negligibly small (less than e). The convergence criteria e in this program must be specified in the data file.

Two convergence criteria can be specified in the input data; ERROR is the convergence criterion for iterations at a given station (i.e., radial and circumferential directions), and ERRAX is the convergence criterion for axial marches. A suggested value for ERROR is 10^{-3} and if the axial conduction is not significant (thin wall low pressure engine) then the axial conduction is negligible and ERRAX should be set to any number greater than 1. When ERRAX < 1, the program makes axial marches (iterations) and it includes the axial heat conduction in the analysis. A reasonable value for ERRAX is 10^{-2}. Very small values of ERRAX cause excessive numbers of axial marches, and in some cases, the coolant properties calculated via GASP or WASP subroutines fluctuate about the correct answer without reaching convergence. Smaller values of convergence criteria will substantially increase computational time without significantly improving the accuracy of the results. To avoid excessive number of iterations, the user can specify limits for the number of iterations. These limits are: MAXITER for maximum number of iterations at each station, and MAXPASS for maximum number of axial passes (axial marches).

Listings of the original subroutines BONNIE and GASP are given in references [1] and [2]. Major modifications were made to the aforementioned subroutines to conjugate them with the conduction/convection and radiation modules of RTE.

For certain types of fuels (e.g., hydrocarbon fuels), radiation from hot gas is significant and the user may include this mode of heat transfer in the thermal analysis by setting IGASRAD=1 in the input file. The major part of radiation calculation is the evaluation of total exchange factors. Values of these exchange factors are functions of the engine geometry and hot gas radiative properties. In order to conserve computational time, these exchange factors can be evaluated once for a given engine and inputted to the RTE. A separate FORTRAN program based on the DEF method [27-31], namely, RTE_RAD (radiation module of RTE) has been developed.

INPUT FILES OF RTE

The main input data file for RTE is called RTE.INP, which consists of two parts, the RTEDATA namelist and reactants information. For user defined thermal conductivity an additional namelist (CONDDATA) is needed. Two exchange factor files, which contain radiative exchange factors for surface to surface (TSS.DAT) and gas to surface (TGS.DAT) are also needed if the radiative heat transfer option is selected. To illustrate the input procedure, a sample input for the Space Shuttle Main Engine (SSME) is presented in Appendix B.

The three sets of input data in RTE.INP file are as follows:

RTEDATA is the main input data file of RTE. RTEDATA has a NAMELIST format and it includes: coolant name (COOLANT); case code for the run (CASECODE)[1]; coolant and total propellant weight flow rate (WC & WGAS); percentage of fuel in the mixture at all stations (RMIX); chamber pressure (PGO); coolant stagnation pressure and

[1] This code can be a character input to recognize the output of RTE. This code will be printed on every output of RTE

temperature at the entrance to the cooling channel (PCO, TCO); number of stations (NOFS); type of correlation to be used for coolant heat transfer coefficient (ITYPE)[2]; exponent of Reynolds number (REEXP)[3]; exponent of Prandtl number (PREXP)[3]; exponent of density ratio (DENEXP)[3] ; exponent of viscosity ratio (VISCEXP)[3]; exponent of conductivity ratio (CONDEXP)[3]; exponent of specific heat ratio (SHEXP)[3]; pressure ratio exponent (PRESEXP)[3]; critical pressure (PCRIT)[3];number of blocked channels (NBLOCK)[4]; entrance effect correction factor (IENT)[5]; gas radiation flag (IGASRAD)[6]; initial guess of temperature for the first pass (TSTART); convergence criterion for conduction in radial and circumferential directions (ERROR); maximum number of iterations at each station (MAXITER); convergence criterion for conduction in axial direction (ERRAX); maximum number of axial passes (MAXPASS); axial location of stations (X); heat transfer coefficient correlation factor for hot-gas and coolant sides (CG & CC); gas-side chamber and nozzle diameters (DG); cooling channel width and height (CCW & CCH); distance between the cooling channel bottom and inner surface of the nozzle (DCIN); wall and coating thickness (THKNS & TCOAT); number of cooling channels (NCC); number of nodes in circumferential (NPHIL for land and NPHIC for channel) and radial (NRCLO, NRCHT, NRCHB and NRCOAT for close-out, channel top, channel bottom, and coating, respectively) directions; types of materials used in different wall layers (MTCLO, MTCH and MTCOAT for close out, channel and coating, respectively)[7]; the boundary condition at the outer surface (IHOUT)[8]; heat transfer coefficient at the outer surface in the case of forced convection (HO1); outer surface emissivity (EM); type of cooling system (ICOOL)[9]; outside temperature in the case of convection at the outer surface (TO); radius of curvature for cooling channel (RCURVE); gas scattering albedo (OMEGA); gas extinction coefficient (KTG); emissivity of inner surface (EPSILON); swiler angle (SANGLE); flag for swiler or no swiler at a station (ISW)[10]; edge effect for cooling channel (IEDGE)[11] cooling channel surface roughness (RGHNS); flag for units (IUNIT)[12]; flags for detailed outputs of the main program (IFLAGM)[13], subroutines GASP and BONNIE (IFLAGG)[10] and subroutine COND (IFLAGC)[10]; flag for using enthalpy difference or temperature difference in calculating hot-gas-side heat flux (ENTHALPY)[14]; flag for known or unknown wall heat flux

[2] Equal to1, 2, 3, 4 or 5 for equations (34), (35), (36), (37) or (38), respectively. Equal to 0 for user defined correlation, equation (39).
[3] Needed for user-defined coolant correlation.
[4] Equal to 0 for no blocked channel and 1 for one blocked channel
[5] Equal to 1, 2, 3 or 4 for equations (35), (36), (37) and (38), respectively
[6] Equal to 1 for gas radiation and 2 for no gas radiation
[7] Equal to 1 for copper; 2 for nickel; 3 for soot; 4 for NARloy-Z; 5 for columbium; 6 for zirconia; 7 for SS-347; 8 for amzirc; 9 for Platinum; 10 for Glidcop; 11 for Inconel718; 12 for Nicraly; -1 for user definefd #1; -2 for user defined #2 and -3 for user defined #3.
[8] Equal to 1 for forced convection; 2 for natural convection; and 3 for radiation.
[9] Equal to1 for regeneratively cooled and 2 for radiatively cooled engines.
[10] Equal to 1 for swiler and 0 for no swiler.
[11] Equal to 0 for no edge effect, 1 for two edges and 2 for four edges.
[12] 1 for English, 2 for SI
[13] Equal to 0 for no detailed output and 1 for detailed output
[14] Equal to 0 for temperature difference (equation (11)) and equal to 1 for enthalpy difference (equation (12)).

(IWFLUX)[15]; wall heat flux array along axial direction (QW); hot-gas static temperature (TGS). QW array is required when IWFLUX is set 1, also TGS is required when both IWFLUX and IGASRAD are set 1; station number for which wall temperature isotherm plots are requested (ISOST)[16].

A sample of RTEDATA data and its nomenclature are given in Appendix B.

CONDDATA is needed if MTCH, MTCLO or MTCOAT is set to –1, -2 or –3. CONDDATA defines up to three user defined material conductivities as functions of the temperature profile. For each material up to ten temperature points can be defined. CONDDATA has a NAMLIST format and it includes: number of temperature points for material –1 (NP1); temperature array of material –1 (T1); conductivity array of material -1 corresponding to temperature array T1 (K1); number of temperature points for material –2 (NP2); temperature array of material –2 (T2); conductivity array of material -2 corresponding to temperature array T2 (K2); number of temperature points for material –3 (NP3); temperature array of material –3 (T3); conductivity array of material -3 corresponding to temperature array T3 (K3). All temperatures should be in Rankin and conductivities in Btu/(s.ft.R).

REACTANT describes the chemical composition of the fuel and oxidant (propellant). In the sample of REACTANT data for (RP1, O2), (LH2, LO2) and (CH4,O2) are given in Appendix B. REACTANT data is an input to the BONNIE subroutine and a complete description of its format is given in [1].

In addition to the main data file, which described above, RTE requires thermal and transport properties for combustion gases species. These properties are provided via the following two files:

THERMO.DAT is data for the thermodynamic properties of the hot gas species. A complete list of THERMO data is given in [1]. An ASCII form of THERMO.DAT (named THERMOSA.DAT in RTE files) is required for the first run of the program. Subroutine BONNIE generates a binary form of THERMO.DAT, which is used in the next runs. THERMO.DAT in the file package is in binary form suitable for running the executable RTE on a WINDOWS operating systems. If RTE is being used in other operating systems, before running any case, the REACTANT data should be replaced by the ASCII file of THERMO.DAT (THERMOSA.DAT) and then run RTE. This run will produce the binary form of THERMO.DAT.

TRANS.DAT is data for the transport properties of the hot-gas species and are taken from reference [1]. Similar to the THERMO.DAT data file, the ASCII form of TRANS.DAT data (TRANSSA.DAT) is required for the first run and for the next runs, the transport properties are read from TRANS.DAT which is a binary file.

[15] Equal to 0 for unknown wall heat flux, 1 for known wall heat flux and 2 when a matrix of wall heat flux is provided via file flux.dat
[16] For a maximum of ten stations

Note that the ASCII forms of both THERMO.DAT and TRANS.DAT must be attached to the main data file RTEDATA and REACTANTS for the first run only. For the subsequent runs THERMO.DAT and TRANS.DAT must be removed from the main data file.

FLUX.DAT is needed if WFLUX in RTEDATA is set to 2, RTE expects a matrix of fluxes. Often hot-gas side boundary layer programs can be used to determine the hot-gas-side heat fluxes. The wall heat fluxes are evaluated along the nozzle and chamber by holding the wall temperature in the hot-gas-side constant. This provides a vector of heat fluxes for various positions along the engine. By repeating this for all possible temperatures, a number of vectors of heat fluxes can be formed. Each of these vectors corresponds to constant wall temperatures and their elements give fluxes at different locations along the engine. These vectors form columns of the matrix of fluxes in FLUX.DAT.

The first row in FLUX.DAT contains two integers. The first one is the number of rows (locations at which fluxes are given) and the second one is the number of columns (temperatures at which fluxes are evaluated). The second line of FLUX.DAT gives temperatures for which wall fluxes are specified (starting from the lowest to the highest temperature). From the third line on, each line, gives the x-coordinate (distance from the throat) and the corresponding heat flux for each temperature. A sample of FLUX.DAT for a typical engine is given in Appendix B.

Only RTEDATA and CONDDATA provide data for RTE. The input data given by REACTANT, THERMO and TRANS correspond to the BONNIE subroutine and, TSS.DAT and TGS.DAT are used to evaluate the radiative heat flux at the inner surface. Note that for certain types of combustion gases, such as LH_2/LO_2, the gas radiation is insignificant and there is no need to include radiation within the chamber. Under these conditions, IGASRAD in RTEDATA must be set to 2 and TSS.DAT and TGS.DAT must be excluded from the inputs.

Radiation Module Input Files

When IGASRAD is set to 1 in RTEDATA then the program takes into consideration the hot-gas radiation. Under this condition the exchange factors, as well as, weight factors are required for input to RTE. The exchange and weight factors are read by RTE via two files TSS.DAT (total exchange factors between surface elements) and TGS.DAT (total exchange factors from volume elements to surface elements). RTE's radiation module (RTE_RAD) generates these two files. The inputs of RTE_RAD are: axial position of stations (X); contour diameter at all stations (DG); hot-gas extinction coefficient (KTG) and hot-gas scattering albedo (OMEGA). RTE_RAD's data is a part of RTEDATA, hence to make user's job easy RTEDATA can also be used as the radiation module input data (i.e., NAMELIST of RTE_RAD is the same as RTEDATA).

Generating RTE's Data Using its Preprocessor

RTE can be run in two ways: via its Graphic User Interface (GUI) preprocessor, or by typing its executable file name. The GUI of RTE is based on Excel, which consists of a single data sheet with text boxes, combo boxes and help in producing input data (see Figures 10 -12 for parts of RTE's GUI). A user can enter engine specifications and dimensions in appropriate boxes and then by clicking on "Generate RTE Input" generate the ASCII file of RTE' data file.

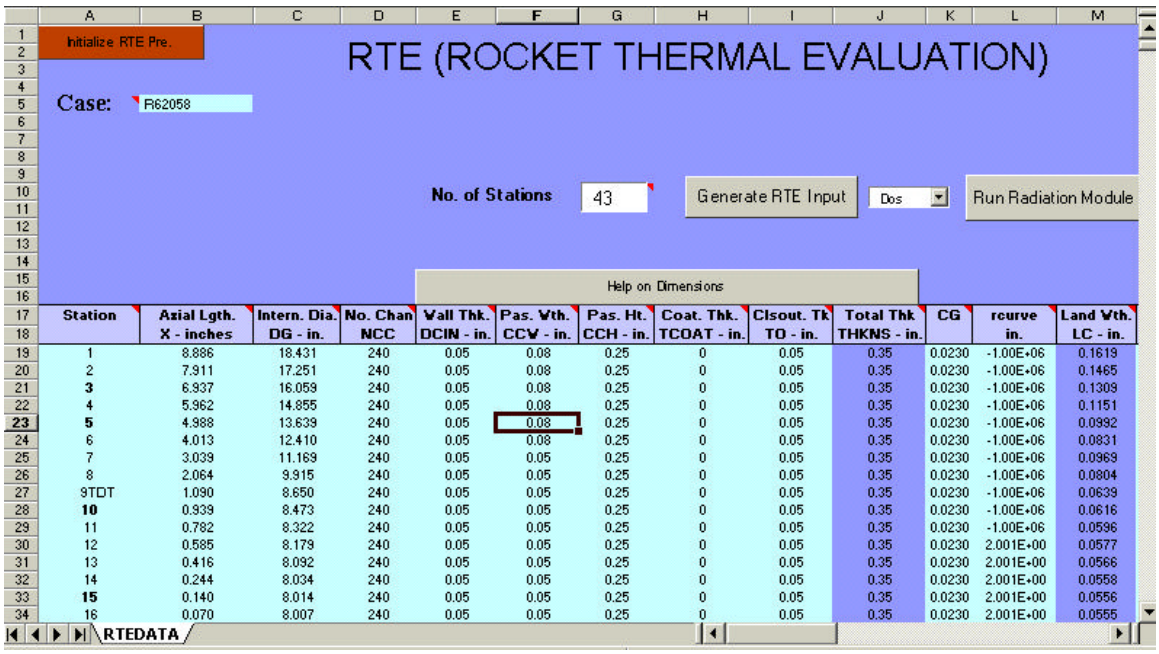

Station	Axial Lgth. X - inches	Intern. Dia. DG - in.	No. Chan NCC	Wall Thk. DCIN - in.	Pas. Wth. CCW - in.	Pas. Ht. CCH - in.	Coat. Thk. TCOAT - in.	Clsout. Tk TO - in.	Total Thk THKNS - in.	CG	rcurve in.	Land Wth. LC - in.
1	8.886	18.431	240	0.05	0.08	0.25	0	0.05	0.35	0.0230	-1.00E+06	0.1619
2	7.911	17.251	240	0.05	0.08	0.25	0	0.05	0.35	0.0230	-1.00E+06	0.1465
3	6.937	16.059	240	0.05	0.08	0.25	0	0.05	0.35	0.0230	-1.00E+06	0.1309
4	5.962	14.855	240	0.05	0.08	0.25	0	0.05	0.35	0.0230	-1.00E+06	0.1151
5	4.988	13.639	240	0.05	0.08	0.25	0	0.05	0.35	0.0230	-1.00E+06	0.0992
6	4.013	12.410	240	0.05	0.08	0.25	0	0.05	0.35	0.0230	-1.00E+06	0.0831
7	3.039	11.169	240	0.05	0.05	0.25	0	0.05	0.35	0.0230	-1.00E+06	0.0969
8	2.064	9.915	240	0.05	0.05	0.25	0	0.05	0.35	0.0230	-1.00E+06	0.0804
9TDT	1.090	8.650	240	0.05	0.05	0.25	0	0.05	0.35	0.0230	-1.00E+06	0.0639
10	0.939	8.473	240	0.05	0.05	0.25	0	0.05	0.35	0.0230	-1.00E+06	0.0616
11	0.782	8.322	240	0.05	0.05	0.25	0	0.05	0.35	0.0230	-1.00E+06	0.0596
12	0.585	8.179	240	0.05	0.05	0.25	0	0.05	0.35	0.0230	2.001E+00	0.0577
13	0.416	8.092	240	0.05	0.05	0.25	0	0.05	0.35	0.0230	2.001E+00	0.0566
14	0.244	8.034	240	0.05	0.05	0.25	0	0.05	0.35	0.0230	2.001E+00	0.0558
15	0.140	8.014	240	0.05	0.05	0.25	0	0.05	0.35	0.0230	2.001E+00	0.0556
16	0.070	8.007	240	0.05	0.05	0.25	0	0.05	0.35	0.0230	2.001E+00	0.0555

Figure 10: A portion of RTE's GUI

RTE's graphic user interface contains help buttons and it is design to ease generating input data for RTE. In fact a user does not need to know the name of an input variable and by simple entering engine information in corresponding cell and selecting proper condition can generate RTE's input file and run the program. By clicking on the "Generate RTE Input" button the input data files (RTEDATA, CONDDATA, and REACTANTS) of RTE can be generated. Then the user can run the radiation module and RTE by clicking on the corresponding buttons. It should be noted that RTE 's GUI can only run on a WINDOWS operating system. For running the program on a UNIX operating system, the input file can be generated using RTE's GUI on a WINDOWS operating system and then upload it to the UNIX machine. A more detailed description of RTE's GUI is given in Appendix C.

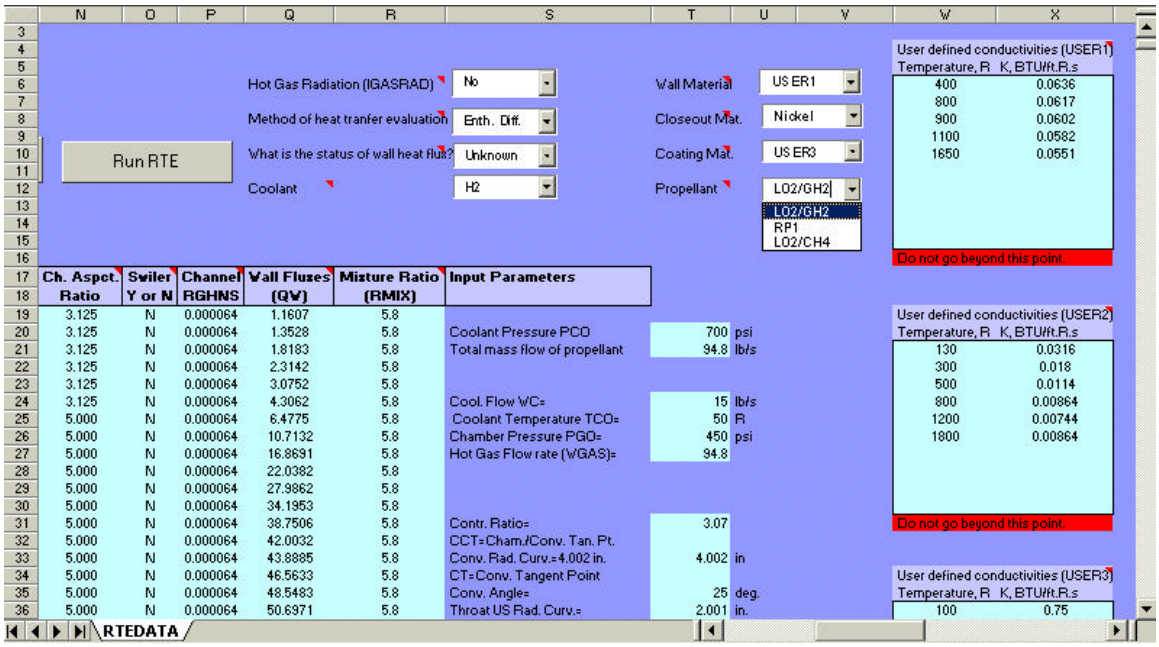

Figure 10: Other parts of RTE's GUI containing various combo boxes and Run RTE button

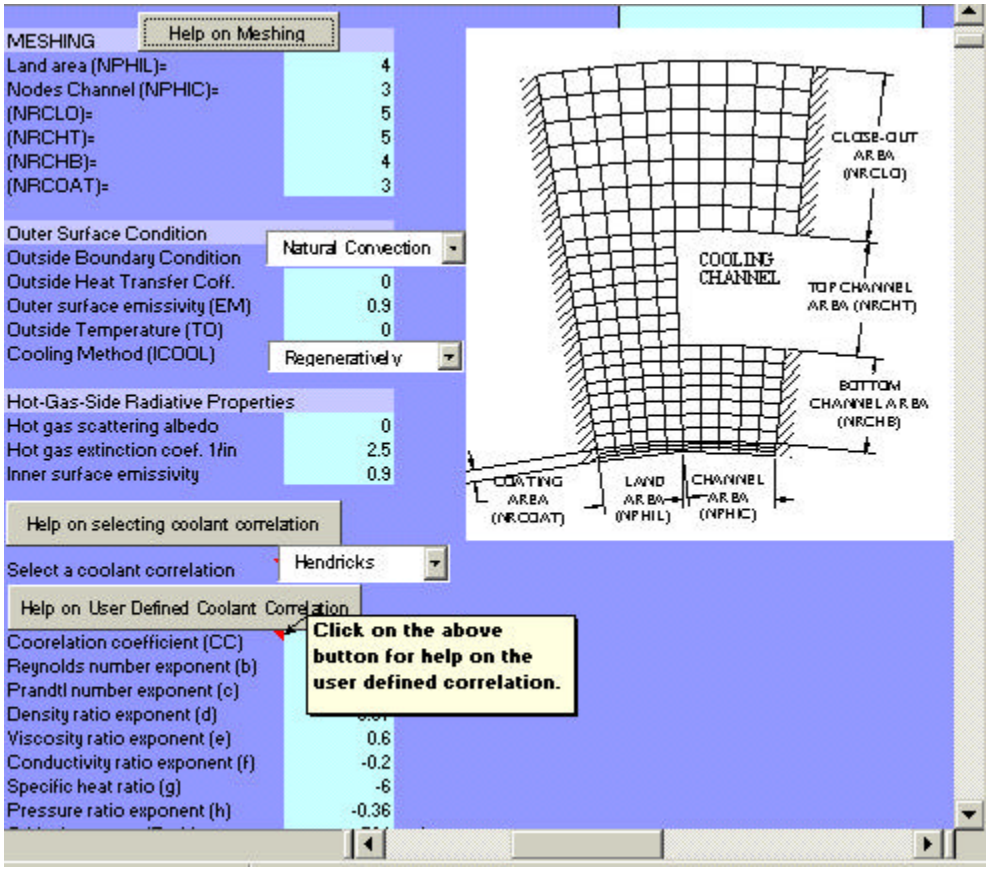

Figure 11: Part of RTE's GUI with help on meshing activated

RTE OUTPUTS

RTE's main output is printed on unit 5 (screen). It contains a printout of the input information given in the RTEDATA. Next, it prints the output nomenclature and the results of the ROCKET subroutine, which includes the static chamber pressure, the temperature, the enthalpy, Mach number, velocity, specific heat ratio and static density of hot-gas for all stations. Following this, the resulting nodal temperature distribution and some hot-gas and coolant thermal/transport properties for all stations are printed. The heat transfer from hot-gas to coolant is also given in the output. This output is a standard output of RTE, which includes the final results for each station. Three FLAG variables are included in the program for printing intermediate iteration results. These FLAG variables are:

IFLAGM	for main RTE program intermediate results
IFLAGC	for COND subroutine intermediate results
IFLAGG	for GASP and BONNIE subroutines intermediate results

When all FLAG variables are zero in RTEDATA, the standard output is printed. Setting its FLAG variable equal to one prints intermediate results of a subroutine or the main program.

RTE also produces some files, which can be read by TECPLOT (a registered software by Amtec Engineering Inc.) to produce graphs for some important output parameters. These files are as follows:

GRCCH.DAT	for cooling channel heights versus axial position.
GRFLUX.DAT	for wall heat flux versus axial position.
GRPC.DAT	for coolant static and stagnation pressures versus axial position.
GRTEMP.DAT	for average wall temperature distribution versus axial position.

These graphs are shown in Figures 13 through 16. Also, the code provides data files for contour (isotherm) plots of temperature distributions (similar to that shown in Figure 18) for up to ten stations. To get the isotherm plots, ISOST in the input file should be set to the station numbers that their plots are needed. The program will then provide up to ten files (ISOST1.DAT, ISOST2.DAT, ..., ISOST10.DAT) which can be read by TECPLOT to produce isotherm plots similar to that shown in Figure 9 for the specified station. Making a station number bold in RTE's preprocessor the graphic file for that station will be generated.

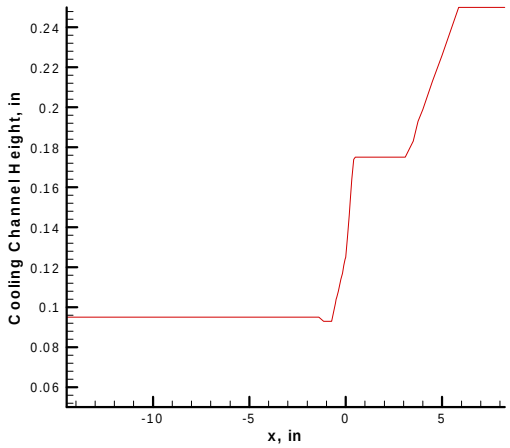

Figure 13: Cooling channel height for the SSME engine versus axial position

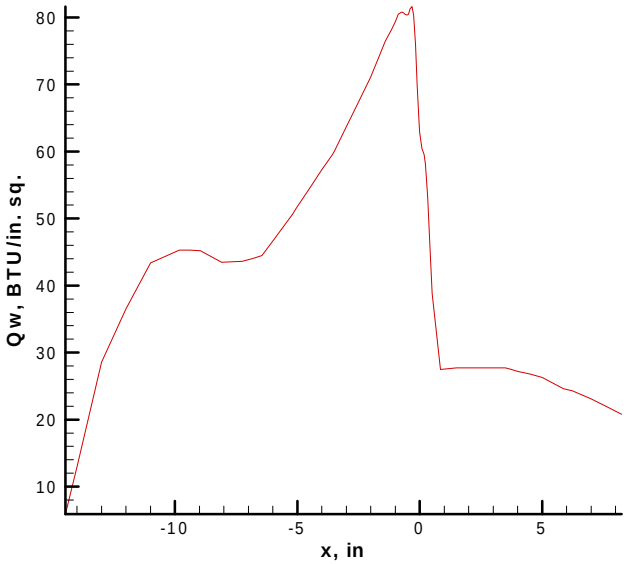

Figure 14: Wall heat flux distribution for the SSME engine versus axial position

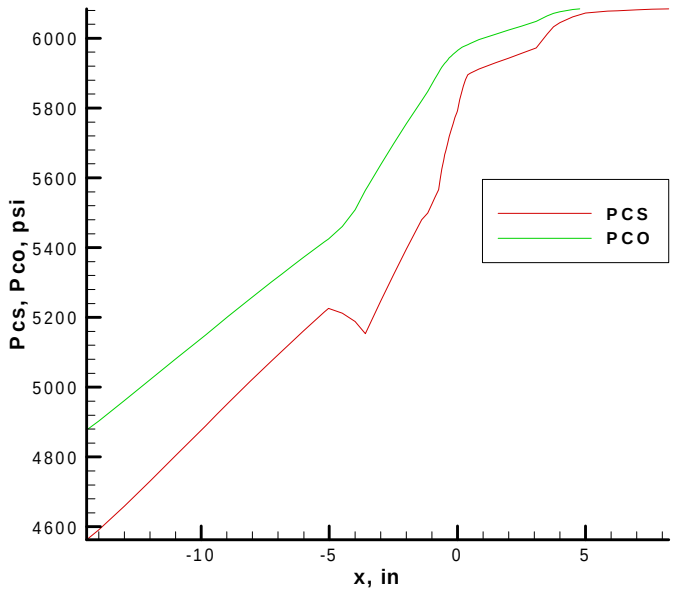

Figure 15: Static and stagnation pressure distribution for the SSME engine versus axial position

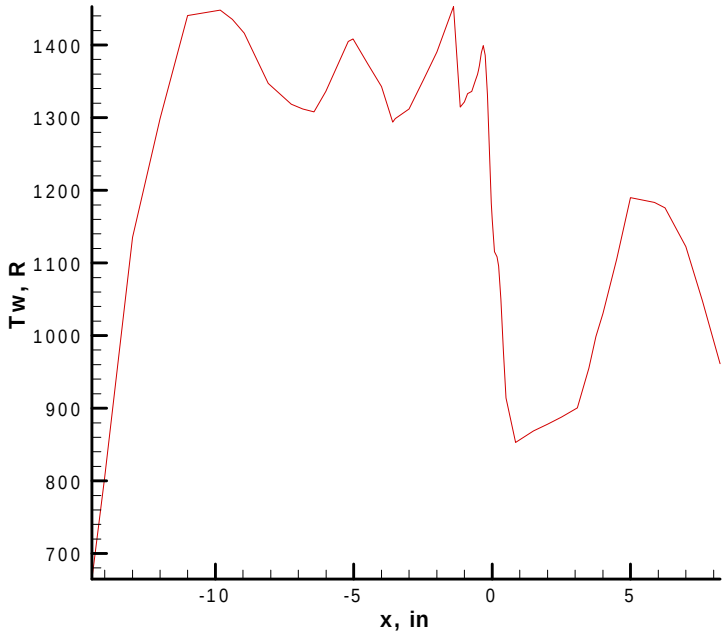

Figure 16: Wall average temperature distribution the SSME engine versus axial position

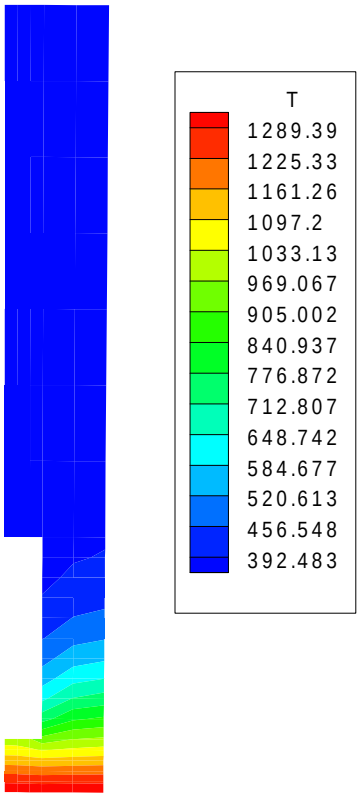

Figure 17: Temperature distribution for a specified station of an engine

A short file showing the summary of results for each station (SHRESULTS.DAT) is also generated. The results printed in SHRESULTS.DAT include: axial position (X), wall temperature (TW), wall heat flux (QW), coolant static pressure (PCS), coolant stagnation pressure (PCO), coolant stagnation (TCO), coolant Mach number (MC).

In addition to its regular outputs, RTE produces two output files, GAS_TEMP.DAT, which is a table of axial position, chamber diameter, gas temperature, wall heat flux and temperature; and RTE_BLM.DAT and RTE_MABL.DAT are output files, which can be used to interface RTE and TDK. The procedure for interfacing RTE and TDK and implementation of these output files will be described in the next section.

HOT-GAS-SIDE BOUNDARY LAYER ANALYSIS INTERFACE

The convective heat transfer coefficients and heat fluxes for the hot-gas-side of RTE are evaluated based on adiabatic wall temperature (enthalpy) correlations [8-9], see equation (3)-(12). To obtain results based on boundary layer analysis, RTE can be linked to a nozzle flow and boundary layer analysis program. The procedure for linking RTE to

TDK (Two-Dimensional Kinetics Nozzle Performance Computer Program [6] is described in this section. A similar approach may be implemented to link RTE to other nozzle boundary layer analysis programs.

An iterative procedure for linking RTE to TDK has been devised. A flowchart of this procedure is given in Figure 5. Initially, the wall fluxes and temperatures are evaluated by running RTE under an unknown wall heat flux condition (i.e., IWFLUX=0). The wall temperatures calculated by RTE are then used in the inputs of TDK. Using one of TDK's boundary layer modules (BLM or MABL), a new wall heat flux distribution is evaluated. The wall heat flux distribution is inserted into the RTE inputs. This time, since the hot-gas-side heat fluxes are known, RTE bypasses all hot-gas-side calculations (e.g., subroutine BONNIE and hot-gas-side heat transfer coefficient correlations) and calculates the wall temperature distribution. The new wall temperature distribution along the axial direction is then input to TDK and a new heat flux distribution is calculated. This iterative procedure continues until convergence is reached.

To automate this iterative process, a shell program has been developed. This program is a C-shell program for the UNIX operating system (rte.com) and a Compaq Visual Fortran System program for MS Windows operating systems (RTECOM.exe). A listing of this program is given in Appendix C. The shell program can be executed by typing its name followed by four arguments: RTE input data[17], TDK input data[18], RTE output and TDK output filenames. Both input data files (i.e., RTE and TDK input files) must end with the word FINISH. Note that the user can run TDK with either BLM (Boundary Layer Module) or MABL (Mass Addition Boundary Layer). Typical input files for both cases are given in Appendix B. Note that in place of a temperature distribution in the TDK input, the word BLM or MABL must be inserted, depending on the boundary layer option in the TDK input. For details of TDK inputs, reference should be made to the TDK user manual [6].

The shell program first cleans up files from the previous run and copies the RTE input data into RTE.INP and then starts the iterative loop by running RTE. In the first loop RTE performs the hot-gas-side as well as wall and cooling channel calculations. The resulting wall temperature distributions along the axial direction are written into two files, RTE_BLM.DAT and RTE_MABL.DAT, which have the same formats as the NAMELISTS in the MABL or BLM modules of TDK. Next, the shell program runs an interfacing program (RTE_TDK.). This program revises the TDK inputs based on the temperature distribution coming out of RTE, (i.e. it inserts the temperature distribution in place of words BLM or MABL). TDK is then executed and generates a table of heat fluxes versus axial positions, which is written to a file TDK_RTE.DAT. An interfacing program (TDK_RTE) reads wall heat fluxes from TDK_RTE.DAT and prints them into the RTE input file, consistent with the NAMELIST format of RTE. In the second and subsequent iterations, RTE runs with a known wall heat flux boundary condition (i.e., it bypasses the hot-gas-side calculations). This iterative procedure continues until the relative difference between heat fluxes of two consecutive iterations becomes negligibly

[17] IWFLUX=0 in the RTE input
[18] In place of wall temperature distribution in the TDK input word TEMPERATURES must be inserted.

small. The convergence criterion and the number of iterations are specified in CONVERGE.DAT.
A typical file for CONVERGE.DAT is given in Appendix B. CONVERGE.DAT has a NAMELIST format, which consists of the following variables:

ITER	shell iteration number. Initially, =1.
ERROR	convergence criterion for the shell. The C-shell iteration stops when the difference between wall heat fluxes of two consecutive iterations become smaller than ERROR.
XSTART	coordinate of the boundary layer leading edge. When X > XSTART, the boundary layer heat fluxes are used. Otherwise, the results of RTE based on equation (7) are implemented.
NSKIP	The BLM option makes the resulting wall heat fluxes close to the leading edge very ustable. NSKIP allows the user to skip (eliminate) heat fluxes close to the leading edge. If NSKIP=10, the interface skips 10 rows (heat fluxes) from the top of the heat flux table (TDK_RTE.DAT).
QW1	wall heat flux. Initially, =0.

At each iteration the resulting wall heat fluxes are written into CONVERGE.DAT and are read by TDK_RTE at the next iteration to compare with the revised fluxes. If the convergence criterion is satisfied the calculation stops, otherwise the loop continues. At each iteration, the RTE_TDK writes the resulting wall fluxes and wall temperatures into PLOT.DAT. This file can be used to plot final results of each iteration. A listing of RTE-TDK input files is given in Appendix D.

BLOCKED CHANNEL OPTION AND RESULTS

One of the concerns of the rocket designer is what happens to the wall temperature if one of the cooling channels is blocked. The default mode of RTE when all cooling channels are open, due to symmetry of all of the cooling channels at a given station, only models one-half of a cooling channel (a half-rib) in cross-section, similar to that shown in Figure 18a. In order to perform a thermal analysis for a chamber liner that has a blocked channel, the model is represented by two half-channels (a full-rib), one side representing a channel that is blocked in which there is no convective cooling, while the other side represents the adjacent open channel with coolant flowing in it (see Figure 18b).

In order to show the effects of a blocked cooling channel on the wall temperature profile, three different rocket thrust chambers were studied in [34] using RTE interfaced with TDK for hot-gas-side calculations. One chamber was designed to operate at a relatively low chamber pressure (P_c=450 psia), while the other two chambers were designed to operate at a relatively high chamber pressure (P_c=2000 psia). The high pressure chambers used in this analysis are modified designs of the high-pressure chamber designed and tested at the NASA-Glenn Research Center [35, 36]. The liners for all three chambers are made of copper, closed out with nickel, incorporating high- aspect-ratio cooling channels (HARCC) in their designs. The result presented in [34] show that for the blocked channel

cases, the analysis showed the effect on the wall temperature for the blocked channel and the adjacent open channel. The results indicated that there is a significant increase in the hot-gas-side wall temperature of the blocked channel and the adjacent open channel and a significant reduction in the coolant mass flow in the adjacent open channel. The increase in wall temperature due to a blocked channel for the low chamber pressure case was not at a level that would cause significant wall damage. However, the peak wall temperatures in the blocked channels for the high chamber pressure cases were at levels that could result in severe plastic deformation occurring in the cooling channel hot-gas-side wall, especially for the 150 channel high-pressure chamber.

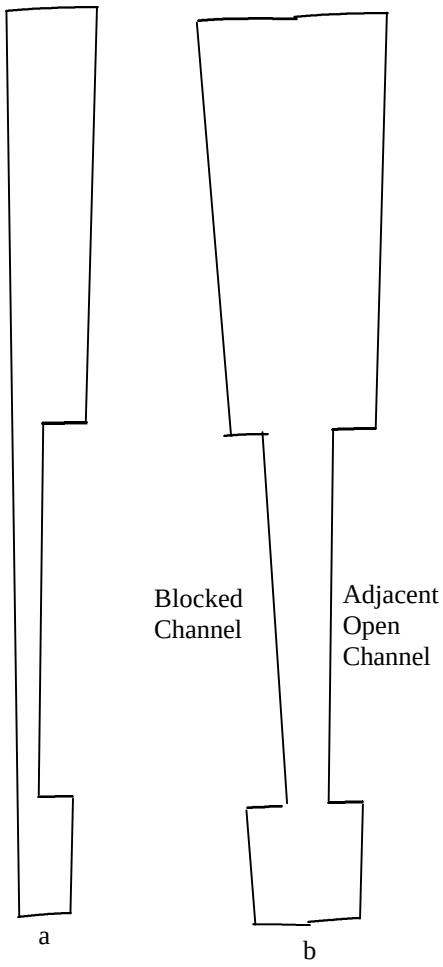

Figure 18: (a) One-half cooling channel and half-rib cross-section (b) One-half blocked channel and one-half open channel with full-rib.

If one of the cooling channels in a rocket thrust chamber liner is blocked, obviously, the resulting wall temperature of the blocked channel will be higher than that of the cooled channels. However, the channel adjacent to the blocked channel will also have a higher wall temperature than the channels further away from the blocked-channel region due to conduction of heat from the blocked channel to the adjacent channel. This has the effect of reducing the maximum wall temperature in the blocked channel for a liner made of a

high conductivity material. As a result, this causes the coolant temperature in the channel adjacent to the blocked channel to rise to a level higher than that for the channels further away from the blocked channel region. This would result in an increase in coolant Mach number and pressure drop in the adjacent channel, assuming the coolant mass flow in that channel is the same as all of the other channels. However, the pressure drop across the cooling jacket must be equal for all channels. Since the pressure drop across the channel adjacent to the blocked channel must be the same as that of the other channels, the mass flow in that channel will become less than that of the other channels. Therefore, in order to calculate the hot-gas-side wall temperature of the blocked channel and the adjacent channel, the mass flow in the adjacent channel must be determined.

To obtain the mass flow in the cooling channel adjacent to the blocked channel, RTE was first run for a given cooling jacket geometry in which there is no blocked channel in order to determine the pressure drop across the cooling jacket. Then, another case was run using the full-rib conduction model in order to obtain the temperature profile in the rib with no cooling on one side and coolant flowing on the other side (see figure 18b). The mass flow in the adjacent channel is reduced through an iterative scheme until the pressure drop matches that for the case with no blocked channel. Through this procedure the wall temperature and the temperature profile in the blocked channel and the adjacent channel can be calculated.

To demonstrate RTE's results for a blocked channel case consideration is given to a high-pressure chamber [blocked paper] with 150 and 200 cooling channels. The specifications of the engine are:

Chamber pressure	2000 psia	2000 psia
O/F	5.8	5.8
Contraction ratio	3.41	3.41
Expansion ratio	6.63	6.63
Throat diameter	2.6 inches	2.6 inches
Propellant	GH2-LO2	GH2-LO2
Coolant	LH2	LH2
Total coolant flow rate	6.45 lb/sec	6.45 lb/sec
Coolant inlet temperature	50	50R
Coolant inlet stagnation pressure	200 psia	2900 psia
Approximate throat heat flux	77 $\frac{Btu}{in^2-\sec}$	75 $\frac{Btu}{in^2-\sec}$
Number of cooling channels	200	150
Throat region channel aspect ratio	5-7.8	6
Channel width step changes at	X=0.947 inches X=-3.906 inches	X=0.947 inches X=-3.906 inches

The rocket thrust chamber and nozzle contour is shown in Figure 19 with the station locations denoted on the contour. The 200 channel chamber was evaluated first. In order to allow for the pressure drop across the injector, the coolant inlet pressure required was 3200 psia, resulting in a pressure drop of 834 psi in the cooling jacket, which is relatively

high for this chamber pressure. However, the wall temperature just upstream of the throat is only 1058R, which is relatively low for a high-pressure chamber, showing the effectiveness of HARCC in this design. The temperature profile for this location is given in Figure 20. The dashed line in Figure 21 shows the average hot-gas-side wall temperature as a function of axial position for the unblocked-channel case. This figure also shows that there are step changes in the wall temperature, just before and just after step changes in the cooling channel width in the nozzle and chamber respectively, at x ≈1.0 inches and x ≈-4.0 inches.

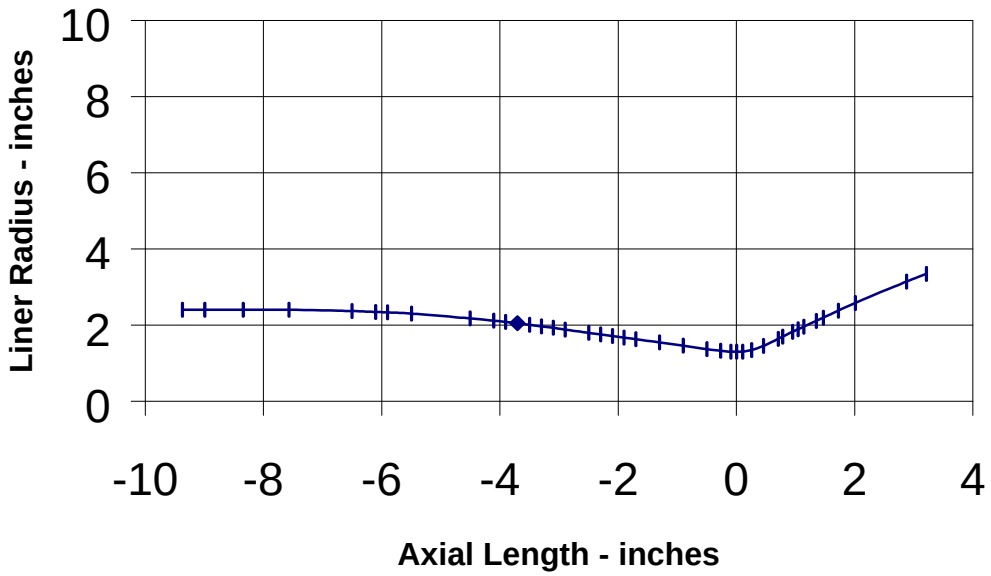

Figure 19: The high-pressure rocket thrust chamber contour showing station locations

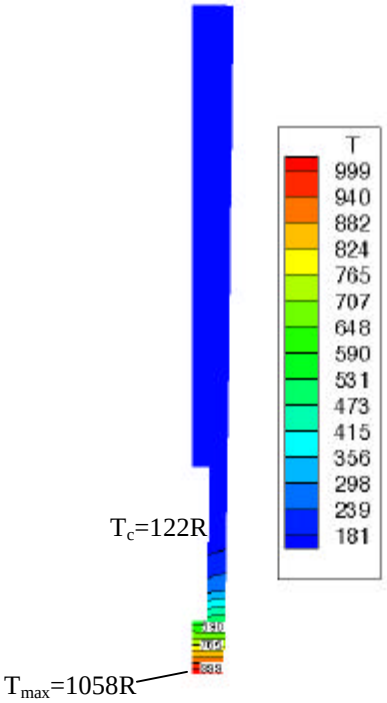

Figure 20: Rib temperature profile upstream of the throat (x=-0.1 inches) for the high-pressure chamber, 200 channels (unblocked)

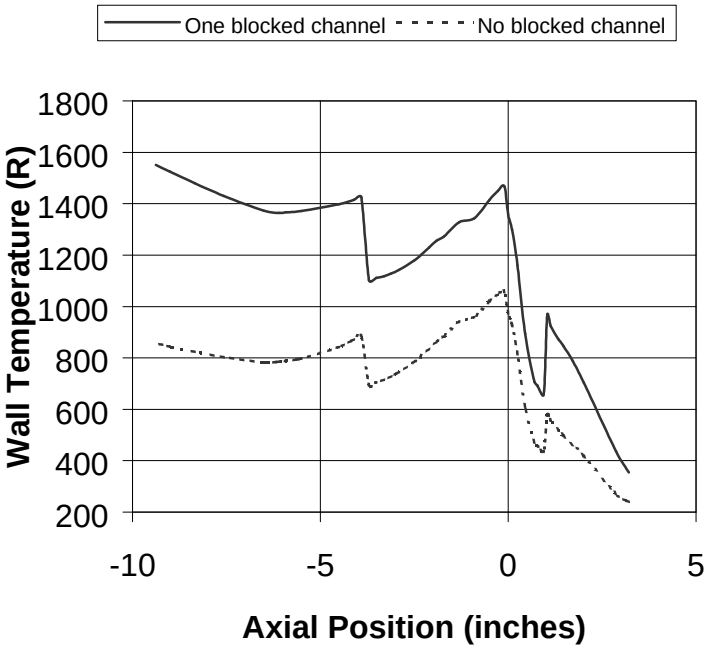

Figure 21: Comparison of the maximum wall temperature profile versus axial position for the blocked-channel and unblocked-channel cases for the high-pressure chamber, 200 channels

The same high-pressure chamber was evaluated by running RTE with the blocked-channel option. In order to maintain the pressure drop of 834 psi for the cooling channel adjacent to the blocked channel the mass flow rate of the coolant was reduced to 0.024 lb/sec. compared to 0.032 lb/sec per channel for the no-blocked channel case, a 25% drop in the coolant mass flow. The resulting axial average wall temperature profile for the blocked-channel and the adjacent open channel is shown in Figure 20. As shown in this Figure, the maximum wall temperature occurs at the injector-end of the cooling channels. Another location of high temperature occurs at x ≈ -4. inches, where there is a step change in the cooling channel width. Figures 22 and 23 show the rib temperature profiles for the peak temperatures in the throat-region and injector-end locations

In order to achieve a chamber design with a lower pressure drop, the same chamber was evaluated incorporating 150 cooling channels in the design. Although the channel width for the reduced number of channels is larger, the aspect ratio in the throat region was held at 6 by increasing the height of the channels relative to the 200 channel case. As in the previous cases, the chamber was first evaluated with unblocked channels. In this case, the pressure drop was 587 psi, which resulted in a lower coolant inlet pressure of 2900 psia.

Again, the peak wall temperature occurs just upstream of the throat at a value of 1211R, 153R higher than the 200 channel case. The temperature profile for this location is shown in Figure 24. The dashed line in Figure 25 shows the average hot-gas-side wall temperature as a function of axial position for the unblocked-channel case. This figure also shows the step changes in wall temperature just before and just after the step change in the cooling channel width in the nozzle and chamber respectively, at x ≈1.0 inch and x ≈-4.0 inches.

The same high-pressure chamber was evaluated by running RTE with the blocked-channel option. In order to maintain the pressure drop of 587 psi for the cooling channel adjacent to the blocked channel, the mass flow rate of the coolant was reduced from 0.043 lb/sec per channel to 0.031 lb/sec per channel, a 28% reduction in the coolant mass flow. The resulting average hot-gas-side wall temperature as a function of axial position for the blocked-channel and adjacent open channel is also shown in Figure 25. A maximum wall temperature of 1766R for this case occurs just upstream of the throat and is shown in the temperature profile in Figure26. At the injector end of the cooling channels the maximum wall temperature reached 1738R as shown in Figure 17.

The 150-channel design resulted in a conservative axial wall temperature profile with a reasonable pressure drop across the cooling jacket. However, the peak wall temperatures for the blocked-channel case are in a range where severe plastic deformation of the cooling channel on the hot-gas-side wall could occur.

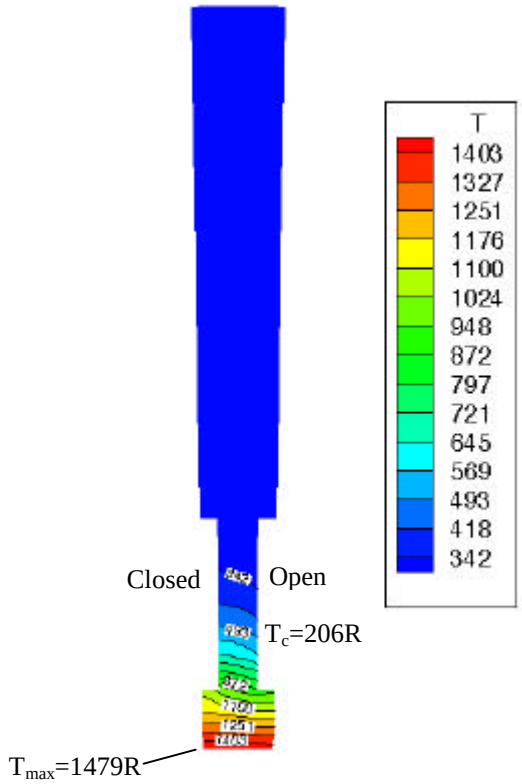

Figure 22: Rib temperature profile upstream of the throat (x=-0.1 inches) of the high-pressure chamber, 200 channels (blocked channel and adjacent open channel)

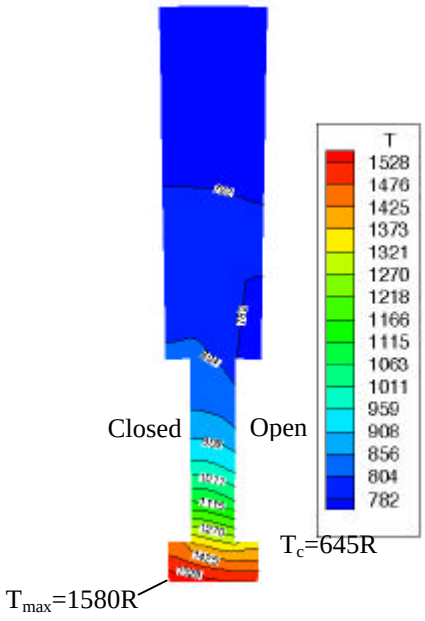

Figure 23: Rib temperature profile at the injector-end station (x=-9.38 inches) for the high-pressure chamber, 200 channels (blocked channel and adjacent open channel)

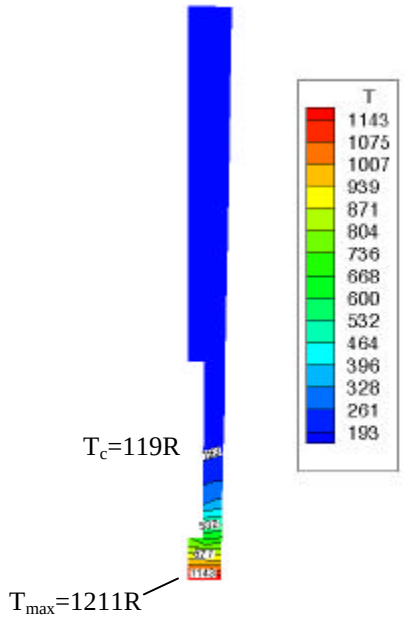

Figure 24: Rib temperature profile upstream of the throat (x=-0.1 inches) for the high-pressure chamber, 150 channels (unblocked)

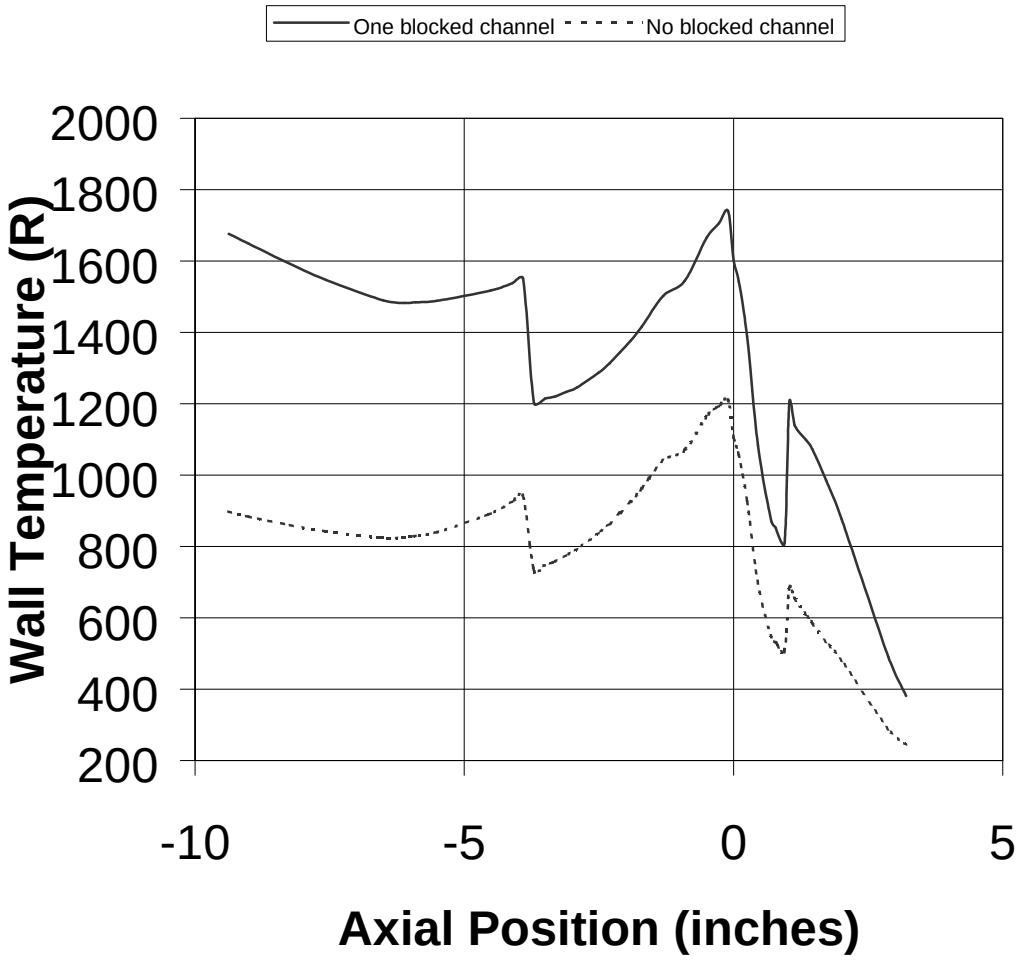

Figure 25: Comparison of the maximum wall temperature profile versus axial position for the blocked-channel and unblocked-channel cases for the high-pressure chamber, 150 channels

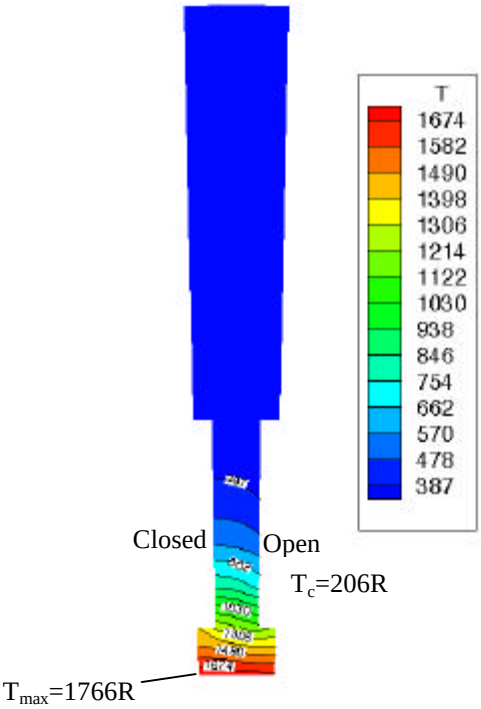

Figure 26: Rib temperature profile upstream of the throat (x=-.01 inches) for the high-pressure chamber, 150 channels (blocked channel and adjacent open channel)

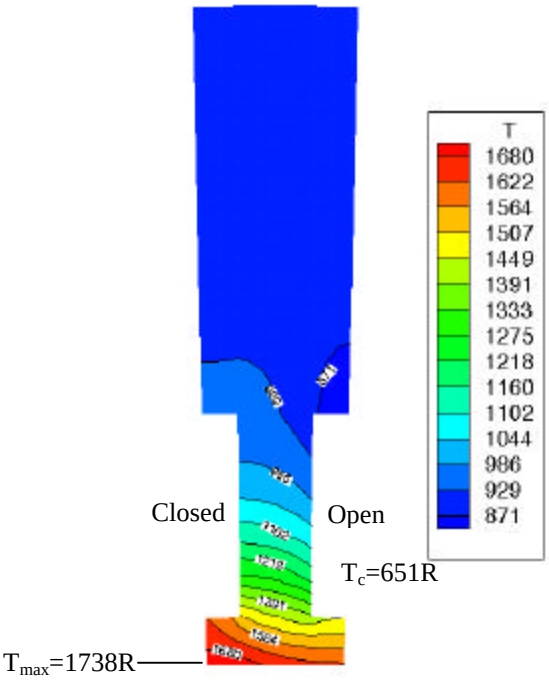

Figure 27: Rib temperature profile at the injector-end station (x=-9.38 inches) for the high-pressure chamber, 150 channels (blocked channel and adjacent open channel)

INSTALLATION AND EXECUTION INSTRUCTIONS

The instruction provided here is to help the user who acquired the source code of RTE and wish to modify the program and generate their executable file. The users with RTE's executable can run RTE by using its graphic user interface; or typing RTE.exe in DOS mode or UNIX systems. Typing their executable file can run other supporting files of RTE. For example, simply typing RTE_RAD.exe run the radiation module of RTE and typing rtecom.exe (rte.com for UNIX along with required parameter) runs RTE-TDK interface. The easiest way of running RTE is through it Graphic User Interface (GUI), which is only available for the Windows operating systems.

Microsoft WINDOWS Operating System

RTE and its modules were successfully compiled and executed on Compaq Visual FORTRAN Version 6. The enclosed CD contains the RTE program, its supporting modules and typical data files. The CD contains the following files:
rte2002.f (RTE main program and its subroutines)
cet.f (combustion properties subroutines, BONNIE)
gasp.f (coolant properties subroutines)
RTE.INP (typical RTE input including RTEDATA)
THERMOSA.DAT (Thermodynamics properties of hot gases, needed in ASCII format only for the first run)
TRANSSA.DAT (Transport properties of hot gases, needed in ASCII format only for the first run)
RTE_RAD.f (Program for gas radiation exchange and weight factors calculations)

After installing these files the user should compile the FORTRAN files (i.e., rte.f, cet.f and gasp.f) and link them into an executable file (rte.exe). The user can run the program by simply typing rte2002.exe. To minimize errors in inputting data RTE's graphic user interface can be used. By clicking on "Run RTE" button RTE runs. The following programs and data files are used for linking RTE and TDK: rtecom.exe (executable of rtecom.f , a Shell program for linking RTE and TDK) RTE_TDK.f (a FORTRAN program for taking RTE_BLM.DAT or RTE_MABL.DAT, outputs of RTE, and inserting wall temperature distribution into TDK input)
TDK_RTE.f (a FORTRAN program for taking TDK_RTE.DAT, an output of TDK, and inserting wall heat flux distribution into RTE input)
CONVERGE.DAT (typical CONVERGE.DAT file)
TDK.DAT (typical TDK data file)

UNIX Operating System

RTE and its modules were successfully compiled and executed on an IBM RISC6000. The enclosed CD contains the RTE program, its supporting modules and typical data files. The CD contains the following files:
rte.f (RTE main program and its subroutines)

cet.f (combustion properties subroutines, BONNIE)
gasp.f (coolant properties subroutines)
RTE.INP (typical RTE input including RTEDATA)
THERMOSA.DAT (Thermodynamics properties of hot gases, needed in ASCII format only for the first run)
TRANSSA.DAT (Transport properties of hot gases, needed in ASCII format only for the first run)
RTE_RAD.f (Program for gas radiation exchange and weight factors calculations)

After installing these files the user should compile the FORTRAN files (i.e., rte2002.f, cet.f and gasp.f) and link them into an executable file (rte.exe). The user can run the program by simply typing rte.exe. The following programs and data files are used for linking RTE and TDK: rte.com (Shell program for linking RTE and TDK) RTE_TDK.f (a FORTRAN program for taking RTE_BLM.DAT or RTE_MABL.DAT, outputs of RTE, and inserting wall temperature distribution into TDK input)
TDK_RTE.f (a FORTRAN program for taking TDK_RTE.DAT, an output of TDK, and inserting wall heat flux distribution into RTE input)
CONVERGE.DAT (typical CONVERGE.DAT file)
TDK.DAT (typical TDK data file)

The program was successfully executed for several types of engines under different conditions and provided results, which are reasonably close to the experimental data. A number of provisions are made in the program to detect possible error in data of unrealistic conditions. It is, however possible that the program fail under certain conditions. The following guidelines may be useful to detect and correct any possible error in the input data:

1. For a new case, set MAXPASS=1 for the first run. Then the program makes one axial pass and prints the results as soon as it finishes calculations for each station. If the program fails, one can tell exactly at what station the failure has occurred and check the data at that station.

2. If failure is indicated in the conduction subroutine (CONDWCC), check dimensions of cooling channels to see if the land between cooling channels becomes zero or negative. Also, check other wall dimensions to make sure that they are consistent. Using RTE's preprocessor ensures a user that dimensions of cooling channels are entered correctly.

3. Failures in the coolant properties subroutines (GASP or WASP) are usually caused by low or negative pressure in the cooling channel. This is due to small size cooling channels or large coolant flow rate causing a large pressure drop in the cooling channels. This problem, most likely, appears close to the throat area where cooling channels contract. Once the coolant passes the throat, cooling channels expand causing an increase in coolant pressure and the possibility of negative coolant pressure vanishes. For this condition RTE stops running at the

station where the coolant runs out of pressure and instructs the user what to do in order to correct the problem.

4. Divide by zero in the Reynolds and Prandtl numbers calculations of the main program is caused by very large coolant temperature. This can happen if the coolant velocity is very low or the wall temperature is very large. The GASP assigns zero to the transport properties of the coolant when its temperature is unrealistically large.

5. Very low wall temperature at the inner surface causes the combustion gases to freeze on the surface. The combustion subroutine (BONNIE) cannot predict the transport properties of frozen combustion gases and the program may fail by sending an OVERFLOW message. Usually this problem occurs at the first station where the coolant temperature is lowest. To overcome this problem, the user may assign a tiny layer of coating with low thermal conductivity to increase the wall temperature at the inner surface.

6. The program has been tested successfully for most commonly used rocket propellants (LH2/LO2 and hydrocarbon fuels). For propellants with metal components (e.g., LH_2/LO_2/AL), the combustion subroutine over predicts the hot-gas temperature causing higher wall and coolant temperature. The program will eventually fail due to an excessive coolant temperature. The program is not recommended for metallized propellants.

For any other failure of the program contact its developer at Tara Technologies LLC via e-mail (mnaraghi@tara-technologies.com).

REFERENCES

1. Gordon, S. and McBride, B. J., "Computer Program for Calculation of complex Chemical Equilibrium Compositions, Rocket Performance, Incident and Reflection Shocks, and Chapman-Jouquet Detonations," NASA SP-270, 1971.

2. Gordon, S., McBride, B. J. and Zeleznik, F. J., "Computer Program for Calculation of Complex Chemical Equilibrium Compositions and Applications Supplement I - Transport Properties," NASA TM-86885, Oct. 1984.

3. Hendricks, R. C., Baron, A. K. and Peller, I. C., "GASP - A Computer Code for Calculating the Thermodynamic and Transport Properties for Ten Fluids: Parahydrogen, Helium, Neon, Methane, Nitrogen, Carbon Monoxide, Oxygen, Fluorine, Argon, and Carbon Dioxide," NASA TN D-7808, Feb. 1975.

4. Hendricks, R. C., Peller, I. C. and Baron, A. K., "WASP - A Flexible Fortran IV Computer Code for Calculating Water and Steam Properties," NASA TN D-7391, Nov, 1973.

5. Muss, J.A., Nguyen, T.V., and Johnson, C.W., *User's Manual for Rocket Combustor Interactive Design (ROCCID) and Analysis Compter Program*, Volumes I and II, NASA Contractor Report 1087109, May 1991.

6. Nickerson, G.R., Coats, D.E., Dang, A.L., Dunn, S.S., and Kehtarnavaz, H., *Two-Dimensional Kinetics (TDK) Nozzle Performance Computer Program*, NAS8-36863, March 1989.

7. CPIA/M4, Liquid Propellant Manual, Unit 20a, September 1997, Chemical Propulsion Information Agency.

8. Eckert, E. R. G. and Drake, R. M., *Analysis of Heat and Mass Transfer*, McGraw-Hill Book Company, 1972.

9. Bartz, D. R., "Turbulent Boundary-Layer Heat Transfer from Rapidly Accelerating Flow of Rocket Combustion Gases and of Heated Air," Advances in Heat Transfer, pp. 2-108, 1965.

10. Colebrook, C.F., "Turbulent Flow in Pipes with Particular Reference to the Transition Region Between the Smooth and Rough Pipe Laws," Journal of Institute of Civil Engineers, Vol. 11, pp. 133-156, 1939.

11. Chen, N.H., "An Explicit Equation for Friction Factor in Pipe," Ind. Eng. Chem. Fundam., Vol. 18, No. 3, pp. 296-297, 1979.

12. Ito, H., “Friction Factors for Turbulent Flow in Curved Pipes,” Journal of Basic Engineering, pp. 123-134, 1959.

13. Moody, L.F., ``Friction Factors for Pipe Flow,” Transactions of ASME, pp. 671-684, 1944.

14. Hendricks, R. C., Niino, M., Kumakawa, A., Yernshenko, V. M., Yaski, L. A., Majumdar, L. A., and Mukerjee, J., “Friction Factors and Heat Transfer Coefficients for Hydrogen Systems Operating at Supercritical Pressures,” Proceeding of Beijing International Symposium on Hydrogen Systems, Beijing, China, May 7-11, 1985.

15. Kumakawa, A., Niino, M., Hendricks, R.C., Giarratano, P.J. and Arp, V.D., “Volume-Energy Parameters for Heat Transfer to Supercritical Fluids,” Proceeding of the Fifteenth International Symposium of Space Technology and Science, Tokyo, pp. 389-399, 1986.

16. Spencer, R.G. and Rousar, D.C., “Supercritical Oxygen Heat Transfer,” NASA CR-135339, 1977.

17. Faith, L.E., Ackerman, Henderson, H.T., Heat Sink Capability of Jet A Fuel: Heat Transfer and Coking Studies, NASA CR-72951, S-14115, 1971.

18. Cook, R.T., “Advanced Cooling Techniques for High Pressure Hydrocarbon – Fueled Rocket Engines,” AIAA-80-1266.

19. Master, P.A., Aukerman, C.A., “Deposit Formation and Heat Transfer in Hydrocarbon Rocket Fuels,” AIAA 84-0512.

20. Niino, M., Kumakawa, A., Yatsuyanagi, N. and Suzuki, A., “Heat Transfer Characteristics of Liquid Hydrogen as a Coolant for the LO2/LH2 Rocket thrust Chamber with the Channel Wall Construction," 18Th. AIAA/SAE/ASME Joint Propulsion Conference, Cheveland, Ohio, June 21-23, 1982, AIAA paper 82-1107.

21. Taylor, M.F., “A Method of Predicting Heat Transfer Coefficients in the Cooling Passages of Nerva and Phoebus-2 Rocket Nozzles,” NASA TM X-52437, June 1968.

22. Owhadi, A., Bell, K.J. and Crain, B., “Forced Convection Boiling Inside Helically-Coiled Tubes,” International Journal of Heat and Mass Transfer, Vol. 11, pp. 1779-1793, 1968.

23. Norris, R.H., “Augmentation of Convection Heat and Mass Transfer,”American Society of Mechanical Engineers, New York, 1971.

24. Date, A.W., “Flow in Tubes Containing Twisted Tapes,” Heating and Ventilating Eng., Vol. 47, pp. 240-249, 1973.

25. Thorsen, R. and Landis, F., “Friction and Heat Transfer Characteristics in Turbulent Swirl Flow Subject to Large Transverse Temperature Gradient,” Journal of Heat Transfer, Vol. 90, pp. 87-89, 1968.

26. Handbook of Heat Transfer Fundamentals, end Ed., Editors: Rohsenow, Hartnet and Ganic, McGraw Hill Book Company, 1985.

27. Naraghi, M.H.N., Chung, B.T.F., and Litkouhi, B., “A Continuous Exchange Factor Method for Radiative Analysis of Enclosures with Participating Media,” Journal of Heat Transfer, Trans. ASME, Vol. 110, pp. 456-462, 1988.

28. Hammad, K.J., and Naraghi, M.H.N., “Exchange Factor Model for Radiative Heat Transfer Analysis in Rocket Engines,” AIAA Journal of Thermophysics and Heat Transfer, Vol. 5, No. 3, pp. 327-334, 1991.

29. Hammad, K.J., ``Radiative Heat Transfer in Rocket Thrust Chambers and Nozzles," M.S. Thesis, Department of Mechanical Engineering, Manhattan College, 1989.

30. Nunes, E.M., Modi, V., and Naraghi, M.H.N., "Radiative Transfer in Arbitrarily-Shaped Axisymmetric Bodies with Anisotropic Scattering Media," International Journal of Heat and Mass Transfer, Vol. 43, pp. 3275-3285, 2000.

31. Nunes, E.M., Naraghi, M.H.N., ``A Model for Radiative Heat Transfer Analysis in Arbitrarily-Shaped Axisymmetric Enclosures", Numerical Heat transfer, Part A, Vol. 33, pp. 495-513, 1998.

32. Ludwig, C.B., Malkmus, W., Reardon, J.E., and Thomson, J.A.L., “Handbook of Infrared Radiation From Combustion Gases,” NASA SP-3080, 1973.

33. Siegel, R., and Howell, J.R., Thermal Radiation Heat Transfer, Hemisphere Publishing Corporation, 3rd Ed., 1992.

34. Naraghi, M.H.N., Quentmeyer, R.J., Mohr, D.H., “ Effect of a Blocked Channel on the Wall Temperature of a Regeneratively Cooled Rocket Thrust Chamber” AIAA 2001-3406, present in the AIAA/ASME/SAE/ASEE 2001 Joint propulsion Conference, Salt Lake City, Utah, July 8-11, 2001.

35. Mary F. Wadel, Richard J. Quentmeyer, and Michael L. Meyer, “A Rocket Engine Design for Validating the High-Aspect-Ratio Cooling Concept,” Preprint from the 1994 Conference on Advanced Earth-To-Orbit Propulsion Technology held at NASA Marshall Space Flight Center, Huntsville, AL, May 17-19, 1994.

36. Mary F. Wadel and Michael L. Meyer, “Validation of High-Aspect-Ratio Cooling in a 89kN (20,000 lbf) Thrust Combustion Chamber,” AIAA/ASME/SAE/ASEE 32nd Joint Propulsion Conference; July 1-3, 1996 / Lake Buena Vista, FL, AIAA-96-258

APPENDIX A

FLOWCHART OF RTE

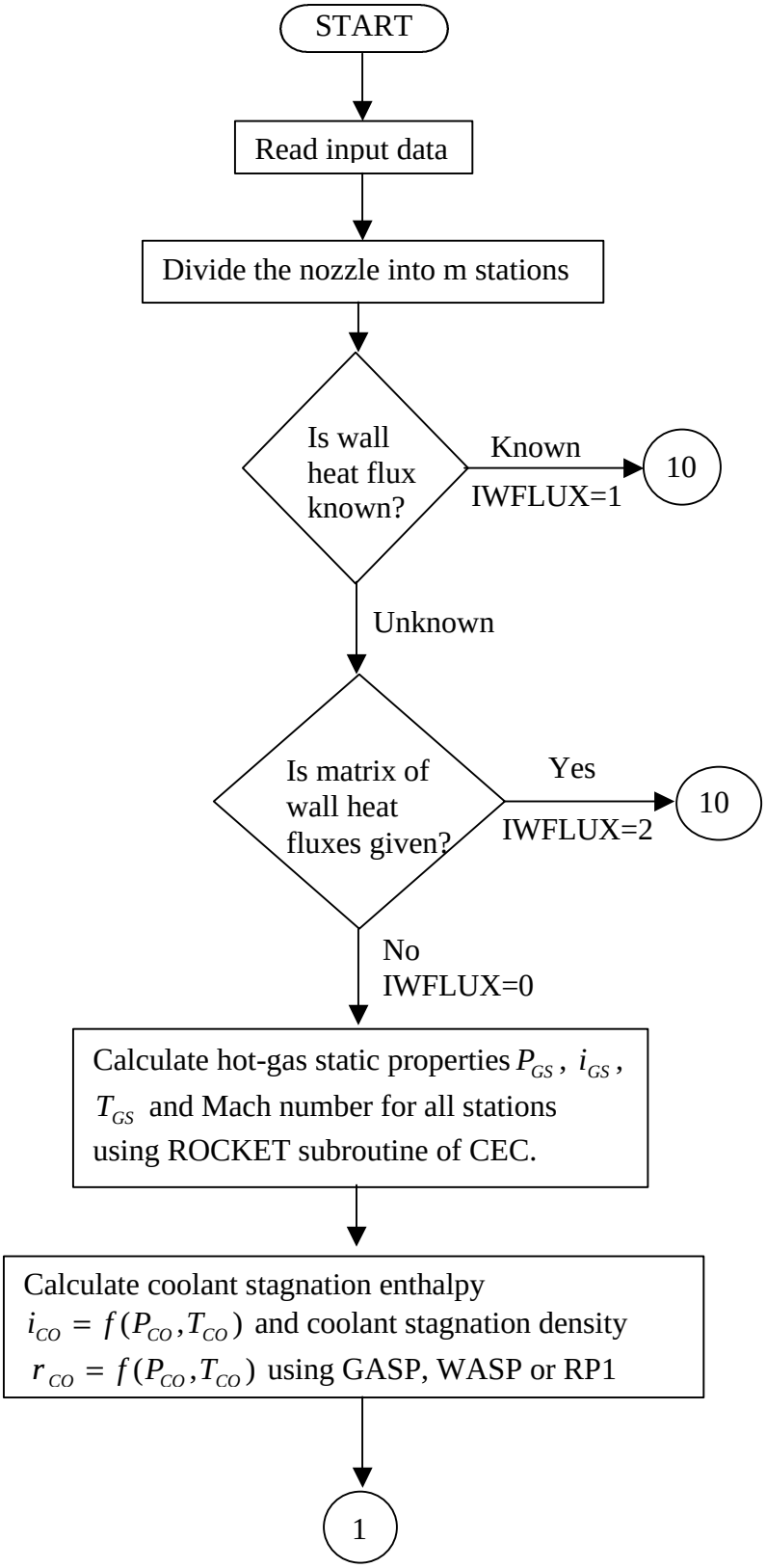

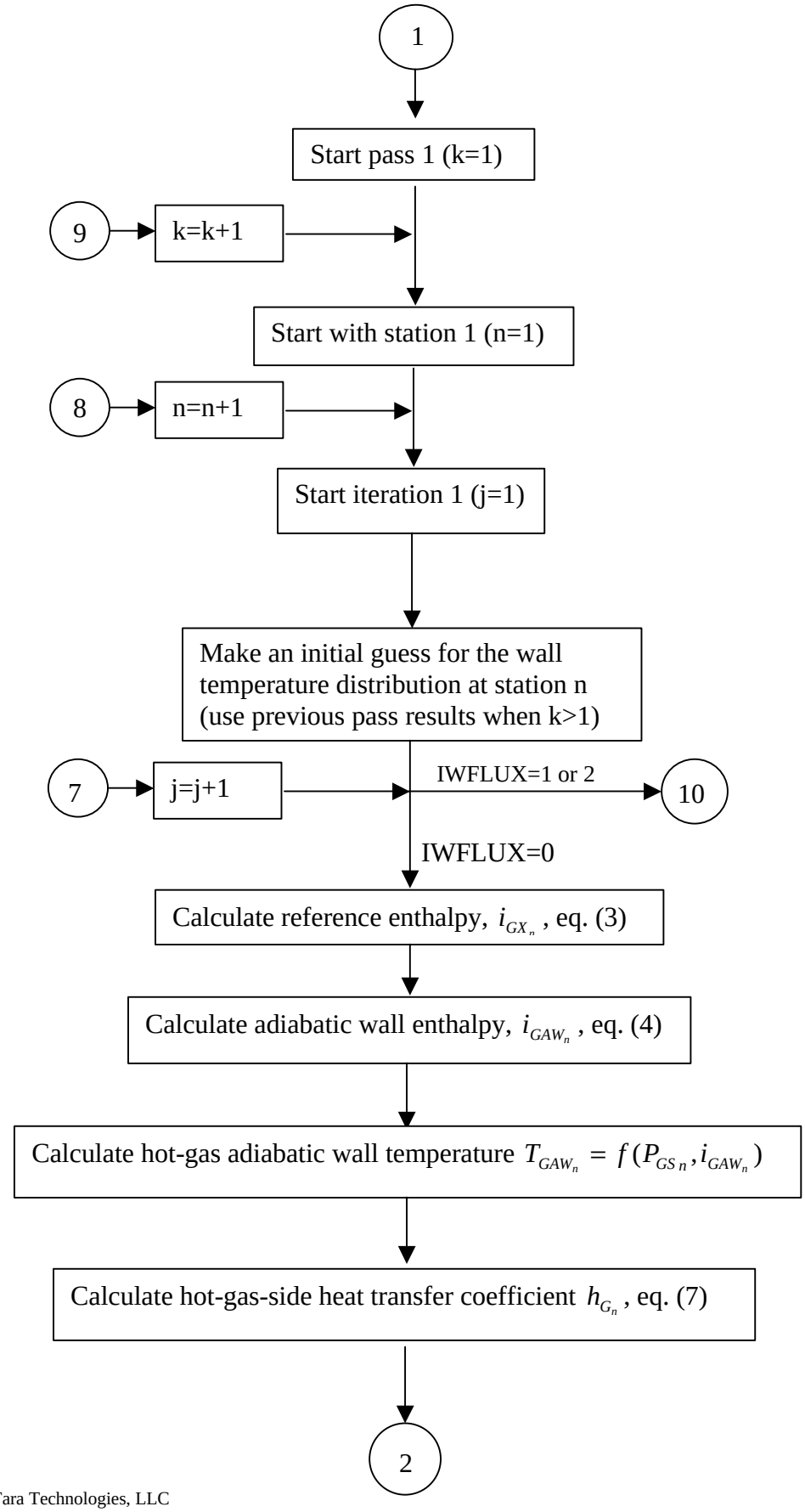

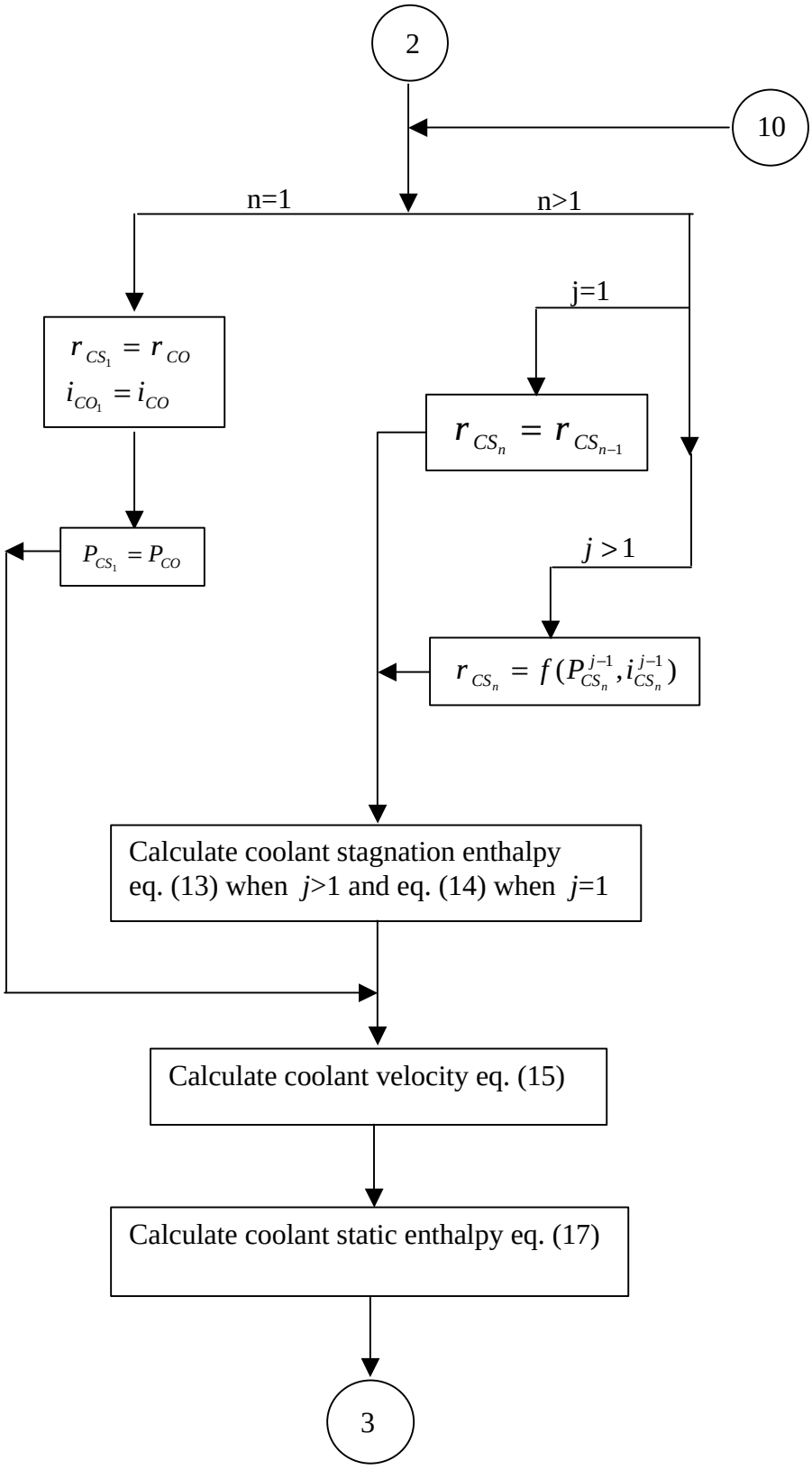

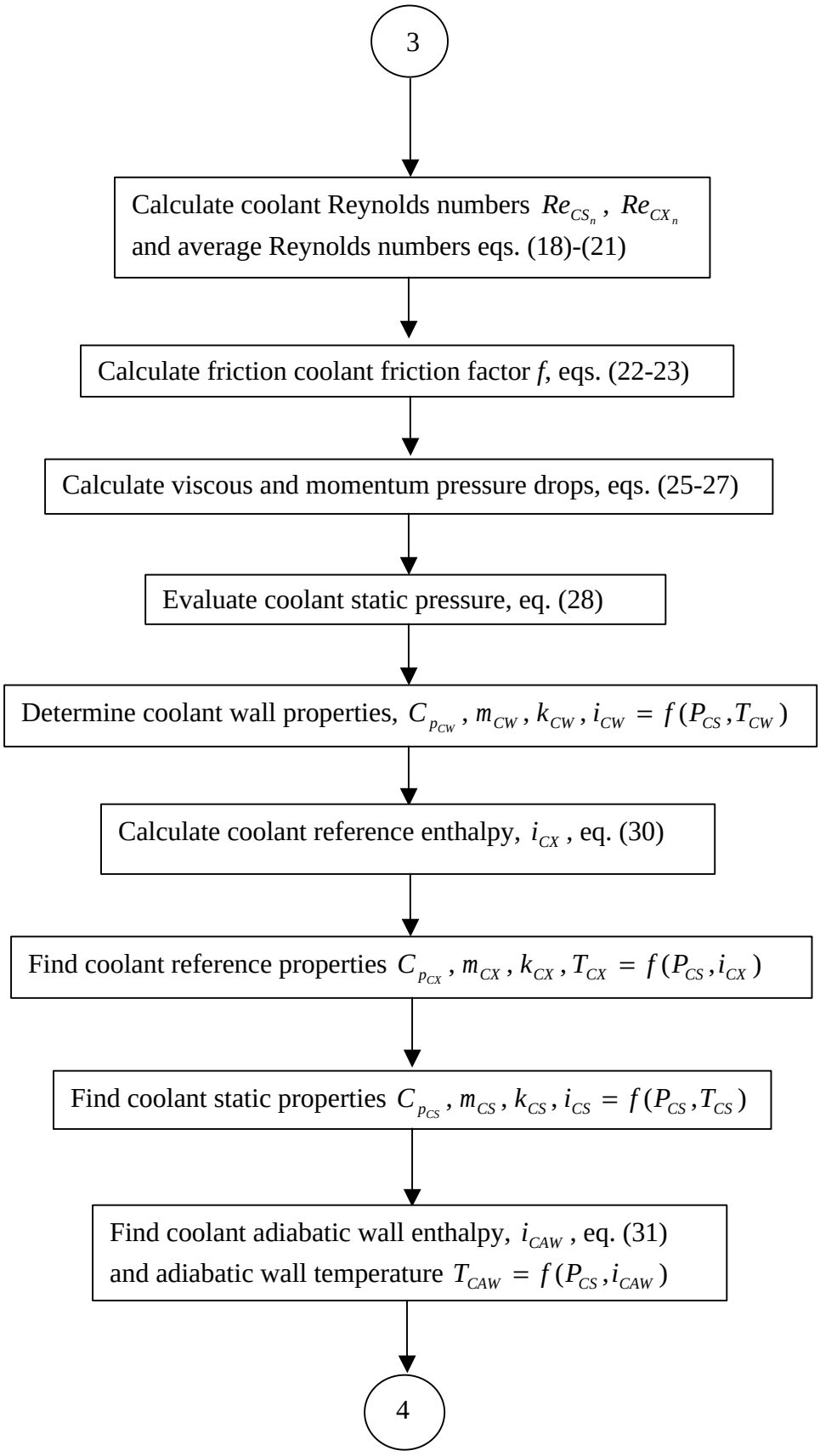

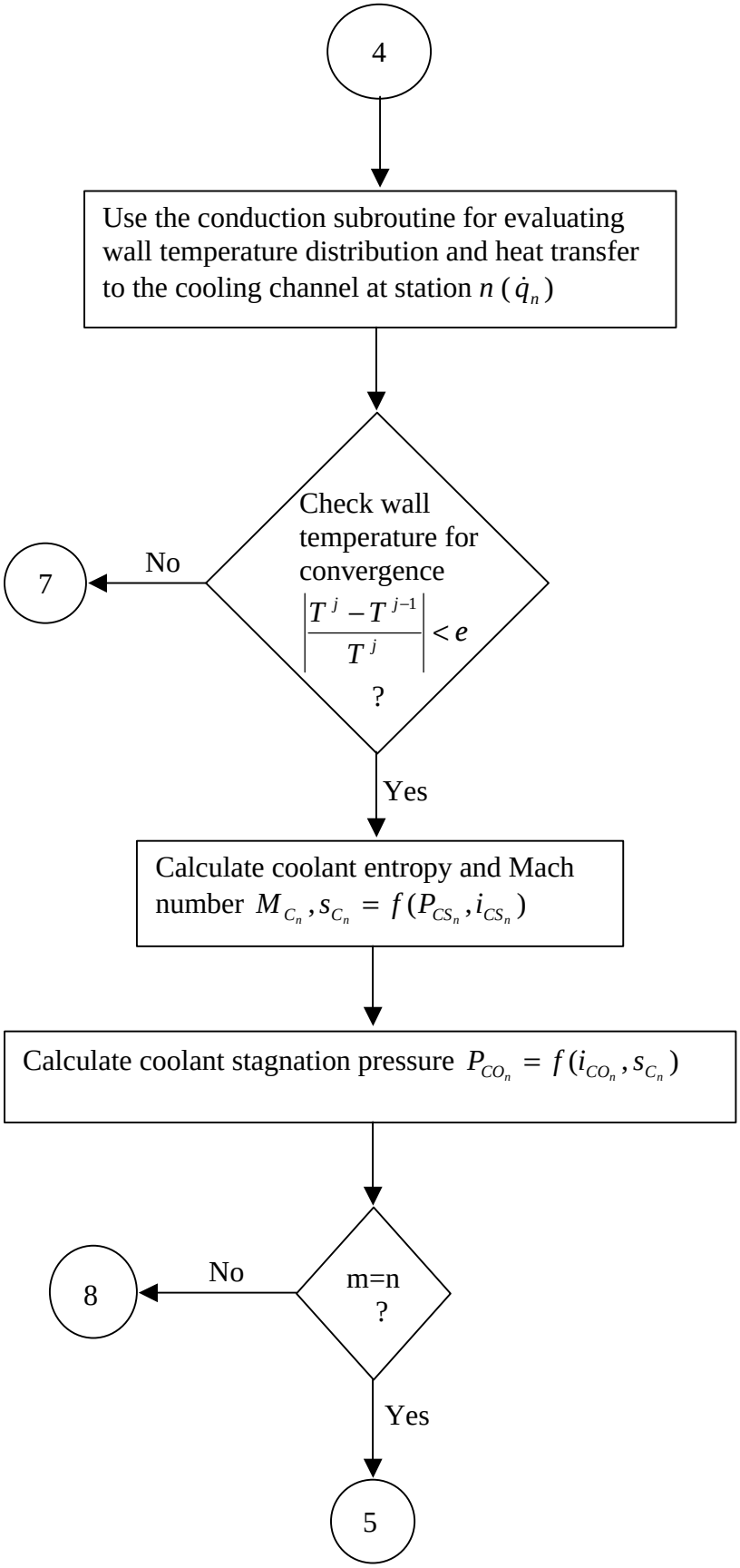

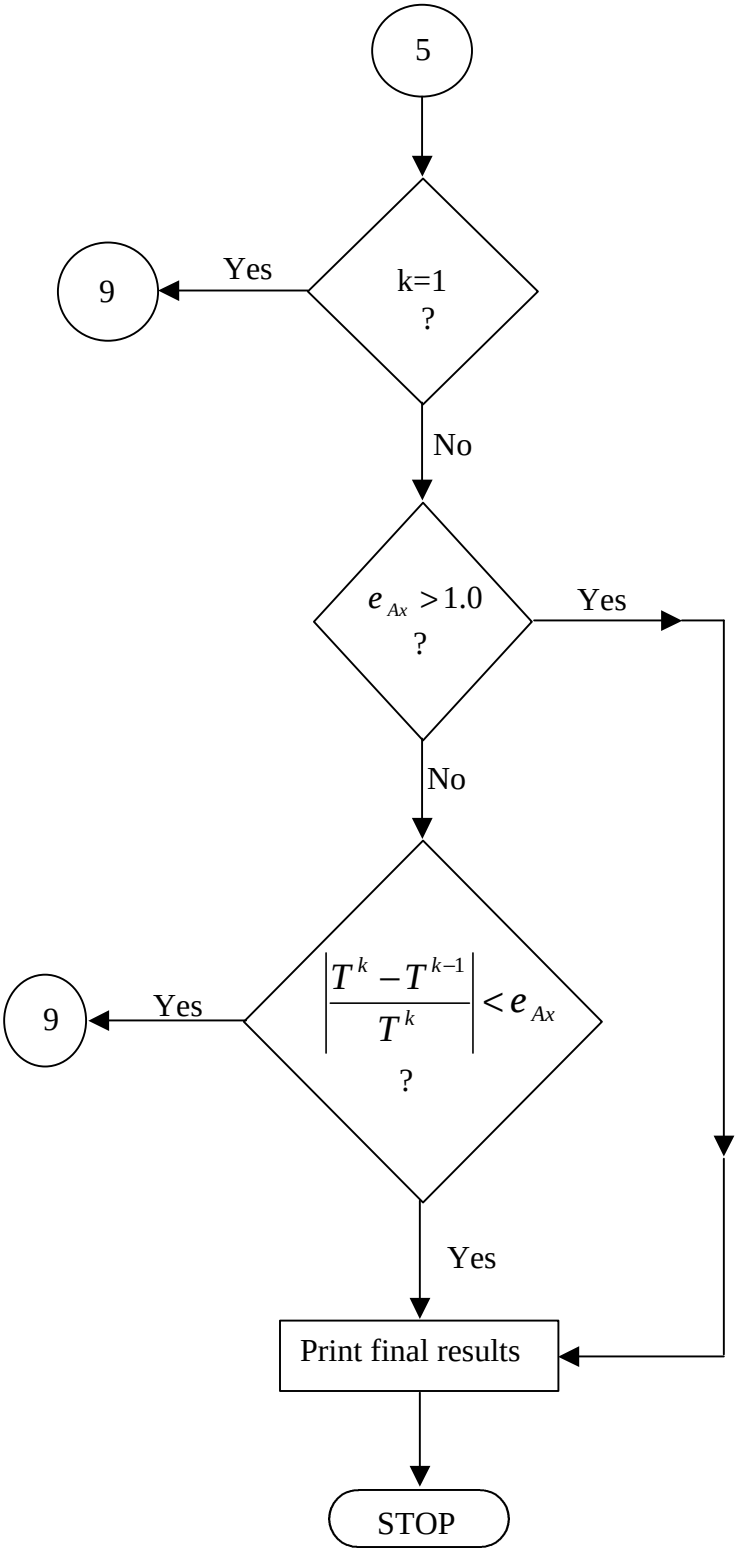

APPENDIX B

INPUT NOMENCLATURE AND SAMPLE INPUTS FOR RTE

STRUCTURE OF RTE'S DATA FILES

The main input data of RTE consists of six parts: &RTEDATA, &RTECOND (needed only if the user defined conductivity option is chosen), REACTANTS, FLUX.DAT, THERMO.DAT and TRANS.DAT. Three files &RTEDATA, &RTECOND and REACTANTS are attached as a single file to RTE.INP, which is read by the default read unit of RTE (unit 5).

&RTEDATA is a namelist data file which defines all specification of the engine, such as, nozzle and cooling channel geometry, coolant flow rate, inlet temperature and pressure.

&RTECOND is a namelist file that is only needed if user-defined conductivities option is chosen (i.e. negative material code). It defines conductivities of up to three user-defined materials as function of temperature.

REACTANT provides information on the fuel and oxidant (propellant) composition. It is needed if the RTE's own hot-gas-side calculation is used (i.e., IWFLUX=0 in &RTEDATA namelist).

FLUX.DAT is a matrix of wall heat flux which gives hot-gas-side heat flux as a function of position and wall temperature. This file is needed if IWFLUX=2.

THERMO.DAT provides the thermodynamic properties of combustion gas species. This file is needed if RTE's own hot-gas-side calculation is used (i.e., IWFLUX=0 in &RTEDATA namelist).

TRANS.DAT provides the transport properties of combustion gas species. This file is needed if RTE's own hot-gas-side calculation is used (i.e., IWFLUX=0 in &RTEDATA namelist).

TGS.DAT is a data file for gas to surface radiation weight and exchange factors. This file is needed if hot-gas side radiation option is selected.

TSS.DAT is a data file for surface radiation weight and exchange factors. This file is needed if hot-gas side radiation option is selected.

NOMENCLATURE FOR **RTEDATA** NAMELIST

CASECODE	case code (for user distinguish different cases)
CC	cooling channel heat transfer correlation coefficient (for each station)
CG	hot-gas-side heat transfer correlation coefficient (for each station)
CCH[19]	cooling channel height (in.) (for each station)
CCW[19]	cooling channel width (in.) (for each station)

[19] See Fig. 3 for notation

CCOLANT	coolant name (e.g., “H2”, “O2”, “H2O”)
DCIN[19]	distance between bottom of the cooling channel and inner surface of the nozzle (in.), excluding coating thickness (for each station)
CONDEXP	exponent of conductivity ratio in equation (39), needed for user-defined coolant correlation (ITYPE=0)
DENEXP	exponent of density ratio in equation (39), needed for user-defined coolant correlation (ITYPE=0)
DG	nozzle diameter (in.) (for each station)
EM	emissivity of the outer surface
ENTHALPY	0 for using temperature difference in calculating wall heat flux (equation (11))1 for using enthalpy difference in calculating wall heat flux (equation (12))
EPSILON	inner surface emissivity
ERROR	convergence criterion for radial and circumferential directions
ERRAX	convergence criterion for axial direction
HO1	outside heat transfer coefficient (Btu/ft^2 s R)
ICOOL	type of cooling system = 1 for regeneratively cooled 2 for radiatively cooled
IENT	entrance effect correction factor =1 for equation (33) 2 for equation (34) 3 for equation (35) 4 for equation (36)
IFLAGC[20]	flag variable for printing intermediate results of COND subroutine
IFLAGG[20]	flag variable for printing intermediate results of GASP and BONNIE subroutines
IFLAGM[20]	flag variable for printing intermediate results of the main program
IHOUT	type of heat transfer at outer boundary 1 for force convection 2 natural convection 3 radiation
IGASRAD	gas radiation flag = 1 for gas radiation 2 no gas radiation
ISOST	station number for which isotherm plots are requested
ISW	flag for swiler or no swiler (for all stations) = 1 for swiler = 0 for no swiler
ITYPE	coolant side heat transfer correlation to be used, ITYPE = 0 for user-defined correlation, equation (39) ITYPE = 1 for the correlation given by equation (34) ITYPE = 2 for the correlation given by equation (35) ITYPE = 3 for the correlation given by equation (36) ITYPE = 4 for the correlation given by equation (37) ITYPE = 5 for the correlation given by equation (38)

[20] Equal to 0 for no intermediate results, and 1 for intermediate results

IWFLUX	flag for known or unknown wall heat flux = for unknown wall heat flux 1 for known wall heat flux 2 for matrix of wall heat flux (FLUX.DAT file is needed for this case)
IUNIT	unit flag = 1 for English units, and 2 for SI units

KTG	extinction coefficient (in^{-1}) (for each station)
MAXITER	maximum number of iterations at each station
MAXPASS	maximum number of passes (axial marches)
MTCH[21]	channel (top and bottom portion) material
MTCLO[21]	close-out material
MTCOAT[21]	coating material
NBLOCK	number of blocked channels (0 for no blocked channel and 1 for one blocked channel)
NCC	number of cooling channels (for each station)
NOFS	number of stations
NPHIC	number of circumferential nodes within channel area
NPHIL	number of circumferential nodes within land area
NRCHB	number of radial nodes in channel area (bottom portion)
NRCHT	number of radial nodes in channel area (top portion)
NRCLO	number of radial nodes in close-out
NRCOAT	number of radial nodes in coating
OMEGA	hot-gas scattering albedo (for hot-gas radiation only)
PCO	coolant inlet pressure (psia)
PGO	chamber pressure (psia)
PCRIT	critical pressure in equation (39), needed for user-defined coolant correlation (ITYPE=0)
PRESEXP	exponent of pressure ratio in equation (39), needed for user-defined coolant correlation (ITYPE=0)
PREXP	exponent of Prandtl number in equation (39), needed for user-defined coolant correlation (ITYPE=0)
QW	hot-gas-side wall heat flux (Btu/in^2) (for each station), needed if IWFLUX=1
RCURVE	cooling channel radius of curvature (in.) (for each station)
REEXP	exponent of Reynolds number in equation (39), needed for user-defined coolant correlation (ITYPE=0)
RGHNS	cooling channel surface roughness (in.)
RMIX	percentage of fuel (for each station)
SANGLE	swiler angle in degrees
SHEXP	exponent of specific heat ration in equation (39), needed for user-defined coolant correlation (ITYPE=0)

[21] Equal to 1 for copper; 2 for nickel; 3 for soot; 4 for NARloy-Z; 5 for columbium; 6 for zirconia; 7 for SS-347; 8 for amzirc; 9 for Platinum; 10 for Glidcop; 11 for Inconel718; 12 for Nicraly; 13 for user defined #1; 14 for user defined #2 and 15 for user defined #3.

TCO	coolant inlet temperature (R)
TCOAT	coating thickness (in.) (for each station)
TGS	hot-gas static temperature (R), needed if IWFLUX=1 and IGASRAD=1
THKNS	wall thickness (in.), excluding coating thickness (for each station)
OPTO	outside temperature (R)
TSTART	initial guess of wall temperature (R)
VISCEXP	exponent of viscosity ratio in equation (39), needed for user-defined coolant correlation (ITYPE=0)
WC	coolant weight flow (lb/sec)
WGAS	total weight flow of oxidant and fuel (lb/sec)
X	axial distance from the throat (in.) (+tive for diverging part) (-tive for converging part) (0 for the throat)

NOMENCLATURE FOR **&CONDDATA** NAMELIST

K1	conductivities of material one (material code of –1 in &RTEDATA), NP1 conductivities are needed (Btu/s.ft.R)
K2	conductivities of material two (material code of –2 in &RTEDATA), NP2 conductivities are needed (Btu/s.ft.R)
K3	conductivities of material three (material code of –3 in &RTEDATA), NP3 conductivities are needed (Btu/s.ft.R)
NP1	number of conductivity points for material one
NP2	number of conductivity points for material two
NP3	number of conductivity points for material three
T1	temperatures for material one (R)
T2	temperatures for material two (R)
T3	temperatures for material three (R)

REACTANT FORMAT

This part of the input data provides information on the chemical composition of the propellant. The following table provides the name and input format of commonly used propellants in liquid propulsion systems [1].

Component	Chemical formula (columns 1 to 45)	Percent (46-52)	Assigned enthalpy cal/mol (54-62)	Phase L liquid G Gas (63)	Temp. K (64-71)	Fuel; F Oxid.; O (72)	Density g/cm3 (73-80)
Air	**N** 1.56176**O** .41959 **AR**.009324 C .000300	100.	-28.2	G	298.15	O	
Hydrogen (g)	**H** 2.	100.	0.	G	298.15	F	
Hydrogen (l)	**H** 2.	100.	-2154.	L	20.27	F	0.0709
JP-5, ASTMA1	**C** 1. **H** 1.9185	100.	-5300.	L	298.15	F	0.807
JP-4, RP-1	**C** 1. **H** 1.9423	100.	-5430	L	298.15	F	.773

Methane (g)	**C** 1. **H** 4.	100.	-17895.	G	298.15	F	
Methane (l)	**C** 1. **H** 4.	100.	-21390.	L	111.66	F	.4239
Methyl alcohol	**C** 1. **H** 4. **O** 1.	100	-57050	L	298.15	F	.78659
Octane	**C** 8. **H** 18.	100	-59740.	L	298.15	F	.69849
Oxygen	**O** 2.	100	0.0	G	298.15	O	
Oxygen	**O** 2.	100	-3102.	L	90.18	O	1.149
Propane	**C** 3. **H** 8.	100	-30372.	L	231.08	F	

Typical data file for two commonly used propellants are given bellow.

For RP1-O2:

```
REACTANTS
C 1.000  H 1.9423                              100.    -5430.   L 298.15 F
O 2.000                                        100.    -3146.9  L  83.3  O
END
```

For GH2-LO2:

```
REACTANTS
H 2.000                                        100.00       0.0 G 298.15 F
O 2.000                                        100.00   -3102.0 L  90.0  O
```

SAMPLE MAIN INPUT FILE FOR RTE (RTE.INP)

The main input file of RTE is RTE.INP, which is read by unit 5 (default FORTRAN read unit). This file consists if &RTEDATA and RTECOND namelists, and REACTANT data file.

```
&RTEDATA

CASECODE='HARCC-PC2000',
COOLANT = 'H2',
WC =4.62,
WGAS =43.9,
RMIX =   5.8, 5.8,
         5.8, 5.8, 5.8, 5.8, 5.8, 5.8, 5.8, 5.8, 5.8, 5.8,
         5.8, 5.8, 5.8, 5.8, 5.8, 5.8, 5.8, 5.8, 5.8, 5.8,
         5.8, 5.8, 5.8, 5.8, 5.8, 5.8, 5.8, 5.8, 5.8, 5.8,
         5.8, 5.8, 5.8, 5.8, 5.8, 5.8, 5.8, 5.8, 5.8,
PGO =2000,
PCO =2900,
TCO =50,
NOFS = 41,
ITYPE =  0 ,
NBLOCK =  0 ,
REEXP = 0.99,
PREXP = 0.4,
DENEXP = 0.37,
VISCEXP = 0.6,
CONDEXP = -0.2,
SHEXP = -6,
PREXP = -0.36,
PCRIT = 731,
IENT = 4,
IGASRAD = 2,
TSTART = 400,
```

```
ERROR = 0.1000000E-03,
MAXITER = 50,
ERRAX = 0.1000000E-02,
MAXPASS = 1,

NPHIL =4,
NPHIC =3,
NRCLO =5,
NRCHT =5,
NRCHB =4,
NRCOAT =3,
MTCLO =14,
MTCH =13,
MTCOAT =15,
IHOUT =2,
HO1 =0,
EM = 0.9,
ICOOL =1,
TO =0,
OMEGA = 0,
EPSILON =0.9,
SANGLE =30,
IUNIT = 1,
IEDGE = 1,
KTG = 41*2.5,
IFLAGM = 0,
IFLAGG = 0,
IFLAGC = 0,
ENTHALPY = 1,
X =      3.208,2.872,
         2.009,1.719,1.464,1.347,1.135,1.038,0.947,0.778,0.701,0.452,
         0.25,0.1,0,-0.1,-0.274,-0.506,-0.906,-1.306,-1.706,-1.906,
         -2.106,-2.306,-2.506,-2.906,-3.106,-3.306,-3.506,-3.706,-3.906,-4.106,
         -4.506,-5.5,-5.906,-6.106,-6.506,-7.572,-8.35,-9,-9.375,
DG =      6.694 , 6.28 ,
          5.154 , 4.754 , 4.392 , 4.226 , 3.916 , 3.776 , 3.64 , 3.388 , 3.272 , 2.902 ,
          2.686 , 2.613 , 2.6 , 2.608 , 2.656 , 2.746 , 2.924 , 3.092 , 3.264 , 3.344 ,
          3.432 , 3.516 , 3.602 , 3.77 , 3.86 , 3.94 , 4.022 , 4.1 , 4.17 , 4.236 ,
          4.358 , 4.6 , 4.666 , 4.694 , 4.744 , 4.8 , 4.8 , 4.8 , 4.8 ,
NCC =    150,150,
         150,150,150,150,150,150,150,150,150,150,
         150,150,150,150,150,150,150,150,150,150,
         150,150,150,150,150,150,150,150,150,150,
         150,150,150,150,150,150,150,150,150,
DCIN =   0.035,0.035,
         0.035,0.035,0.035,0.035,0.035,0.035,0.035,0.035,0.035,0.035,
         0.035,0.035,0.035,0.035,0.035,0.035,0.035,0.035,0.035,0.035,
         0.035,0.035,0.035,0.035,0.035,0.035,0.035,0.035,0.035,0.035,
         0.035,0.035,0.035,0.035,0.035,0.035,0.035,0.035,0.035,
CCW =    0.05, 0.05,
         0.05, 0.05, 0.05, 0.05, 0.05, 0.05, 0.025, 0.025, 0.025, 0.025,
         0.025, 0.025, 0.025, 0.025, 0.025, 0.025, 0.025, 0.025, 0.025, 0.025,
         0.025, 0.025, 0.025, 0.025, 0.025, 0.025, 0.025, 0.025, 0.05, 0.05,
         0.05, 0.05, 0.05, 0.05, 0.05, 0.05, 0.05, 0.05, 0.05,
CCH =    0.125, 0.125,
         0.125, 0.125, 0.125, 0.125, 0.125, 0.125, 0.125, 0.125, 0.125, 0.125,
         0.125, 0.125, 0.125, 0.125, 0.125, 0.125, 0.125, 0.134, 0.145, 0.15,
         0.156, 0.156, 0.156, 0.156, 0.156, 0.156, 0.156, 0.156, 0.156, 0.156,
         0.156, 0.156, 0.156, 0.156, 0.156, 0.156, 0.156, 0.156, 0.156,
TCOAT =  0, 0,
         0, 0, 0, 0, 0, 0, 0, 0, 0, 0,
         0, 0, 0, 0, 0, 0, 0, 0, 0, 0,
         0, 0, 0, 0, 0, 0, 0, 0, 0, 0,
         0, 0, 0, 0, 0, 0, 0, 0, 0,
THKNS =  0.36, 0.36,
         0.36, 0.36, 0.36, 0.36, 0.36, 0.36, 0.36, 0.36, 0.36, 0.36,
         0.36, 0.36, 0.36, 0.36, 0.36, 0.36, 0.36, 0.369, 0.38, 0.385,
         0.391, 0.391, 0.391, 0.391, 0.391, 0.391, 0.391, 0.391, 0.391, 0.391,
         0.391, 0.391, 0.391, 0.391, 0.391, 0.391, 0.391, 0.391, 0.391,
CC =      0.0095 ,  0.0095 ,
```

```
          0.0095 ,  0.0095 ,  0.0095 ,  0.0095 ,  0.0095 ,  0.0095 ,  0.0095 ,  0.0095 ,
0.0095 ,  0.0095 ,
          0.0095 ,  0.0095 ,  0.0095 ,  0.0095 ,  0.0095 ,  0.0095 ,  0.0095 ,  0.0095 ,
0.0095 ,  0.0095 ,
          0.0095 ,  0.0095 ,  0.0095 ,  0.0095 ,  0.0095 ,  0.0095 ,  0.0095 ,  0.0095 ,
0.0095 ,  0.0095 ,
          0.0095 ,  0.0095 ,  0.0095 ,  0.0095 ,  0.0095 ,  0.0095 ,  0.0095 ,  0.0095 ,
0.0095 ,
CG =      0.023, 0.023,
          0.023, 0.023, 0.023, 0.023, 0.023, 0.023, 0.023, 0.023, 0.023, 0.023,
          0.023, 0.023, 0.023, 0.023, 0.023, 0.023, 0.023, 0.023, 0.023, 0.023,
          0.023, 0.023, 0.023, 0.023, 0.023, 0.023, 0.023, 0.023, 0.023, 0.023,
          0.023, 0.023, 0.023, 0.023, 0.023, 0.023, 0.023, 0.023, 0.023,
RCURVE = -1000000, -1000000,
          -1000000, -1000000, -1000000, -1000000, -1000000, -1000000, -1000000, -1000000,
-1000000, 2.001,
          2.001, 2.001, 2.001, 2.001, 2.001, 2.001, 2.001, 2.001, 2.001, 2.001,
          2.001, 1000000, 1000000, 1000000, 1000000, 1000000, 1000000, 1000000, -4.002, -
4.002,
          -4.002, -4.002, 1000000, 1000000, 1000000, 1000000, 1000000, 1000000, 1000000,
ISW =     0, 0,
          0, 0, 0, 0, 0, 0, 0, 0, 0, 0,
          0, 0, 0, 0, 0, 0, 0, 0, 0, 0,
          0, 0, 0, 0, 0, 0, 0, 0, 0, 0,
          0, 0, 0, 0, 0, 0, 0, 0, 0, 0,
RGHNS =   0.000064, 0.000064,
          0.000064, 0.000064, 0.000064, 0.000064, 0.000064, 0.000064, 0.000064, 0.000064,
0.000064, 0.000064,
          0.000064, 0.000064, 0.000064, 0.000064, 0.000064, 0.000064, 0.000064, 0.000064,
0.000064, 0.000064,
          0.000064, 0.000064, 0.000064, 0.000064, 0.000064, 0.000064, 0.000064, 0.000064,
0.000064, 0.000064,
          0.000064, 0.000064, 0.000064, 0.000064, 0.000064, 0.000064, 0.000064, 0.000064,
0.000064,
ISOST =
IWFLUX = 0,
QW =      0, 0,
          0, 0, 0, 0, 0, 0, 0, 0, 0, 0,
          0, 0, 0, 0, 0, 0, 0, 0, 0, 0,
          0, 0, 0, 0, 0, 0, 0, 0, 0, 0,
          0, 0, 0, 0, 0, 0, 0, 0, 0,
&END
&CONDDATA
NP1=      5 ,
T1=       400 , 800 , 900 , 1100 , 1650 ,
K1=       0.0636 , 0.0617 , 0.0602 , 0.0582 , 0.0551 ,
NP2=      6 ,
T2=       130 , 300 , 500 , 800 , 1200 , 1800 ,
K2=       0.0316 , 0.018 , 0.0114 , 0.00864 , 0.00744 , 0.00864 ,
NP3=      2 ,
T3=       100 , 2000 ,
K3=       0.75 , 0.0125 ,
&END
REACTANTS
H 2.000                                    100.00       0.0 G 298.15 F
O 2.000                                    100.     -3146.9 L  83.3  O

END

FINISH
```

SAMPLE OF **THERMO.DAT** FILE

THERMO.DAT is needed as a separate file if IWFLUX is set to zero (IWFLUX=0) in &RTEDATA. This file is supplied as an ASCII file (THERMOSA.DAT). If the program is moved to a new operating system THERMOSA.DAT must be attached to RTE.INP for the first run, instead of REACTANT data. Then by running RTE the binary format of

THERMO.DAT will be generated. Note that if you have received the WINDOWS version of RTE the binary file of THERMO.DAT is already a part of the package. A partial listing of ASCII format of THERMO.DAT is given bellow:

```
THERMO
   300.000  1000.000  5000.000
E                 L02/67E  1.0  0.0  0.0  0.G   300.000  5000.000      0.00000 1
 0.25000000E 01     0.00000000     0.00000000     0.00000000     0.00000000    2
-0.74537496E 03-0.11734026E 02 0.25000000E 01     0.00000000     0.00000000    3
     0.00000000     0.00000000-0.74537500E 03-0.11734026E 02     0.00000000    4
AL                J 6/79AL 1.   0.   0.   0.G   300.000  5000.000     26.98154 1
 0.25561389E 01-0.10072150E-03 0.68901481E-07-0.20503307E-10 0.22331058E-14    2
 0.38899208E 05 0.52516077E 01 0.28588767E 01-0.16963453E-02 0.32120695E-05    3
-0.27578166E-08 0.88926440E-12 0.38853482E 05 0.38750889E 01     0.00000000    4
AL+               J 6/79AL 1.E -1.   0.   0.G   300.000  5000.000     26.98154 1
 0.25078778E 01-0.17718291E-04 0.13696497E-07-0.43266360E-11 0.48066244E-15    2
 0.10713754E 06 0.37356724E 01 0.24948978E 01 0.38124702E-04-0.99507420E-07    3
 0.10964185E-09-0.43146931E-13 0.10714056E 06 0.37990113E 01     0.00000000    4
AL-               J 6/79AL 1.E  1.   0.   0.G   300.000  5000.000     26.98154 1
 0.20396369E 01 0.83502844E-03-0.33224315E-06 0.54948566E-10-0.33528088E-14    2
 0.33916449E 05 0.84890118E 01 0.26297902E 01-0.43426365E-03 0.34020091E-06    3
 0.20861285E-09-0.15032237E-12 0.33727771E 05 0.53309683E 01     0.00000000    4
ALBO2             J 6/66AL 1.B  1.O  2.   0.G   300.000  5000.000     69.79034 1
 0.71722995E 01 0.29780741E-02-0.12431107E-05 0.23188779E-09-0.16041208E-13    2
-0.67683682E 05-0.99949242E 01 0.23087234E 01 0.18890539E-01-0.20633348E-04    3
 0.10251324E-07-0.16941283E-11-0.66482167E 05 0.14463834E 02     0.00000000    4
ALBR              J 9/79AL 1.BR 1.   0.   0.G   300.000  5000.000    106.88554 1
 0.43822424E 01 0.21200707E-03-0.70764447E-07 0.10659018E-10 0.14830266E-15    2
 0.57616849E 03 0.37259456E 01 0.34900611E 01 0.45476797E-02-0.81935578E-05    3
 0.68666152E-08-0.21765058E-11 0.72945306E 03 0.78734846E 01     0.00000000    4
ALBR3             J 9/79AL 1.BR 3.   0.   0.G   300.000  5000.000    266.69354 1
 0.96150590E 01 0.44468546E-03-0.19902983E-06 0.39251818E-10-0.28427975E-14    2
-0.52349544E 05-0.13132272E 02 0.62537206E 01 0.16080217E-01-0.28659758E-04    3
 0.23616076E-07-0.73931314E-11-0.51735211E 05 0.26704951E 01     0.00000000    4
ALC               J 6/63AL 1.C  1.   0.   0.G   300.000  5000.000     38.99254 1
 0.41564478E 01 0.44692490E-03-0.17467040E-06 0.34304336E-10-0.24772706E-14    2
 0.81606605E 05 0.28915623E 01 0.26422483E 01 0.64465161E-02-0.95892376E-05    3
 0.69040805E-08-0.19430779E-11 0.81929874E 05 0.10254199E 02     0.00000000    4
ALCL              J 9/79AL 1.CL 1.   0.   0.G   300.000  5000.000     62.43454 1
 0.43395271E 01 0.24838874E-03-0.82921852E-07 0.12342319E-10-0.23755818E-16    2
-0.75281081E 04 0.25241385E 01 0.31222286E 01 0.59280474E-02-0.10415832E-04    3
 0.85551065E-08-0.26722380E-11-0.73075839E 04 0.82402004E 01     0.00000000    4
ALCL+             J 6/76AL 1.CL 1.E -1.   0.G   300.000  5000.000     62.43454 1
 0.46284965E 01-0.34750535E-03 0.22997351E-06-0.24279798E-10-0.26440544E-15    2
 0.10220447E 06 0.14172573E 01 0.28698352E 01 0.66534586E-02-0.11327707E-04    3
 0.90702974E-08-0.27794640E-11 0.10259741E 06 0.10006810E 02     0.00000000    4
ALCLF             J 6/76AL 1.CL 1.F  1.   0.G   300.000  5000.000     81.43294 1
 0.64262622E 01 0.67861168E-03-0.31186392E-06 0.62142379E-10-0.42519573E-14    2
-0.60938769E 05-0.30754283E 01 0.32175968E 01 0.14524549E-01-0.23922488E-04    3
 0.18621609E-07-0.55903667E-11-0.60305508E 05 0.12258661E 02     0.00000000    4
ALCLF+            J 6/76AL 1.CL 1.F  1.E -1.G   300.000  5000.000     81.43294 1
 0.68835905E 01 0.70509366E-03-0.31366088E-06 0.61607310E-10-0.44490537E-14    2
 0.31005990E 05-0.84952610E 01 0.37341292E 01 0.13889043E-01-0.22222539E-04    3
 0.16937683E-07-0.50061342E-11 0.31647755E 05 0.66560000E 01     0.00000000    4
ALCLF2            J 6/76AL 1.CL 1.F  2.   0.G   300.000  5000.000    100.43135 1
 0.88674544E 01 0.12933319E-02-0.57468796E-06 0.11278419E-09-0.81398154E-14    2
-0.12309250E 06-0.15613943E 02 0.34905245E 01 0.23410622E-01-0.36730802E-04    3
 0.27577485E-07-0.80570874E-11-0.12197857E 06 0.10346676E 02     0.00000000    4
                      .
                      .
                      .
                      .
                      .
                      .
                      .
                      .
                      .
                      .
                      .
```

```
                    .
                    .
                    .
                    .
                    .
                    .
                    .
                    .
                    .
                    .
                    .
                    .
                    .
ZRN(S)            J 6/61ZR 1.N  1.   0.   0.S   300.000  3225.000    105.22670 1
 0.55407820E 01 0.61839353E-03 0.29542110E-06-0.11784311E-09 0.15241430E-13    2
-0.45751324E 05-0.27420654E 02 0.28556290E 01 0.86166970E-02-0.53486638E-05    3
-0.28804219E-08 0.31087849E-11-0.45112020E 05-0.13901069E 02     0.00000000    4
ZRN(L)            J 6/61ZR 1.N  1.   0.   0.L  3225.000  5000.000    105.22670 1
 0.70451164E 01     0.00000000     0.00000000     0.00000000     0.00000000    2
-0.38105527E 05-0.34436264E 02 0.70451164E 01     0.00000000     0.00000000    3
     0.00000000     0.00000000-0.38105527E 05-0.34436264E 02     0.00000000    4
ZRO2(A)           J12/65ZR 1.O  2.   0.   0.S   300.000  1478.000    123.21880 1
-0.22144395E 02 0.99639763E-01-0.12006688E-03 0.64686736E-07-0.13004881E-10    2
-0.12732797E 06 0.11100891E 03-0.79537106E 00 0.43933458E-01-0.81214444E-04    3
 0.69567648E-07-0.22380947E-10-0.13311967E 06 0.53221009E 00     0.00000000    4
ZRO2(B)           J12/65ZR 1.O  2.   0.   0.S  1478.000  2950.000    123.21880 1
 0.89573629E 01     0.00000000     0.00000000     0.00000000     0.00000000    2
-0.13414354E 06-0.45274017E 02 0.89573629E 01     0.00000000     0.00000000    3
     0.00000000     0.00000000-0.13414354E 06-0.45274017E 02     0.00000000    4
ZRO2(L)           J12/65ZR 1.O  2.   0.   0.L  2950.000  5000.000    123.21880 1
 0.10567675E 02     0.00000000     0.00000000     0.00000000     0.00000000    2
-0.12842745E 06-0.54592264E 02 0.10567675E 02     0.00000000     0.00000000    3
     0.00000000     0.00000000-0.12842745E 06-0.54592264E 02     0.00000000    4
END                        0.   0.   0.   0.      0.000     0.000
```

SAMPLE OF **TRANS.DAT** FILE

Similar to THERMO.DAT, transport properties file of hot-gas (TRANS.DAT) is needed as a separate file if IWFLUX is set to zero (IWFLUX=0) in &RTEDATA. This file is supplied as an ASCII file (TRANSSA.DAT). If the program is moved to a new operating system TRANSSA.DAT must be attached to RTE.INP for the first run (second run after performing the same task for THERMO.DAT), instead of REACTANT data. Then by running RTE the binary format of TRANS.DAT will be generated. Note that if you have received the WINDOWS version of RTE the binary file of TRANS.DAT is already a part of the package. A listing of ASCII format of TRANS.DAT is given bellow:

```
TRANSPORT PROPERTY COEFFICIENTS
C                                V2C2  GORDON; NASA TM86885, OCT 1984
 V    50.00   500.00 0.57664156E 00-0.35019433E 02 0.12224627E 04 0.19526199E 01
 V   500.00  5000.00 0.63946695E 00-0.17638455E 02 0.47303914E 04 0.15133911E 01
 C    50.00   500.00 0.62665106E 00-0.18331584E 02 0.83902096E 03 0.25707432E 01
 C   500.00  5000.00 0.80309997E 00 0.26034111E 03-0.46773038E 05 0.11072852E 01
CH                               V2C2  GORDON; NASA TM86885, OCT 1984
 V    50.00   500.00 0.51572122E 00-0.74707840E 02 0.19719001E 04 0.23318835E 01
 V   500.00  5000.00 0.63895175E 00-0.21086915E 02 0.39704839E 04 0.14508179E 01
 C    50.00   500.00 0.52513903E 00-0.73145794E 02 0.19408307E 04 0.34518423E 01
 C   500.00  5000.00 0.64819976E 00-0.34110542E 03 0.84313328E 05 0.28934974E 01
CH4                              V2C2  GORDON; NASA TM86885, OCT 1984
 V    50.00   500.00 0.61285983E 00-0.82167119E 02 0.18475609E 04 0.14747394E 01
 V   500.00  5000.00 0.65340841E 00 0.25977551E 02-0.20120034E 05 0.10943269E 01
 C    50.00   500.00 0.15044605E 01 0.11382256E 03-0.26842459E 04-0.30431470E 01
 C   500.00  5000.00 0.45982942E 00-0.10509052E 04 0.15791881E 06 0.51358693E 01
CO                               V2C2  GORDON; NASA TM86885, OCT 1984
 V    50.00   500.00 0.51840229E 00-0.86401891E 02 0.21168247E 04 0.24881742E 01
 V   500.00  5000.00 0.63942307E 00-0.16043078E 02-0.34528052E 03 0.16052082E 01
```

```
 C    50.00   500.00 0.62893503E 00-0.59279284E 02 0.14545124E 04 0.21849702E 01
 C   500.00  5000.00 0.59002712E 00-0.35600085E 03 0.70771415E 05 0.27429431E 01
CO2                                V2C2  GORDON; NASA TM86885, OCT 1984
 V    50.00   500.00 0.71298372E 00-0.65673504E 02 0.14963183E 04 0.11548638E 01
 V   500.00  5000.00 0.65015925E 00 0.18410033E 02-0.27377624E 05 0.14926219E 01
 C    50.00   500.00 0.12325046E 01 0.17577905E 02-0.82083093E 03-0.18858575E 01
 C   500.00  5000.00 0.62902371E 00-0.22453540E 03-0.15727615E 05 0.24083935E 01
H                                  V2C2  GORDON; NASA TM86885, OCT 1984
 V    50.00   500.00 0.55995219E 00-0.43305205E 02 0.13988573E 04 0.12513079E 01
 V   500.00  5000.00 0.63779530E 00-0.23016980E 02 0.60571893E 04 0.70833314E 00
 C    50.00   500.00 0.55942885E 00-0.43471877E 02 0.13985506E 04 0.46873025E 01
 C   500.00  5000.00 0.63745095E 00-0.23949330E 02 0.62706766E 04 0.41438921E 01
H2                                 V2C2  GORDON; NASA TM86885, OCT 1984
 V   50.000  500.000 0.52212423E 00-0.67665387E 02 0.18585313E 04 0.17199202E 01
 V  500.000 5000.000 0.63757943E 00-0.24838511E 02 0.55837133E 04 0.90185688E 00
 C   50.000  500.000 0.12836605E 01 0.11455825E 03-0.24998764E 04-0.42170152E 00
 C  500.000 5000.000 0.88550133E 00 0.30164014E 03-0.99040245E 05 0.20646994E 01
H2O                                V2C2  GORDON; NASA TM86885, OCT 1984
 V  200.000 1000.000 0.94668769E 00-0.69050351E 02 0.11018645E 05-0.60008112E 00
 V 1000.000 5000.000 0.58468518E 00-0.46488533E 03 0.27934880E 05 0.22794623E 01
 C  200.000 1000.000 0.14468338E 01 0.17203212E 03-0.38723374E 04-0.31068889E 01
 C 1000.000 5000.000 0.50651995E 00-0.14110690E 04 0.31752127E 06 0.46502768E 01
H2O2                               V2C2  GORDON; NASA TM86885, OCT 1984
 V   50.000  500.000 0.90482890E 00-0.21439944E 02 0.69480678E 03-0.51475862E 00
 V  500.000 5000.000 0.62689431E 00-0.62039801E 02-0.23897053E 05 0.13920631E 01
 C   50.000  500.000 0.14029337E 01 0.56011042E 02-0.14091735E 04-0.30326144E 01
 C  500.000 5000.000 0.59326745E 00-0.49202617E 03 0.34391846E 05 0.29520144E 01
O                                  V2C2  GORDON; NASA TM86885, OCT 1984
 V   50.000  500.000 0.53932114E 00-0.87466991E 02 0.20749216E 04 0.24324848E 01
 V  500.000 5000.000 0.64852989E 00 0.84773546E 01-0.82600710E 04 0.16032465E 01
 C   50.000  500.000 0.52921368E 00-0.74978154E 02 0.18304585E 04 0.31659144E 01
 C  500.000 5000.000 0.73002806E 00 0.16087118E 03-0.32030077E 05 0.15816751E 01
OH                                 V2C2  GORDON; NASA TM86885, OCT 1984
 V   50.000  500.000 0.51566598E 00-0.81060512E 02 0.20553653E 04 0.25894132E 01
 V  500.000 5000.000 0.64201860E 00-0.12095925E 02 0.60829603E 03 0.16720403E 01
 C   50.000  500.000 0.44556585E 00-0.10023169E 03 0.25434520E 04 0.39610822E 01
 C  500.000 5000.000 0.70273668E 00-0.23912109E 03 0.69412155E 05 0.23731702E 01
O2                                 V2C2  GORDON; NASA TM86885, OCT 1984
 V   50.000  500.000 0.53917653E 00-0.87475338E 02 0.20721199E 04 0.25236763E 01
 V  500.000 5000.000 0.64854183E 00 0.84278487E 01-0.82330148E 04 0.16934280E 01
 C   50.000  500.000 0.78398875E 00-0.29780881E 02 0.68993582E 03 0.12373559E 01
 C  500.000 5000.000 0.75890427E 00-0.49408342E 01-0.86556363E 04 0.13809483E 01
LAST

END
```

FLUX.DAT input file

This file is a matrix of heat fluxes for different temperatures and all points along the axial direction of the nozzle. Rows of this matrix correspond different locations and its columns are different temperature. The first row of this file consists of two integers: the first integer gives the number of rows in the matrix (number of position points) and the second integer gives the number columns (number of temperature points). The sample FLUX.DAT file in the next page has 252 rows and 16 columns. Temperatures in this file are from 1000R to 2500R with increments of 100R and positions cover the whole nozzle and thrust chamber.

```
   252   16
       1010  1110  1210  1310  1410  1510  1610  1710  1810  1910  2010  2110  2210  2310  2410  2510
-6.377  25.11 24.75 24.35 23.92 23.42 22.88 22.23 21.54 20.78 19.99 19.24 18.63 18.11 17.71 17.34 17.01
-5.997  25.11 24.75 24.35 23.92 23.42 22.88 22.23 21.54 20.78 19.99 19.24 18.63 18.11 17.71 17.34 17.01
-5.012  25.11 24.75 24.35 23.92 23.42 22.88 22.23 21.54 20.78 19.99 19.24 18.63 18.11 17.71 17.34 17.01
-3.998  25.11 24.75 24.35 23.92 23.42 22.88 22.23 21.54 20.78 19.99 19.24 18.63 18.11 17.71 17.34 17.01
-3.014  25.11 24.75 24.35 23.92 23.42 22.88 22.23 21.54 20.78 19.99 19.24 18.63 18.11 17.71 17.34 17.01
-2.001  25.11 24.75 24.35 23.92 23.42 22.88 22.23 21.54 20.78 19.99 19.24 18.63 18.11 17.71 17.34 17.01
-1.495  25.11 24.75 24.35 23.92 23.42 22.88 22.23 21.54 20.78 19.99 19.24 18.63 18.11 17.71 17.34 17.01
-1.020  33.29 32.88 32.41 31.88 31.27 30.59 29.76 28.87 25.38 24.46 23.59 22.90 22.32 21.87 21.47 21.10
-0.997  35.16 34.72 34.21 33.66 32.00 32.27 31.40 30.45 27.06 26.07 25.13 24.40 23.78 23.30 22.88 22.48
-0.974  36.90 36.44 35.90 35.31 34.61 33.85 32.93 31.92 28.63 27.57 26.57 25.79 25.14 24.63 24.18 23.75
-0.952  38.59 38.10 37.54 36.92 36.18 35.37 34.40 33.33 30.09 28.97 27.92 27.08 26.39 25.85 25.38 24.93
-0.931  40.30 39.79 39.20 38.54 37.77 36.92 35.91 34.79 31.44 30.26 29.16 28.28 27.56 26.99 26.50 26.03
-0.911  42.06 41.52 40.90 40.21 39.41 38.52 37.45 36.28 32.79 31.57 30.41 29.50 28.74 28.15 27.62 27.14
-0.891  43.80 43.23 42.58 41.86 41.02 40.09 38.96 37.74 34.22 32.93 31.71 30.76 29.96 29.35 28.81 28.30
-0.872  45.51 44.91 44.23 43.47 42.61 41.63 40.46 39.18 35.64 34.29 33.02 32.03 31.19 30.55 29.99 29.45
-0.853  47.23 46.61 45.90 45.11 44.20 43.18 41.97 40.64 37.04 35.62 34.30 33.26 32.40 31.72 31.13 30.58
                              .
                                    .
                                    .
                                    .
                                    .
-0.277  92.80 91.43 89.88 88.13 86.10 83.81 81.04 78.02 74.01 70.86 67.96 65.87 64.10 62.71 61.44 60.21
-0.264  93.38 92.00 90.43 88.66 86.61 84.30 81.50 78.44 74.43 71.23 68.33 66.24 64.47 63.06 61.78 60.56
-0.252  93.93 92.54 90.95 89.17 87.10 84.78 81.95 78.85 74.83 71.63 68.70 66.60 64.83 63.42 62.13 60.89
-0.240  94.46 93.05 91.46 89.64 87.56 85.22 82.36 79.24 75.22 71.99 69.05 66.94 65.16 63.75 62.45 61.21
-0.227  94.94 93.52 91.90 90.08 87.98 85.62 82.72 79.58 75.59 72.34 69.38 67.28 65.49 64.07 62.77 61.52
-0.215  95.40 93.99 92.35 90.50 88.38 86.01 83.08 79.92 75.93 72.65 69.68 67.58 65.80 64.36 63.07 61.80
-0.203  95.83 94.40 92.75 90.88 88.76 86.36 83.41 80.22 76.25 72.94 69.96 67.87 66.07 64.64 63.34 62.07
                                    .
                                    .
                                    .
                                    .
                                    .
-0.023  98.22 96.68 94.92 92.89 90.56 87.95 84.68 81.17 77.58 74.18 71.18 69.25 67.59 66.20 64.88 63.57
-0.015  97.95 96.42 94.65 92.63 90.31 87.67 84.40 80.88 77.42 74.00 70.99 69.11 67.48 66.10 64.78 63.47
-0.008  97.61 96.09 94.32 92.29 89.96 87.31 84.04 80.53 77.17 73.75 70.79 68.91 67.30 65.92 64.60 63.30
-0.001  97.20 95.67 93.89 91.85 89.52 86.87 83.62 80.14 76.83 73.44 70.48 68.63 67.06 65.70 64.39 63.08
 0.000  96.77 95.25 93.48 91.47 89.14 86.51 83.27 79.79 76.50 73.15 70.22 68.37 66.78 65.43 64.12 62.82
 0.001  96.86 95.35 93.59 91.56 89.23 86.60 83.37 79.93 76.13 72.79 69.88 68.06 66.46 65.11 63.80 62.52
 0.002  97.04 95.53 93.77 91.75 89.42 86.80 83.58 80.14 76.12 72.83 69.99 68.16 66.59 65.26 63.95 62.67
 0.003  97.08 95.58 93.82 91.80 89.47 86.83 83.62 80.18 75.89 72.64 69.81 68.02 66.46 65.14 63.83 62.55
 0.005  97.03 95.53 93.77 91.74 89.39 86.74 83.56 80.12 74.94 71.76 68.98 67.22 65.68 64.36 63.06 61.80
 0.007  96.89 95.39 93.62 91.58 89.22 86.59 83.39 79.97 73.49 70.40 67.69 65.97 64.46 63.14 61.87 60.62
 0.009  96.65 95.14 93.39 91.33 88.98 86.32 83.13 79.72 71.80 68.80 66.17 64.47 62.99 61.71 60.47 59.24
 0.011  96.28 94.77 93.02 90.95 88.59 85.93 82.75 79.36 69.88 66.99 64.46 62.83 61.37 60.13 58.92 57.72
```

```
 0.015  95.73 94.22 92.47 90.39 88.03 85.36 82.22 78.85 67.87 65.09 62.65 61.04 59.64 58.44 57.24 56.07
 0.018  94.94 93.43 91.68 89.61 87.24 84.57 81.44 78.12 65.77 63.09 60.75 59.21 57.84 56.65 55.50 54.35
 0.023  93.84 92.34 90.59 88.53 86.17 83.51 80.42 77.15 63.61 61.05 58.79 57.30 55.98 54.85 53.73 52.62
 0.028  92.40 90.92 89.18 87.12 84.76 82.11 79.08 75.87 61.39 58.94 56.80 55.38 54.09 52.98 51.89 50.82
                                      .
                                      .
                                      .
                                      .
                                      .
 0.854  31.97 31.30 30.50 29.51 28.42 27.30 26.38 25.50 22.57 21.85 21.19 20.69 20.22 19.79 19.36 18.95
 0.878  31.37 30.72 29.93 28.95 27.88 26.79 25.89 25.02 22.15 21.45 20.81 20.31 19.85 19.43 19.02 18.62
 0.902  30.81 30.17 29.40 28.44 27.39 26.30 25.42 24.57 21.74 21.05 20.43 19.93 19.49 19.07 18.66 18.27
 0.926  30.22 29.62 28.87 27.91 26.89 25.82 24.96 24.12 21.32 20.65 20.03 19.56 19.11 18.71 18.30 17.92
 0.950  29.71 29.07 28.34 27.41 26.38 25.34 24.49 23.67 20.93 20.28 19.68 19.22 18.77 18.38 17.99 17.60
 0.974  29.15 28.54 27.81 26.89 25.88 24.85 24.02 23.22 20.56 19.93 19.34 18.88 18.45 18.05 17.67 17.30
 0.998  28.62 28.02 27.30 26.39 25.41 24.40 23.57 22.79 20.19 19.57 18.99 18.54 18.12 17.74 17.36 16.99
 1.023  28.09 27.50 26.80 25.90 24.94 23.94 23.13 22.37 19.83 19.21 18.66 18.21 17.80 17.42 17.05 16.69
 1.047  27.57 26.98 26.29 25.41 24.46 23.47 22.69 21.94 19.48 18.88 18.32 17.89 17.48 17.11 16.76 16.40
                                      .
                                      .
                                      .
                                      .
                                      .
                                      .
                                      .
 9.752   3.06  2.97  2.87  2.74  2.61  2.49  2.42  2.37  2.32  2.27  2.23  2.19  2.15  2.10  2.06  2.02
10.003   3.02  2.93  2.83  2.71  2.58  2.46  2.40  2.35  2.29  2.24  2.21  2.17  2.12  2.08  2.04  1.99
10.256   2.99  2.91  2.81  2.69  2.56  2.44  2.38  2.33  2.26  2.22  2.18  2.14  2.10  2.06  2.02  1.98
10.513   2.95  2.87  2.78  2.65  2.52  2.41  2.35  2.30  2.26  2.22  2.18  2.14  2.09  2.05  2.01  1.97
10.758   2.94  2.85  2.76  2.63  2.51  2.39  2.33  2.28  2.24  2.20  2.17  2.13  2.08  2.04  2.00  1.96
11.000   2.91  2.82  2.73  2.61  2.49  2.37  2.31  2.26  2.23  2.19  2.16  2.11  2.07  2.03  1.99  1.94
```

TGS.DAT data file

This file is generated by the radiation module of RTE (RTE_RAD) and contains weight factors of the volume nodes and total exchange factor from gas nodes to surface nodes. It begins with the case code assigned in RTEDATA to ensure that RTE reads the right exchange factor numbers. If there is a mismatch between the case code of RTEDATA and the radiation exchange factor's case code RTE stops and send a message of the mismatched case code.

A partial listing of TGS.DAT is given below:

```
CASECODE
    1    0.008839
    2    0.008839
    3    0.008839
    4    0.008839
    5    0.008839
    6    0.008368
       .
       .
       .
       .
  177    0.001736
  178    0.001736
  179    0.001736
  180    0.001736
  181    0.001736
  182    0.001736
  183    0.001736
  184    0.001736
  185    0.001736
   1    1   0.76654E+00
   1    2   0.58044E-01
   1    3   0.33586E-02
   1    4   0.21049E-03
   1    5   0.15036E-04
   1    6   0.38147E-04
 185   35   0.48987E-09
 185   36   0.50041E-08
 185   37   0.88018E-07
 185   38   0.16163E-05
 185   39   0.31476E-04
 185   40   0.68707E-03
 185   41   0.22496E-01
 185   42   0.25675E+01
 185   43   0.24126E+01
 185   44   0.86659E+00
 185   45   0.22498E+00
 185   46   0.53916E-01
 185   47   0.10362E-01
```

TSS.DAT data file

Similar to TGS.DAT, this file contains weight factors of surface nodes and exchange factors between surface nodes. The radiation module of RTE (RTE_RAD) generates this file. It begins with the case code assigned in RTEDATA to ensure that RTE reads the right exchange factor numbers. If there is a mismatch between the case code of RTEDATA and radiation exchange factor's case code RTE stops and send a message of mismatched case code.

A partial listing of TGS.DAT is given below:

```
CASECODE
   1     0.073592
   2     0.073592
   3     0.073592
   4     0.073592
   5     0.073592
   6     0.124826
   7     0.126371
   8     0.107213
   9     0.086943
  10     0.088059
            .
            .
            .
            .
  41     0.083333
  42     0.083333
  43     0.020833
  44     0.020833
  45     0.020833
  46     0.020833
  47     0.020833
   1    1   0.17160E-11
   1    2   0.31344E-10
   1    3   0.51322E-09
   1    4   0.95474E-08
   1    5   0.22111E-06
   1    6   0.22806E-04
   1    7   0.24689E-04
   1    8   0.48731E-05
            .
            .
            .
            .
            .
            .
   5    3   0.13283E-04
   5    4   0.30072E-03
   5    5   0.73070E-02
   5    6   0.75514E+00
   5    7   0.12975E-02
   5    8   0.18175E-04
   5    9   0.69979E-06
```

```
 5   10   0.40166E-07
          .
          .
          .
          .
          .
47   35   0.71164E-09
47   36   0.75104E-08
47   37   0.13896E-06
47   38   0.27236E-05
47   39   0.57129E-04
47   40   0.12742E-02
47   41   0.26951E-01
47   42   0.20755E+00
47   43   0.25406E-02
47   44   0.20393E-02
47   45   0.69162E-03
47   46   0.19391E-03
47   47   0.40446E-04
```

Note that the exchange factor data presented here is for an engine with RP1 propellant, which has a significant gas radiation.

APPENDIX C

WORKING WITH GRAPHIC USER INTERFACE (PREPROCESSOR) OF RTE

RTE's GRAFIC USER INTERFACE (GUI) PREPROCESSOR

RTE's graphic user interface preprocessor is the easiest way to generate a data file and run the program and its radiation module. This preprocessor is based on Microsoft's Excel Spreadsheet and has combo boxes and help buttons to facilitate inputting data. This file is RTE GUI.xls and should be saved in the same directory that all RTE's executable and data files are located.

RTE GUI.xls can be saved under any other name; for example, if it is used to generate the Space Shuttle Main Engine data it can be saved as SSME.xls, or any relevant name that a user chooses. It should be noted that the RTE preprocessor can only be used on a Microsoft Windows operating system with Excel. UNIX users can use it to generate an input data file and upload the resulting file to the UNIX machine.

WORKING WITH RTE's PREPROCESSOR

Loading it into Excel or double clicking on the file can start RTE GUI.xls. After the file is loaded a message box similar to that shown in Figure C-1 appears. Make sure to click

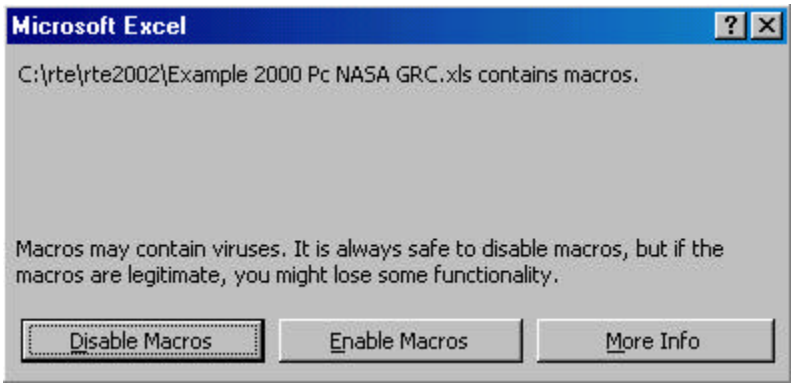

Figure C-1: Microsoft Excel warning message during loading of RTE's GUI

on the Enable Macros button. The macros are legitimate and virus free. After RTE's GUI is loaded a screen similar to that shown in Figure C-2 comes up. Scroll bars (horizontal and vertical) can be used to move around the interface. Note that the initial screen can be at a different location of the interface, depending on the position of the scroll bars when the file was last saved. Make sure to move the horizontal scroll bar to the left of the sheet and vertical scroll bar to the top of the sheet, such that the red button with caption "Initialize RTE's Pre." appears on the top left side of the screen. Then click on this red button. This initiates the combo boxes and inserts all possible options for these boxes. If the initialization is not performed correctly the preprocessor will not work correctly.

After initializing the preprocessor the user should assign a case code to the data file. All outputs of RTE will be marked with this code and helps to separate results of different cases. The case code for the example of Figure C-2 is HARCC-PC2000 (High Aspect Ratio Cooling Channel with a chamber pressure of 2000 psi). The next step is to enter the

number of stations in the appropriate box. RTE's preprocessor has help associated with any input item. A help window appears if the mouse is moved on the red spot at the upper right corner of any title box, or by clicking on the help buttons provided next to some items that need graphic help. Figure C-3 shows the help window for "number of stations" and Figure C-4 shows the help window for "dimensions of cooling channels", and "wall layers".

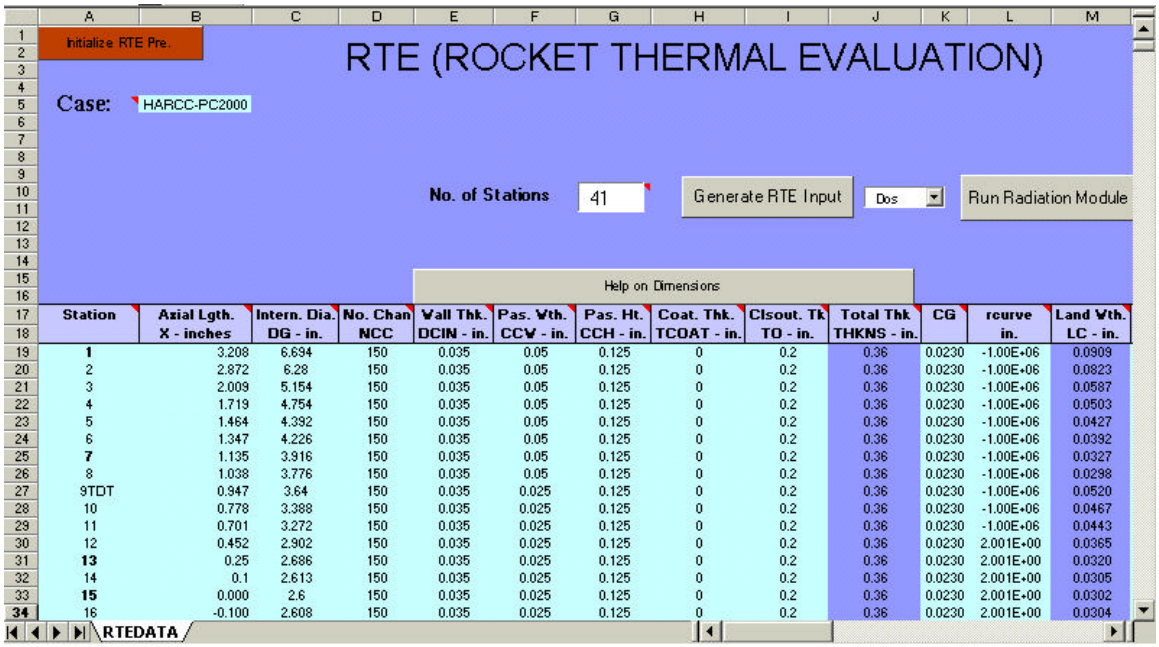

Station	Axial Lgth. X - inches	Intern. Dia. DG - in.	No. Chan NCC	Wall Thk. DCIN - in.	Pas. Wth. CCW - in.	Pas. Ht. CCH - in.	Coat. Thk. TCOAT - in.	Clsout. Tk TO - in.	Total Thk THKNS - in.	CG	rcurve in.	Land Wth. LC - in.
1	3.208	6.694	150	0.035	0.05	0.125	0	0.2	0.36	0.0230	-1.00E+06	0.0909
2	2.872	6.28	150	0.035	0.05	0.125	0	0.2	0.36	0.0230	-1.00E+06	0.0823
3	2.009	5.154	150	0.035	0.05	0.125	0	0.2	0.36	0.0230	-1.00E+06	0.0587
4	1.719	4.754	150	0.035	0.05	0.125	0	0.2	0.36	0.0230	-1.00E+06	0.0503
5	1.464	4.392	150	0.035	0.05	0.125	0	0.2	0.36	0.0230	-1.00E+06	0.0427
6	1.347	4.226	150	0.035	0.05	0.125	0	0.2	0.36	0.0230	-1.00E+06	0.0392
7	1.135	3.916	150	0.035	0.05	0.125	0	0.2	0.36	0.0230	-1.00E+06	0.0327
8	1.038	3.776	150	0.035	0.05	0.125	0	0.2	0.36	0.0230	-1.00E+06	0.0298
9TDT	0.947	3.64	150	0.035	0.025	0.125	0	0.2	0.36	0.0230	-1.00E+06	0.0520
10	0.778	3.388	150	0.035	0.025	0.125	0	0.2	0.36	0.0230	-1.00E+06	0.0467
11	0.701	3.272	150	0.035	0.025	0.125	0	0.2	0.36	0.0230	-1.00E+06	0.0443
12	0.452	2.902	150	0.035	0.025	0.125	0	0.2	0.36	0.0230	2.001E+00	0.0365
13	0.25	2.686	150	0.035	0.025	0.125	0	0.2	0.36	0.0230	2.001E+00	0.0320
14	0.1	2.613	150	0.035	0.025	0.125	0	0.2	0.36	0.0230	2.001E+00	0.0305
15	0.000	2.6	150	0.035	0.025	0.125	0	0.2	0.36	0.0230	2.001E+00	0.0302
16	-0.100	2.608	150	0.035	0.025	0.125	0	0.2	0.36	0.0230	2.001E+00	0.0304

Figure C-2: RTE's graphic user interface preprocessor

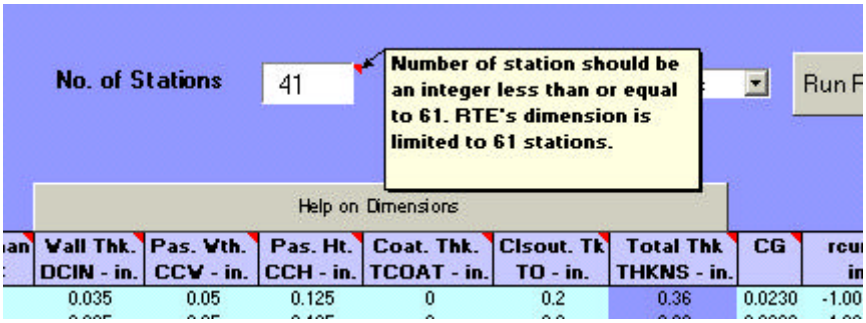

Figure C-3: A typical interactive help window of RTE

Interactive helps are provided for every input item of RTE and a user should ask for them to make sure that data are prepared correctly. A text help window disappears when the pointer is moved away from the corresponding cell. A graphic help window disappears by clicking on the corresponding help button or window.

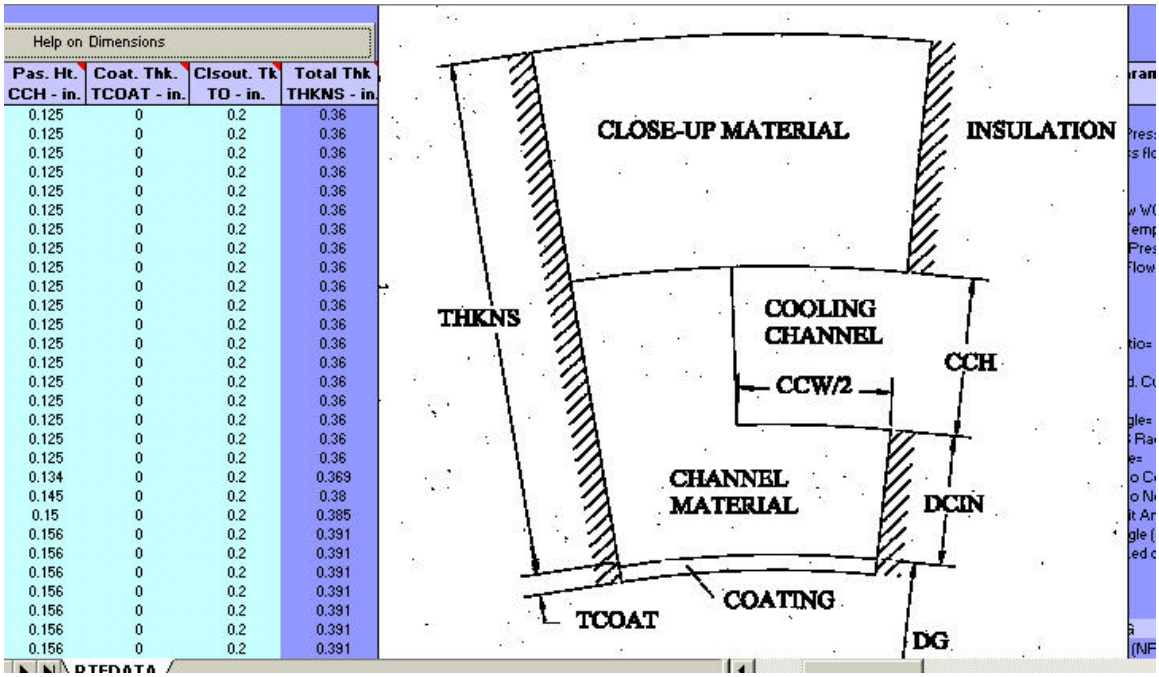

Figure C-4: Help window for dimensions of cooling channels

After entering the number of stations the user can enter station numbers, and nozzle, wall and cooling channel dimensions in their respective boxes, as shown in Figure C5. The user can only enter numbers in those cells with a light blue color. Other cells, which are darker blue or red colors, are protected and their numbers are calculated automatically based on other inputs. By making a station number bold RTE will provide isotherm data file for that station, which can be read and plotted using TecPlot. Up to ten isotherm data files can be generated by RTE (do not make more than ten station number bold). Some stations, in the data of Figure C-5, are identified with different tangent points. These tangent point identifications are not used in RTE and are only for identifying different tangent points and they can be eliminated from the input data. Note that the maximum allowable number of stations is 61. Additional four columns for swiler, surface roughness, wall heat flux and O/F are in the RTE's preprocessor, which is not shown in the Figure C-5 due to space limitation.

Figure C-6 shows various combo boxes for selecting engine specifications. For example, for coolant the user can select from the listed coolants that RTE support. Material selection offers a listing of 13 built-in material conductivities for each layer of the wall, which are listed in the main section of the manual (see Figure C-7). In addition to these materials the user has an option to input user-defined conductivities. For user-defined conductivities either USER1, USER2 or USER3 must be selected from the material combo boxes. Then the corresponding conductivities as functions of temperature can be

defined in the tables shown in Figure C-7. There are three tables for user-defined thermal conductivity, with only two tables shown in the figure. Each material's thermal conductivities can be defined as a function of temperature using maximum of ten points.

Axial Lgth. X - inches	Intern. Dia. DG - in.	No. Chan NCC	Wall Thk. DCIN - in.	Pas. Wth. CCW - in.	Pas. Ht. CCH - in.	Coat. Thk. TCOAT - in.	Clsout. Tk TO - in.	Total Thk THKNS - in.	CG	rcurve in.	Land Wth. LC - in.	Ch. Aspct. Ratio
3.208	6.694	150	0.035	0.05	0.125	0	0.2	0.36	0.0230	-1.00E+06	0.0909	2.500
2.872	6.28	150	0.035	0.05	0.125	0	0.2	0.36	0.0230	-1.00E+06	0.0823	2.500
2.009	5.154	150	0.035	0.05	0.125	0	0.2	0.36	0.0230	-1.00E+06	0.0587	2.500
1.719	4.754	150	0.035	0.05	0.125	0	0.2	0.36	0.0230	-1.00E+06	0.0503	2.500
1.464	4.392	150	0.035	0.05	0.125	0	0.2	0.36	0.0230	-1.00E+06	0.0427	2.500
1.347	4.226	150	0.035	0.05	0.125	0	0.2	0.36	0.0230	-1.00E+06	0.0392	2.500
1.135	3.916	150	0.035	0.05	0.125	0	0.2	0.36	0.0230	-1.00E+06	0.0327	2.500
1.038	3.776	150	0.035	0.05	0.125	0	0.2	0.36	0.0230	-1.00E+06	0.0298	2.500
0.947	3.64	150	0.035	0.025	0.125	0	0.2	0.36	0.0230	-1.00E+06	0.0520	5.000
0.778	3.388	150	0.035	0.025	0.125	0	0.2	0.36	0.0230	-1.00E+06	0.0467	5.000
0.701	3.272	150	0.035	0.025	0.125	0	0.2	0.36	0.0230	-1.00E+06	0.0443	5.000
0.452	2.902	150	0.035	0.025	0.125	0	0.2	0.36	0.0230	2.001E+00	0.0365	5.000
0.25	2.686	150	0.035	0.025	0.125	0	0.2	0.36	0.0230	2.001E+00	0.0320	5.000
0.1	2.613	150	0.035	0.025	0.125	0	0.2	0.36	0.0230	2.001E+00	0.0305	5.000
0.000	2.6	150	0.035	0.025	0.125	0	0.2	0.36	0.0230	2.001E+00	0.0302	5.000
-0.100	2.608	150	0.035	0.025	0.125	0	0.2	0.36	0.0230	2.001E+00	0.0304	5.000
-0.274	2.656	150	0.035	0.025	0.125	0	0.2	0.36	0.0230	2.001E+00	0.0314	5.000
-0.506	2.746	150	0.035	0.025	0.125	0	0.2	0.36	0.0230	2.001E+00	0.0332	5.000
-0.906	2.924	150	0.035	0.025	0.125	0	0.2	0.36	0.0230	2.001E+00	0.0370	5.000
-1.306	3.092	150	0.035	0.025	0.134	0	0.2	0.369	0.0230	2.001E+00	0.0405	5.360
-1.706	3.264	150	0.035	0.025	0.145	0	0.2	0.38	0.0230	2.001E+00	0.0441	5.800
-1.906	3.344	150	0.035	0.025	0.15	0	0.2	0.385	0.0230	2.001E+00	0.0458	6.000
-2.106	3.432	150	0.035	0.025	0.156	0	0.2	0.391	0.0230	2.001E+00	0.0476	6.240
-2.306	3.516	150	0.035	0.025	0.156	0	0.2	0.391	0.0230	1.00E+06	0.0494	6.240
-2.506	3.602	150	0.035	0.025	0.156	0	0.2	0.391	0.0230	1.00E+06	0.0512	6.240
-2.906	3.77	150	0.035	0.025	0.156	0	0.2	0.391	0.0230	1.00E+06	0.0547	6.240
-3.106	3.86	150	0.035	0.025	0.156	0	0.2	0.391	0.0230	1.00E+06	0.0566	6.240
-3.306	3.94	150	0.035	0.025	0.156	0	0.2	0.391	0.0230	1.00E+06	0.0583	6.240
-3.506	4.022	150	0.035	0.025	0.156	0	0.2	0.391	0.0230	1.00E+06	0.0600	6.240
-3.706	4.1	150	0.035	0.025	0.156	0	0.2	0.391	0.0230	1.00E+06	0.0616	6.240
-3.906	4.17	150	0.035	0.05	0.156	0	0.2	0.391	0.0230	-4.002E+00	0.0381	3.120
-4.106	4.236	150	0.035	0.05	0.156	0	0.2	0.391	0.0230	-4.002E+00	0.0395	3.120
-4.506	4.358	150	0.035	0.05	0.156	0	0.2	0.391	0.0230	-4.002E+00	0.0420	3.120
-5.5	4.6	150	0.035	0.05	0.156	0	0.2	0.391	0.0230	-4.002E+00	0.0471	3.120
-5.906	4.666	150	0.035	0.05	0.156	0	0.2	0.391	0.0230	1.00E+06	0.0485	3.120
-6.106	4.694	150	0.035	0.05	0.156	0	0.2	0.391	0.0230	1.00E+06	0.0490	3.120
-6.506	4.744	150	0.035	0.05	0.156	0	0.2	0.391	0.0230	1.00E+06	0.0501	3.120
-7.572	4.8	150	0.035	0.05	0.156	0	0.2	0.391	0.0230	1.00E+06	0.0513	3.120
-8.35	4.8	150	0.035	0.05	0.156	0	0.2	0.391	0.0230	1.00E+06	0.0513	3.120
-9	4.8	150	0.035	0.05	0.156	0	0.2	0.391	0.0230	1.00E+06	0.0513	3.120
-9.375	4.8	150	0.035	0.05	0.156	0	0.2	0.391	0.0230	1.00E+06	0.0513	3.120
								0				
								0				

DO NOT GO BEYOND THIS POINT, RTE TAKES MAXIMUM OF 61 STATIONS

Figure C-5: Input data for the geometry of nozzle, wall and cooling channel

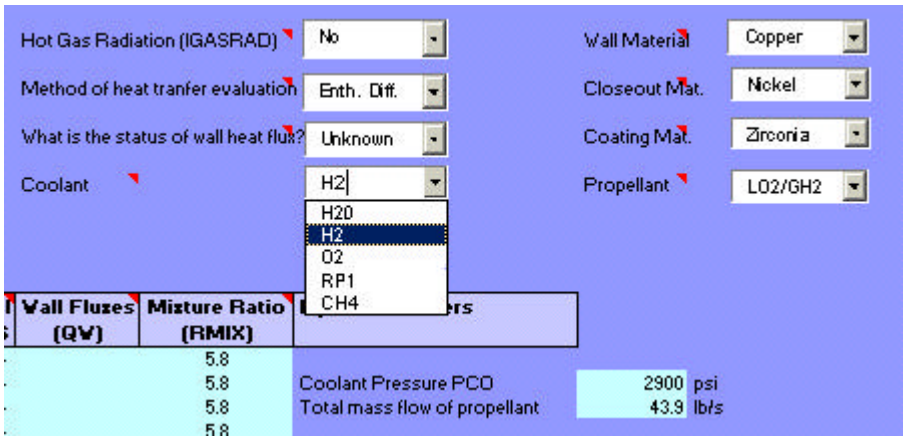

Figure C-6: Combo boxes in the RTE's preprocessor for selecting engine specifications

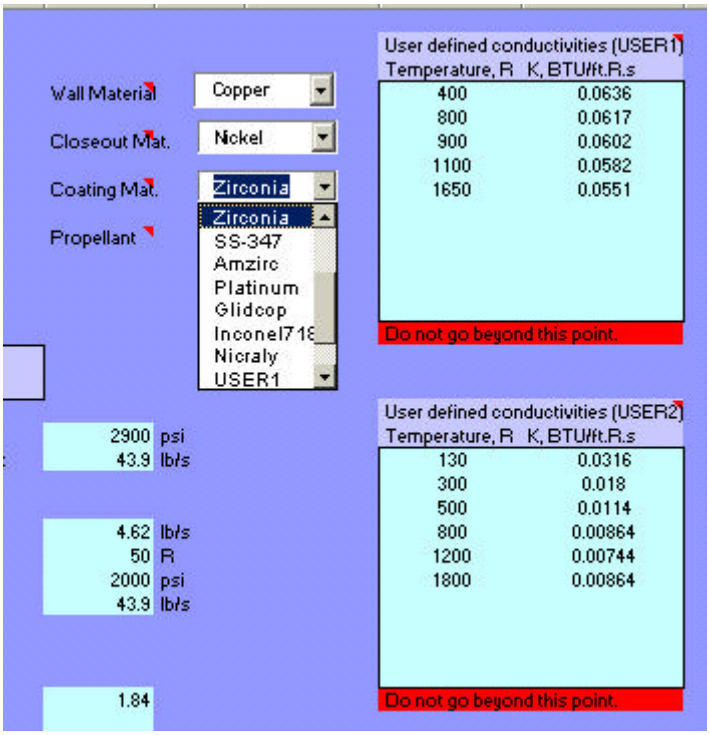

Figure C-7: Material selection from combo boxes from RTE's preprocessor

Figure C-8 shows the meshing of a wall section at various layers. By clicking on the "Help on Meshing" button a window containing meshing nomenclature appears on the screen, which can be used to specify the number of nodes at different sections of the wall (i.e., NPHIL, NPHIC, NRCLO, NRCHT, NRCHB and NRCOAT). Other parts shown in Figure C-8 include: outer surface boundary conditions (Natural Convection, Forced Convection or Radiation), method of cooling (Regeneratively or Radiatively) and coolant side correlation selections. Five built-in correlations that are discussed in the main part of this manual are available for the user to choose from. These correlations can be viewed by clicking on "Help on selecting coolant correlation." The cells shown if Figure C-9

must be filled if the USER-DEFINED correlation is selected, otherwise, they are ignored. Numbers in these cells are the coefficient and exponents of the user-defined correlation that is shown in the help window.

After all numbers are entered and appropriate selections are made in the combo boxes the user can click on “Generate RTE data” button to produce the input file of RTE. Before clicking on this button make sure appropriate the editor is selected for viewing RTE’s input file. Three editors are available for viewing the data file: DOS, Notepad and Word. The DOS editor is the most reliable option since it can be called from any directory. Notepad and Word in some cases do not show the results since they might be installed in different directories that RTE’s preprocessor is not pointed to.

After clicking on “Generate RTE’s Input” a window similar to that shown in Figure C-11 appears on the screen and requests the name of the file that RTE’s input file should be save in. After entering a file name and clicking on OK button RTE’s input in its namelist format will be generated.

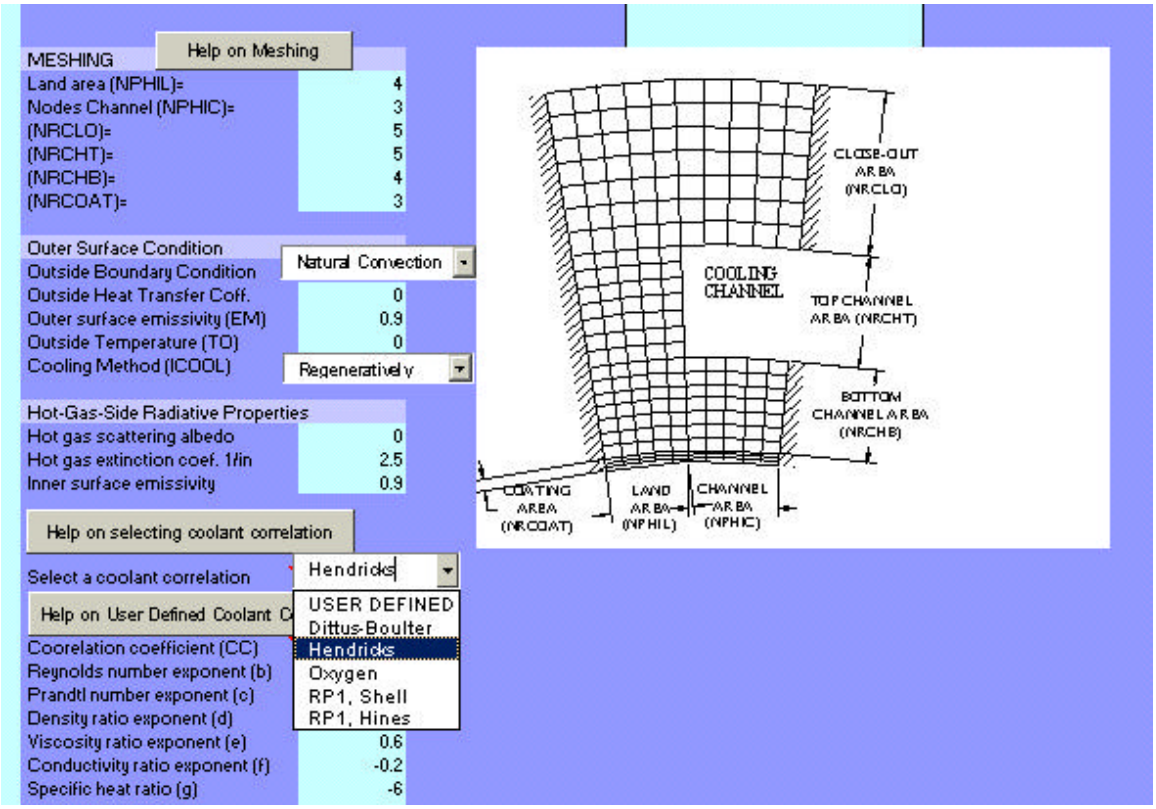

Figure C-8: Other parts of RTE’s preprocessor for meshing and cooling options

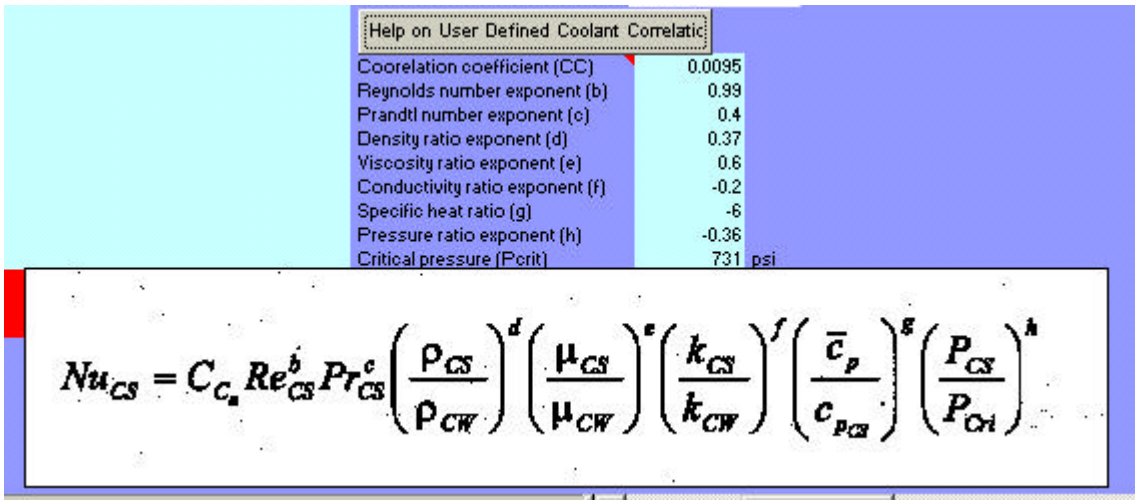

Figure C-9: User-defined coolant correlation input section with help window

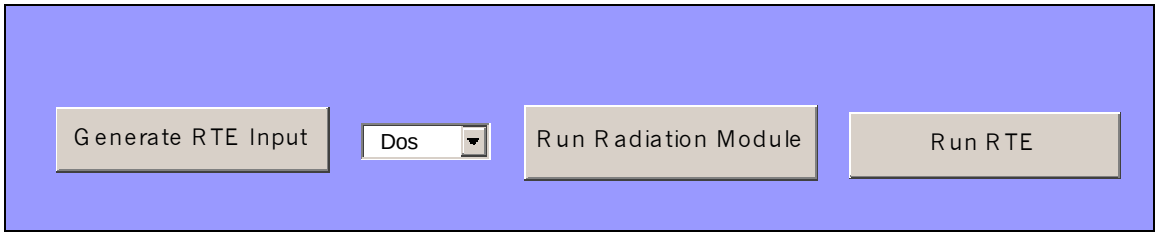

Figure C-10: Command buttons for generating rte input file, running radiation module and RTE.

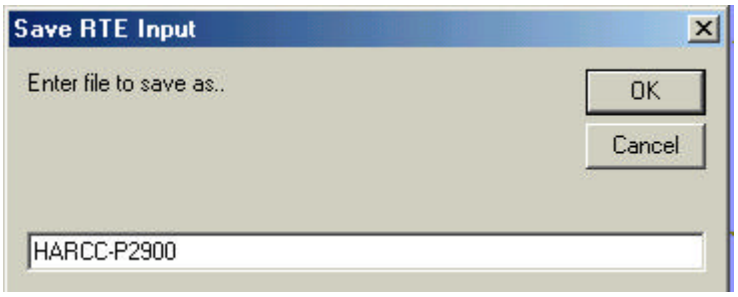

Figure C-11: Input box requesting name of the file that RTE's input data should be saved in

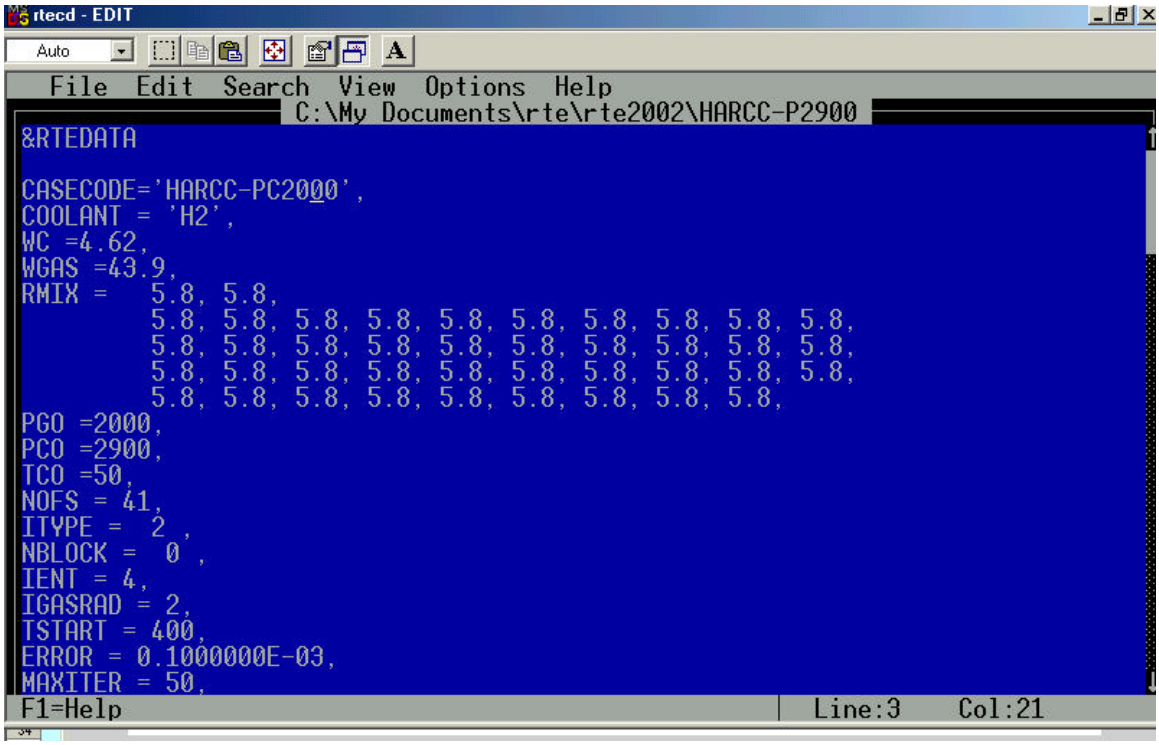

Figure C-12: RTE's input file generated by its preprocessor

After generating the RTE's input file the selected editor will be invoked and shows a listing of the data file similar to that shown in Figure C-12. The user should scroll over the file to make sure selections are made correctly. Special attention should be given to the directory name to ensure that it is the same directory that the executable files of RTE reside in. If the directory name is correct, then by selecting exit from file list the control returns to the RTE's preprocessor. By clicking on "Generate RTE's Input", the preprocessor generates another data file, RTE.INP, which is directly read by unit 5 of RTE and its radiation module. Before running RTE the user should make sure that RTE.INP is saved in the same directory that executable files or RTE are located.

By clicking on "Run Radiation Module" the exchange factors files of RTE (TSS.DAT and TGS.DAT) are generated. Note that depending on the speed of your computer and number of stations in the input file running this file can take between one to 30 minutes. The DOS window generated after clicking on this button should be checked for the status of this run. Note that if a case with no gas radiation is considered this step can be skipped.

Finally, RTE can be executed by clicking on "Run RTE" button. The results are automatically placed in rte.out (output file of RTE). To have more control on the output and execution of RTE a user may choose to run RTE manually after generated input data files via the preprocessor. This can be done by going to the DOS mode, changing the directory to where the executable files of RTE are located and simply typing:
rte_rad (for running the radiation module), or

rte2002 > *outputfilename* (for running RTE).

UNIX operating system users can generate RTE's input on WINDOWS and then ftp the data file to the UNIX computer.

APPENDIX D

RTE –TDK Interface

Shell Program for Interfacing RTE and TDK

Shell programs based on the flowchart of Figure 1, for both WINDOWS and UNIX are developed for interfacing RTE and TDK. These shell programs have two input files, (inputs of RTE and TDK) and two output files (outputs of RTE and TDK).

For the MS WINDOWS operating systems this shell program can be run by typing its executable file (rtecom.exe) in the DOS mode or by double clicking on the executable file. RTE's input file must be named rte.in or copied onto rte.in (RTE's input file name is hardwired in the shell program as rte.in). The format of RTE's input file is the same as RTE.INP file described in Appendix B, with IWLFUX set to 0. TDK's input file must be named tdk.in and it has a format the same as that described in its manual [6], except that its BLM or MABL namelists must be replaced by the word BLM or MABL, respectively.

Sample input of TDK

```
TITLE HYDROGEN COOLED ENGINE DATA - BLM FOR BOUNDARY LAYER DATA
 $DATA
 ODE = 1, ODK = 0, TDE = 1, BLM = 1,
 SHOCK = 0, IRPEAT=0, IRSTRT=0,
 NZONES = 1,
 XIC(1)=6, NXIC=1,
 ECRAT=3.4082, ASUB=3.4082, 2.1025, 1.2648, NASUB=3,
 ASUP = 1.0720, 1.7121, 3.5315, 6.629, NASUP=4,
 RSI = 1.3, RWTU = 1.555, RWTD = 0.77, THETAI = 14.5, RI = 15.564,
 THETA=36.868,
 IWALL=2, RMAX=2.5746, ZMAX=2.4677,
 IOFF=3,
 $END

REACTANTS
H 2.                                              100.       0.0 G 298.15
F
O 2.                                              100.   -3102.0 L  90.56
O 1.149

NAMELISTS
 $ODE
 RKT = T, OF = T, OFSKED = 5.80,
 P = 2000, XP = 1, PSIA = T, DELH = 0,
 $END
REACTIONS
H + H = H2     ,M1, A = 6.4E17, N = 1.0, B = 0.0, (AR) BAULCH 72 (A)
30U
H + OH = H2O   ,M2, A = 8.4E21, N = 2.0, B = 0.0, (AR) BAULCH 72 (A)
10U
O + O = O2     ,M3, A = 1.9E13, N = 0.0, B =-1.79,(AR) BAULCH 76 (A)
10U
O + H = OH     ,M7, A =3.62E18, N = 1.0, B = 0.0, (AR) JENSEN 78 (B)
30U
END TBR REAX
O2 + H = O + OH    , A = 2.2E14, N = 0.0, B =16.8,   BAULCH 72 (A) 1.5U
H2 + O = H + OH    , A = 1.8E10, N = -1., B = 8.9,   BAULCH 72 (A) 1.5U
```

```
H2 + OH = H2O + H  , A = 2.2E13, N = 0.0, B =5.15,   BAULCH 72 (A) 2U
OH + OH = H2O + O  , A = 6.3E12, N = 0.0, B =1.09,   BAULCH 72 (A) 3U
LAST REAX
THIRD BODY REAX RATE RATIOS
M1 = 25*H,4*H2,10*H2O,25*O,25*OH,1.5*O2,
M2 = 12.5*H,5*H2,17*H2O,12.5*O,12.5*OH,6*O2,
M3 = 12.5*H,5*H2,5*H2O,12.5*O,12.5*OH,11*O2,
M7 = 12.5*H,5*H2,5*H2O,12.5*O,12.5*OH,5*O2,
LAST CARD
 $ODK
 JPRNT=-2,
 EP = 7.203,
 $END
 $TRANS
 MP = 200,
 XM = 1,
 $END
 $MOC
 NC = 0,
 ISHCK=0,
 IMAX=40, IMAXF=1,
 $END
 $BLM
 IHFLAG=0,
BLM
 $END
FINISH
```

In addition to RTE and TDK's input files another file is needed to control convergence of wall heat fluxes. This file is CONVERGE.DAT and has a NAMELIST format. Its variables include:

ITER	Iteration number which should be set to 0 before every TDK-RTE run. During iterations its value indicates iteration number.
ERROR	Convergence criterion, iteration stops when relative difference between wall heat fluxes of two consecutive iterations is less than this number.
XSTART	Position of the boundary layer leading edge. It is better to set this point behind the injector in order to have stable wall fluxes. Note, if XSTART is placed after the injectors, RTE will be used to calculate heat fluxes for those stations between the injector and the leading edge of the boundary layer.
NSKIP	Number of station to be skipped after XSTART. If NSKIP=0, heat fluxes for all stations after XSTART will be evaluated based on TDK.
QW1	an array of wall heat fluxes. Should be equal to zero at the beginning of the run. Number of these heat fluxes is equal to the number of stations. After the calculation is finished it gives an array of heat fluxes for different stations.

Sample of CONVERGE.DAT

Sample CONVERGE.DAT at the beginning of the run

```
$CONVERGE
 ITER=    0,
 ERROR=   .010000,
 XSTART= -17.80000,
 NSKIP=    0,
 QW1=      43*0,
$END
```

Sample CONVERGE.DAT at the beginning of the run

```
$CONVERGE
 ITER=    3,
 ERROR=   .010000,
 XSTART= -17.80000,
 NSKIP=    0,
 QW1=      3.36077,
       3.78935,
       4.32674,
       4.82563,
       5.50660,
       5.95934,
       6.70223,
       7.09922,
       8.63991,
       9.81184,
      11.03034,
      12.55929,
      13.87093,
      15.20585,
      16.01301,
      16.55629,
      16.70487,
      16.81964,
      16.93441,
      17.10493,
      17.38694,
      17.71813,
      18.09195,
      16.51487,
      14.04131,
      12.19678,
      10.47431,
       8.78109,
       7.76877,
       7.39723,
       7.10463,
       6.94462,
       6.77984,
       6.61363,
       6.59601,
```

```
        6.65873,
        6.72459,
        6.80522,
        6.89900,
        7.00498,
        7.13237,
        7.30026,
        7.49020,
 $END
```

Running RTE-TDK interface

For **WINDOWS**, copy RTE's input file onto rte.dat and TDK's input file onto tdk.dat. Then, in DOS mode go to the rte directory and type rtecom.exe, or double click on rtecom.exe. The outputs of TDK and RTE will be printed onto rte.out and tdk.out. During the iteration, CONVERGE.DAT can be viewed for the status of convergence.

For **UNIX** systems, type the following command:

`rte.com` *`rteinputfilename tdkinputfilename rteoutputfilename tdkoutputfilename`*

rte.com takes `rteinputfilename` and `tdkinputfilename` for inputs of RTE and TDK respectively. The results of each run will be printed onto `rteoutputfilename`, for RTE's output and `tdkoutfilename` for TDK's output.